Aix*Marseille université
Socialement engagée

NNT : 2024AIXM0000

THÈSE DE DOCTORAT

Soutenue à Aix-Marseille Université
le 3 juillet 2024 par

Magali JAY

Dynamique des billards dans les pavages

Renormalisation des échanges d'intervalles et des surfaces de demi-translation

Discipline
Mathématiques

École doctorale
École doctorale en Mathématiques et Informatique de Marseille - ED 184

Laboratoire
Institut de Mathématiques de Marseille
I2M - UMR 7373

Composition du jury

Jayadev ATHREYA PR, Université de Washington	Rapporteur
Stefano MARMI PR, ENS de Pise	Rapporteur
Erwan LANNEAU PR, Université de Grenoble	Examinateur
Carlos MATHEUS DR, École Polytechnique	Examinateur
Anja RANDECKER CR, Université de Heidelberg	Examinatrice
Pierre ARNOUX PR, Université d'Aix-Marseille	Président du jury
Pascal HUBERT PR, Université d'Aix-Marseille	Directeur de thèse
Olga PARIS-ROMASKEVICH CR, Université d'Aix-Marseille	Codirectrice de thèse

INSTITUT
de MATHÉMATIQUES
de MARSEILLE

Il me semble que j'imite
Et pourtant je cherche qui.

J'ai vu le sable et le vent
Essayer de faire un corps.

J'ai vu l'eau se soulever
Mais le plan est fait pour elle.

J'ai vu durer les rochers
Plus informes que le ciel.

Moi j'ai la stabilité,
J'ai la force dans ma base,

La patience dans mes faces
Et l'esprit dans mon sommet.

J'ai de coupantes arêtes,
Je suis on ne peut plus nette.

Et puis qui n'imite pas,
Qui n'est pas un peu pareil

A tout cela qu'il n'est pas,
Qui ne lui ressemble pas ?

Nous, figures, nous n'avons
Après tout qu'un vrai mérite,

C'est de simplifier le monde,
D'être un rêve qu'il se donne.

« Pyramide », Eugène Guillevic, in *Euclidiennes*

En souvenir de Marcel

Affidavit

Je soussignée, Magali Jay, déclare par la présente que le travail présenté dans ce manuscrit est mon propre travail, réalisé sous la direction scientifique de Pascal Hubert et Olga Paris-Romaskevich, dans le respect des principes d'honnêteté, d'intégrité et de responsabilité inhérents à la mission de recherche. Les travaux de recherche et la rédaction de ce manuscrit ont été réalisés dans le respect à la fois de la charte nationale de déontologie des métiers de la recherche et de la charte d'Aix-Marseille Université relative à la lutte contre le plagiat.

Ce travail n'a pas été précédemment soumis en France ou à l'étranger dans une version identique ou similaire à un organisme examinateur.

Fait à Marseille le 28 avril 2024



Cette œuvre est mise à disposition selon les termes de la Licence Creative Commons Attribution - Pas d'Utilisation Commerciale - Pas de Modification 4.0 International.

Liste de publications et participation aux conférences

Liste des publications réalisées dans le cadre du projet de thèse :

(1) Magali Jay. Deviations for generalized tiling billiards in cyclic polygons. Preprint

(2) Magali Jay. An induction to study bi-triangle tiling billiards. En cours de rédaction.

(3) Magali Jay. Tiling billiard in the wind-tree model. En cours de rédaction.

Participation aux conférences et écoles d'été au cours de la période de thèse :

(1) **Paroles aux jeunes chercheurs en géométrie et dynamique**, CIRM - *Poster* Novembre 2021

(2) **École d'hiver d'Aussois** Décembre 2021

(3) **École d'hiver sur les billards**, Autrans - *Oratrice* Janvier 2022

(4) **Combinatoire, dynamique et géométrie dans les espaces de modules** au CIRM - *Poster* Septembre 2022

(5) **Big Mapping Class Group and Diffeomorphism Groups** au CIRM Octobre 2022

(6) **Paroles aux jeunes chercheurs en géométrie et dynamique**, Orsay - *Exposé de 5 min* Novembre 2022

(7) **École d'hiver d'Aussois** - *Oratrice* Décembre 2022

(8) **École de Printemps en Géométrie et Dynamique** du GDR Platon, Lille - *Oratrice* Mars 2023

(9) **Renormalisation et visualisation en géométrie, dynamique et théorie des nombres**, CIRM Juillet 2023

(10) **Renormalisation, programmation et visualisation en géométrie, théorie des nombres et dynamique**, Workshop au CIRM Septembre 2023

(11) **Paroles aux jeunes chercheurs en géométrie et dynamique**, Grenoble - *Oratrice* Novembre 2023

(12) **Mathématiques et art : Création commune** au CIRM - *Animation d'un atelier* Novembre 2023

(13) **Renormalisation et visualisation en géométrie, dynamique et théorie des nombres**, CIRM Décembre 2023

(14) **Weinachtsworkshop**, Karlsruhe - *Oratrice* Décembre 2023

(15) **Sagedays**, workshop de programmation, Le Teich Janvier 2024

(16) **École sur les surfaces plates et interactions**, Le Teich - *Oratrice* Mars 2024

(17) **Surfaces, MAnifolds, and Related Topics**, Luxembourg - *Oratrice* Mars 2024

(18) **New Frontiers in Parabolic Dynamics and Renormalization**, Bologna Juin 2024

(19) Participation aux **Rencontres de l'ANR GALS** à Paris et Lyon Janvier et Juin 2024

Résumé et mots clés

Les billards dans les pavages sont des systèmes dynamiques dont l'étude est motivée par des questions aussi bien physiques que mathématiques. Au début des années 2000, des physiciens ont conçu et réalisé des méta-matériaux dans lesquels les ondes électromagnétiques se réfractent selon la loi de Snell-Descartes avec un coefficient négatif. Le trajet de la lumière dans un arrangement de méta-matériaux d'indices de réfraction opposés constitue la trajectoire d'un billard dans un pavage. C'est une ligne brisée dans le plan, droite à l'intérieur de chaque tuile du pavage, et réfractée à la frontière entre deux tuiles. Que peut-on dire de telles trajectoires ? Sont-elles bornées ou non ? Périodiques ? Comment s'échappent-elles à l'infini ? La littérature répond à ces questions pour un petit nombre de pavages, mais pour l'essentiel des configurations les questions restent ouvertes. Dans la plupart des cas étudiés, chaque trajectoire s'identifie à l'orbite d'un point par un échange d'intervalles avec retournements. Le chapitre 2 présente les outils utilisés.

Dans le chapitre 3, j'introduis une nouvelle notion, celle de billards dans des pavages généralisés, construits avec des polygones inscrits dans des cercles. Les trajectoires étudiées présentent des comportements différents de celles connues auparavant dans les pavages triangulaires et quadrilatéraux cycliques. J'exhibe un ensemble ouvert de paramètres pour lesquels les trajectoires admettent une direction asymptotique et en dévient de façon sous-linéaire. Cela n'arrive jamais dans des pavages triangulaires ou quadrilatéraux. De plus, j'établis le taux de croissance de ces déviations, dans le cas générique et dans certains cas non génériques.

Dans le chapitre 4, j'étudie la classe des échanges d'intervalles associés aux billards dans un pavage bi-triangulaire. Ce sont des échanges d'intervalles définis sur deux cercles de même périmètre, qui admettent chacun trois intervalles de continuité (tous renversés). Je définis une induction pour étudier cette classe d'échanges d'intervalles. Cette induction permet de restreindre l'ensemble des paramètres susceptibles de correspondre à des échanges d'intervalles minimaux.

Le chapitre 5 s'intéresse aux trajectoires obtenues dans un arrangement périodique de rectangles (d'indice -1) dans le plan euclidien (d'indice 1). Cet arrangement est celui du modèle du vent dans les arbres. Je montre que pour presque tout choix de paramètres, les trajectoires restent dans une bande (de largeur bornée) du plan. Ce comportement est semblable à celui des lentilles d'Eaton.

Mots clés : billards dans des pavages, échanges d'intervalles avec ou sans retournements, induction de Rauzy, surfaces de translation ou demi translation, flot de Teichmüller, cocycle de Kontsevich-Zorich

Abstract and keywords

Tiling billiards are dynamical systems studied for both physical and mathematical reasons. In the early 2000's, physicists designed and produced meta-materials that refract electromagnetic waves according to Snell's law with a negative coefficient. The light rays in an array of such meta-material with opposite refraction indices form the trajectories of a tiling billiard. They are broken lines, straight inside each tile of the tiling, and refracted each time they cross a side of a tile. What can we say about such trajectories? Are they bounded or not? Periodic? How do they go to infinity? The answers to these questions are known for a small set of tilings, but for the majority of configurations they are open questions. In most studied cases, each trajectory can be identified to the orbit of a point under the action of an interval exchange transformation with flips on one or more circles. Chapter 2 introduces the mathematical tools that I use.

In Chapter 3, I introduce a new notion, of generalized tiling billiards in cyclic polygons. The behavior of generalized tiling billiards in cyclic N-gons with $N \geqslant 5$ is significantly different from that of triangular and cyclic quadrilateral tiling billiards. I exhibit an open set of parameters for which the trajectories deviate sublinearly from their asymptotic direction, which never happens with triangle or cyclic quadrilateral tilings. Moreover, I establish the rate of deviations both in the generic case and in some non-generic cases.

In Chapter 4, I study a class of interval exchange transformations corresponding to bi-triangle tiling billiards. To study this class, I define an induction, which allows to restrict the possible parameters for minimal interval exchange transformations with flips (IETFs) in this class.

Finally, in Chapter 5, I consider the trajectories of a light ray in a periodic array of rectangles (of index -1) in the plane $\mathbb{R}^2$ (of index 1). This array is the one of the so-called wind-tree model. I show that for almost every choice of parameters, the trajectories stay in a strip of bounded width. This behavior is similar to that of Eaton lenses.

Keywords: tiling billiards, interval exchange transformations with or without flips, Rauzy induction, translation and half-translation surfaces, Teichmüller flow, Kontsevich-Zorich cocycle

Remerciements

J'ai eu la chance de vivre trois passionnantes années de thèse, au cours desquelles je me suis sentie à l'aise et ne me suis jamais ennuyée. Cela doit beaucoup à mes directeur et directrice de thèse, **Pascal Hubert** et **Olga Paris-Romaskevich**. Je vous remercie tous les deux de m'avoir proposé un sujet aussi riche, sur lequel j'ai eu plaisir à travailler avec vous. Je vous suis très reconnaissante de toutes les maths que vous m'avez transmises. J'ai bénéficié de votre recul sur le domaine, que vous avez chaleureusement partagé avec moi. Merci pour votre disponibilité malgré vos emplois du temps très chargés ! Merci à toi Olga de tes conseils précis et ton aide patiente pour améliorer mon travail, à l'écrit comme à l'oral. Merci à toi Pascal d'avoir toujours pris le temps de vérifier jusqu'aux lemmes d'algèbre linéaire lors de nos séances de travail hebdomadaires. Votre confiance en moi, votre enthousiasme pour mon travail, de recherche et de diffusion, m'ont porté pendant trois ans. Je me suis sentie à la fois très libre et bien entourée. Un grand merci à vous !

Merci à **Jayadev Athreya** et **Stefano Marmi** qui me font l'honneur de rapporter cette thèse. Merci pour votre intérêt pour mon travail. Merci Jayadev pour tous nos échanges lors de ton semestre de chaire Jean Morlet à Marseille. Merci Stefano pour ta lecture attentive et ton rapport très détaillé. Merci à **Pierre Arnoux**, **Erwan Lanneau**, **Carlos Matheus** et **Anja Randecker** de participer au jury. Merci Pierre pour nos échanges enrichissants et tes explications toujours passionnées. Merci Erwan de m'avoir le premier proposé de travailler sur les échanges d'intervalles, puis de m'avoir si bien aiguillée jusqu'à Marseille. Merci Carlos pour la mine précieuse de maths que constitue ton blog. Danke schön Anja, dass du einverstanden bist, dass ich auf Französich verteidige ! Ich hoffe, dass ich bald auch auf Deutsch meine Mathe erklären kann.

Je remercie l'ensemble des membres de mon équipe, GDAC, et toutes les personnes du labo, qui m'ont accueillie et intégrée. Je me suis sentie à ma place à l'I2M. Je tiens à remercier **Etienne Moutot** pour son programme qui m'a permis d'illustrer de nombreuses trajectoires de billards de pavages, **Paul Mercat** pour ses programmes de calcul de diagrammes de Rauzy et **Vincent Delecroix** pour son accompagnement à la création d'un nouveau programme Sage qui fournira des simulations des trajectoires que j'étudie. Merci à **Adrien Boulanger** et à **Lionel Nguyen Van-Thé** dont j'ai beaucoup apprécié les cours doctoraux.

Merci à **Maéva Bessi**, **Jessica Bouanane**, **Sarah Darfeuille**, **Kaina Tighilt** et **Valérie Demare** : grâce à leur travail j'ai pu aller en conférences et séminaires

pendant ces trois ans. Merci à **Marie-Christine Tort-Rigat** pour le miel, et à **Evelyne Henri** pour sa belle initiative végétale, qui améliore notre cadre de travail. Merci Evelyne pour tous tes conseils relatifs à l'impression du manuscrit. Ma thèse s'est déroulée à une période charnière, entre le post-covid, pré-déménagement du site du CMI, travaux du site de Luminy. Après des échanges par mail pendant deux ans à cause de cette situation, je suis très heureuse qu'on puisse maintenant se saluer au moment de la pause café et discuter en direct !

Merci à l'ensemble du personnel du CIRM pour l'accueil chaleureux. J'ai hâte de revenir ici en conférence !

Je remercie également les personnes qui nettoient nos locaux et qui m'ont permis de travailler dans un endroit agréable.

Merci à **Adel**, **Alex**, **Max**, **Michael**, **Roméo** et **Sarah** de m'avoir appris patiemment un joli répertoire musical. Ma présence aux séances était malheureusement irrégulière, mais j'en sortais toujours contente et motivée. Elles ont été ma récompense du vendredi soir lors des semaines plus difficiles de rédaction.

Merci aux doctorant.e.s (et celles et ceux qui sont déjà jeunes docteur.e.s) de Marseille et d'ailleurs (rencontré.e.s avant ou en conf) pour les pauses partagées dans la bonne humeur, les maths échangées, et les parties de baby-foot.

Merci à toutes celles et ceux qui font naître de l'émerveillement mathématique chez les enfants et le grand public, et qui ont participé à mon envie de faire des maths. J'ai une pensée pour ma professeure de mathématiques de collège **Evelyne Mialhe**, avec qui j'ai notamment appris à me servir de géogébra, logiciel qui fut bien utile pour concevoir plusieurs figures de ma thèse.

Merci à toutes les personnes qui, aimant ou non les maths, m'ont écouté parler de ma thèse, s'y s'ont intéressées, m'ont posé des questions. J'ai ainsi pris possession du sujet, et de la manière la plus agréable qui soit : pour le partager. Merci à toutes celles et ceux qui se sont venu.e.s parfois de loin jusqu'au CIRM pour assister à ma soutenance. Votre présence me touche beaucoup.

Merci au grand et lumineux **Félix** d'avoir partagé avec moi dans la bonne humeur les jeux de mots de notre appartement pendant un an. Et de m'avoir régulièrement rappelé que *les mathématiques, c'est facile, il suffit d'écrire une succession de choses justes*. Merci à **Maud**, **Antoine**, **Lucas** et **Yaël**, pour nos belles parties de fou rire, nos discussions philosophiques ou de tous les jours. Vous me manquerez l'année prochaine.

Et puis merci **maman** – pour ton soutien constant, pour ton aide précieuse lors du marathon de la dernière année, celle indispensable lors du sprint final de rédaction, et, bien au-delà, pour tout ce qui l'a précédé.

Table des matières

Affidavit 4

Liste de publications et participation aux conférences 5

Résumé et mots clés 7

Abstract and keywords 8

Remerciements 9

Table des matières 11

Table des figures 14

1. Introduction 16
- 1.1. Billards dans des pavages . . . 16
  - 1.1.1. Aperçu historique et motivations . . . 16
  - 1.1.2. Configurations déjà étudiées . . . 18
  - 1.1.3. Situations étudiées dans cette thèse . . . 21
- 1.2. Objets mathématiques associés . . . 26
  - 1.2.1. Aperçu historique et motivations . . . 27
  - 1.2.2. De l'importance de l'induction . . . 29
  - 1.2.3. Dans cette thèse . . . 30

2. Background 32
- 2.1. Interval exchange transformations . . . 32
  - 2.1.1. Definition . . . 32
  - 2.1.2. Description of an IET . . . 34
  - 2.1.3. Topology and measure . . . 35
  - 2.1.4. The Rauzy induction . . . 36
  - 2.1.5. The Rokhlin towers . . . 36
  - 2.1.6. The Kontsevich–Zorich cocycle (combinatorial point of view) 37
  - 2.1.7. The Rauzy diagram . . . 37
  - 2.1.8. Associated substitution . . . 39
  - 2.1.9. Decomposition of the symbolic coding . . . 40
- 2.2. Translation surfaces . . . 42
  - 2.2.1. Definition . . . 42

2.2.2. Suspensions of an IET . . . 43
2.2.3. Teichmüller space and moduli space . . . 44
2.2.4. The Kontsevich-Zorich cocycle (geometric point of view) . . . 45
2.3. The Oseledets theorem . . . 45

3. Deviations for generalized tiling billiards in cyclic polygons 47
3.1. Introduction . . . 47
3.1.1. The generalized tiling . . . 47
3.1.2. Assumptions . . . 48
3.1.3. Results . . . 50
3.1.4. Outline of the proof . . . 51
3.2. The studied system . . . 53
3.2.1. Definition of a generalized tiling billiard . . . 53
3.2.2. A system of coordinates . . . 53
3.2.3. The obtained Interval Exchange Transformation . . . 55
3.3. To approximate the trajectory . . . 56
3.3.1. Lengths of shifts . . . 56
3.3.2. Estimate the trajectory . . . 57
3.3.3. Average shift . . . 58
3.3.4. Normalized deviations . . . 59
3.4. The generic case . . . 60
3.4.1. Expression of H, when $N = 5$ . . . 61
3.4.2. The vector H is almost never in a fixed plane, when $N = 5$ . . . 62
3.4.3. For $N > 5$ . . . 63
3.4.4. Conclusion . . . 65
3.5. A special case . . . 66
3.5.1. Upper bound . . . 67
3.5.2. Lower bound . . . 69
3.6. Concluding remarks . . . 70

4. Bi-triangle tiling billiards 72
4.1. Introduction . . . 72
4.1.1. The bi-triangle tiling . . . 72
4.1.2. Motivations . . . 72
4.2. The associated IETFs . . . 73
4.2.1. How to associated an IETF to a bi-triangle tiling billiard . . . 74
4.2.2. Description of an IETF defined on a union of d circles . . . 75
4.2.3. The IETFs associated to the bi-triangle tiling billiards . . . 76
4.3. The induction . . . 79
4.3.1. Presentation . . . 79
4.3.2. Conditions . . . 79
4.3.3. Computations under conditions (C0), (C1) and (C2) . . . 83
4.3.4. When a condition fails . . . 97

4.4. Perspectives 100
4.4.1. Complete description of bi-triangle tiling billiards 100
4.4.2. Admissible tilings 101

5. The tiling billiard in the wind-tree model **103**
5.1. Introduction 103
5.1.1. Setting 103
5.1.2. Strategy 104
5.2. The corresponding surface 104
5.2.1. From foliations to an appropriate slit surface 104
5.2.2. Equivalent trajectories 107
5.2.3. The finite half-translation surface we will work with 109
5.2.4. How generic is the surface? 110
5.2.5. The new question 112
5.3. Decomposition of the trajectory 113
5.3.1. From a path to a cycle 113
5.3.2. Uniform bounds in a neighborhood of the surface X 115
5.3.3. Decomposition of the cycle 117
5.4. Conclusion 119
5.4.1. Computation of the algebraic intersection number 119
5.4.2. Conclusion using the Oseledets theorem 120
5.5. Perspectives 121

Conclusion **123**

Bibliographie **125**

Table des figures

1.1. Tous les types de trajectoires des billards dans des pavages réguliers 16
1.2. Exemples de deux trajectoires de billard dans un pavage librement inspiré de l'œuvre *Motifs abstraits (masques)* de Sophie Taeuber-Arp 17
1.3. Exemples de trajectoires de billards dans un pavage triangulaire . . 19
1.4. Trajectoires génériques pour un billard de pavage quadrilatéral . . . 19
1.5. La grandeur conservée au cours de la trajectoire 20
1.6. Sommet pliable : la somme des angles bleus et celle des angles rouges sont égales 20
1.7. Exemples de trajectoires du billard dans le pavage trihexagonal. Source : [DH18] 21
1.8. Pavage bi-triangulaire du plan 23
1.9. Le modèle du vent dans les arbres 24
1.10. Une lentille d'Eaton et des rayons lumineux déviés. Source : [FS14] 25
1.11. Trajet d'un rayon lumineux dans un arrangement de lentilles d'Eaton 25
1.12. Exemple de trajectoire dans le système $W(\Lambda, 0.7, 0.5, \frac{17\pi}{60})$ 26

2.1. Example of an IET which is a rotation 32
2.2. The IET R seen as a first recurrence map on the torus 33
2.3. Composition of IETs 33
2.4. Example of an IET and its inverse 35
2.5. The simplex representing IET_π and $T = (\pi, \lambda(T))$ from examples 2.3 and 2.8 36
2.6. Rauzy induction 37
2.7. Rokhlin towers of orders 1 to 5 for the Rauzy induction of an IET . 38
2.8. The link between the orbit of x and the Rokhlin towers 41
2.9. Suspensions data for the example of Figure 2.6 43
2.10. The suspension data may not give a polygon 43

3.1. The way we put polygons together to play tiling billiards will not tile the plane with N-gons, $N \geqslant 5$. 47
3.2. Examples of trajectories in generalized pentagonal tiling billiards . . 48
3.3. Notations for cyclic polygons and assumption (C) 49
3.4. The modulus of the deviations, depending on the number of steps of the trajectory, has a sublinear growth 52
3.5. Notations for generalized tiling billiards 53
3.6. Moving frame of reference 54
3.7. Coordinates x_i and x_{i+1} are related by a a linear equation 55

3.8. Example of the IETs Φ and Φ^2, corresponding to a tiling billiard. . 56
3.9. Translations f_i when crossing sides a_i followed by side a_5 57

4.1. Setting for bi-triangle tiling billiards 72
4.2. Notation for the bi-triangle tiling billiard 74
4.3. Notations for the frame of reference to study the bi-triangle tiling billiard 75
4.4. Coordinates x_{k+1} and x_k are related by a linear equation 77
4.5. The associated IETF 78
4.6. "Criss-crossed" singularities 80
4.7. Rauzy diagram for the induction without relabeling 83
4.8. Induction on $p_1(A)$ with loser A: we get $p_1(A)$ 85
4.9. Induction on $p_2(A)$ with loser A: we get $p_2(A)$ 85
4.10. Induction on $p_1(A)$ with loser B: we get $p_2(C)$ 86
4.11. Induction on $p_2(A)$ with loser B: we get $p_1(C)$ 86
4.12. Induction on $p_1(A)$ with loser C: we get $p_2(B)$ 87
4.13. Induction on $p_2(A)$ with loser C: we get $p_1(B)$ 87
4.14. Rauzy diagram for the induction with relabeling 89
4.15. The matrices of the the induction in the new basis 95
4.17. An induced IETF with a new combinatorial data 98
4.16. When $(C1)$ is not satisfied, T admits periodic points 102

5.1. Example of a trajectory 103
5.2. The different ways to go through the obstacle 105
5.3. From a rectangular obstacle to a slit with identifications 105
5.4. Identifications of the slit 106
5.5. The surface $S_{(\Lambda,a,b,\theta)}$ 106
5.6. An example where (Λ, a, b, θ) is admissible but not strongly admissible 107
5.7. Definition of the set $\tilde{F}$ 108
5.8. Changing the surface from $\mathbb{R}^2$ to $S_{(\Lambda,a,b,\theta)}$ changes the parametrization of γ 109
5.9. Singularities on the slit 109
5.10. Two equivalent trajectories 110
5.11. The cycles which we consider 112
5.12. Illustration of the different curves 117

1. Introduction

1.1. Billards dans des pavages

1.1.1. Aperçu historique et motivations

Dans leur article [DDRS18], Davis, DiPietro, Rustad et St-Laurent définissent et étudient une classe de systèmes dynamiques qu'ils appellent *tiling billiards*, que je traduis par *billards dans des pavages* ou *billards de pavages* pour alléger. Ce sont des systèmes dynamiques dans le plan euclidien muni d'un pavage (polygonal). Les trajectoires d'un billard de pavage sont des lignes brisées : rectilignes à l'intérieur des tuiles du pavage, et réfractées aux frontières de celles-ci. La Figure 1.1 illustre de telles trajectoires pour des pavages réguliers. La Figure 1.2 donne l'exemple de deux trajectoires dans un autre pavage.

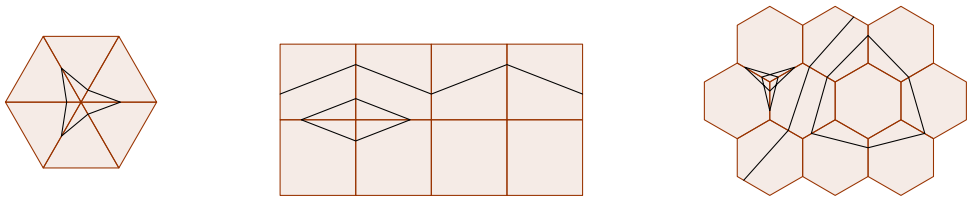

FIGURE 1.1. – Tous les types de trajectoires des billards dans des pavages réguliers

Au début des années 2000, des physiciens ont conçu des méta-matériaux dont l'indice de réfraction optique est négatif [SSS01], [SPW04]. Cette découverte a motivé l'étude des billards de pavages. Notons cependant que le domaine de fréquence pour lequel les ondes électromagnétiques sont réfractées est restreint, et *a priori* en dehors du domaine visible (dans l'article [SSS01], il s'agit de micro-ondes). Depuis, Dynnikov, Hubert, Mercat, Paris-Romaskevich et Skripchenko [DHMPS ; Par21] ont établi le lien entre les billards de pavages et le problème de Novikov, qui est lui motivé par un autre problème de physique : celui du déplacement des électrons dans un métal plongé dans un champ magnétique de faible intensité.

Dans certains cas, les billards de pavages sont en fait un cas particulier des *billards avec retournements* introduits plus tôt par Nogueira à la fin de son article [Nog89]. Il en suggérait l'étude car ils traduisent la dynamique des échanges d'intervalles avec retournements et constituent ainsi une généralisation des billards polygonaux rationnels, étudiés à l'aide d'échanges d'intervalles sans retournements.

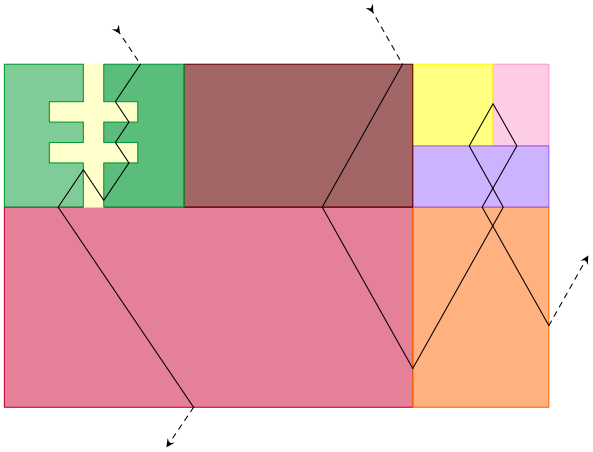

FIGURE 1.2. – Exemples de deux trajectoires de billard dans un pavage librement inspiré de l'œuvre *Motifs abstraits (masques)* de Sophie Taeuber-Arp

On présentera les échanges d'intervalles avec ou sans retournements en seconde partie de cette introduction puis de façon formelle au chapitre suivant.

Quels types de trajectoires sont possibles pour un billard dans un pavage fixé ? Périodiques ? Non bornées ? Denses dans un ouvert du plan ? Ces trajectoires sont-elles *stables* lorsque l'on modifie légèrement le pavage ou le point et la direction initiale de la trajectoire ? Par stable, on entend : la trajectoire modifiée passe par les mêmes tuiles du pavage et dans le même ordre que la trajectoire initiale.

On dispose d'exemples de billards de pavages avec des trajectoires :

- *périodiques*, c'est-à-dire fermées ;
- *périodiques à décalage près – drift-periodic* en anglais – c'est-à-dire invariantes par une certaine translation ;
- *à échappement linéaire*, c'est-à-dire admettant une direction asymptotique, *avec ou sans* déviations sous-linéaires (non bornées) associées ;
- *vagabondes* : non bornées, sans direction asymptotique, et passant au plus une fois par chaque tuile – on peut montrer dans certains cas qu'elles passent par toutes les tuiles du pavage ;
- *denses dans un ouvert du plan.*

Les comportements des trajectoires de billards de pavages ont tendance à se distinguer de ceux des trajectoires de billards polygonaux rationnels classiques, de même que la dynamique typique des échanges d'intervalles avec retournements (EIR) se distingue de celle des échanges d'intervalles sans retournements (EI).

1.1.2. Configurations déjà étudiées

Aucune étude générale des billards de pavages n'est encore faite. Voici un aperçu des configurations traitées dans la littérature avant ma thèse.

1.1.2.a. Pavages triangulaires et pavages quadrilatéraux cycliques

Choisissons un triangle δ. Avec δ et son image par une symétrie centrale, nous formons un parallèlogramme qui pave le plan de façon périodique, cf. Figure 1.3. Remarquons que chaque tuile du pavage $\mathcal{P}(\delta)$ obtenu est l'image de ses voisines par une symétrie centrale. L'étude des billards dans un tel pavage triangulaire commence avec [BDFI24]. Cet article fournit de premiers résultats, notamment grâce à un bel argument de pliage, et énonce plusieurs conjectures, dont certaines sont établies dans [Par19] et [HP22]. Paris-Romaskevich [Par19] a fourni la description complète des trajectoires de billards dans ces pavages triangulaires.

Théorème 1 ([BDFI24], [Par19], [HP22]). *Soit δ un triangle. Soit γ une trajectoire du billard dans le pavage $\mathcal{P}(\delta)$. Une et une seule des propositions suivantes est satisfaite :*

(1) La trajectoire γ est périodique et stable par perturbation de δ ou des conditions initiales. De plus, le nombre de triangles traversés est de la forme $4n+2$ pour un certain entier $n \in \mathbb{N}^*$.

(2) La trajectoire γ est périodique à décalage près et les angles de δ sont rationnellement dépendants.

(3) La trajectoire γ n'est pas périodique à décalage près, mais est à échappement linéaire sans déviations. Dans ce cas, il existe deux mots u, v sur l'alphabet $\mathcal{A} = \{a, b, c\}$ des noms des côtés, tels que la suite des côtés traversés est une suite sturmienne sur l'alphabet $\mathcal{A}' = \{u, v\}$.

(4) La trajectoire γ n'est pas bornée, n'a pas de direction asymptotique et passe par le centre du cercle circonscrit des triangles traversés. De plus, dans l'espace de modules des triangles, δ appartient à la baderne de Rauzy, qui est de mesure de Lebesgue nulle.

Le quatrième cas correspond aux trajectoires que j'ai appelées vagabondes. Il est relié aux échanges d'intervalles avec retournements qui sont minimaux. Dynnikov, Hubert, Mercat, Paris-Romaskevich et Skripchenko [DHMPS] ont pu adapter les techniques utilisées aux cas des pavages construits avec un quadrilatère inscrit dans un cercle, cf. Figure 1.4. Ils montrent alors que presque toute trajectoire d'un billard dans un pavage quadrilatéral cyclique est périodique ou à distance bornée d'une droite – *cyclique* signifie inscrit dans un cercle. Ils obtiennent également une famille de trajectoires vagabondes, qui est de mesure nulle.

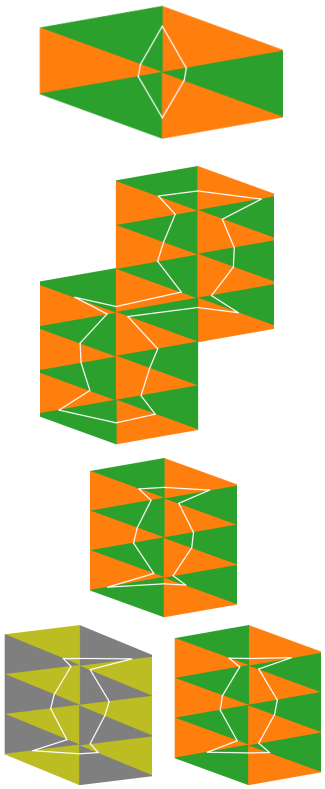

(a) Trois trajectoires périodiques suivies de deux perturbations de la troisième

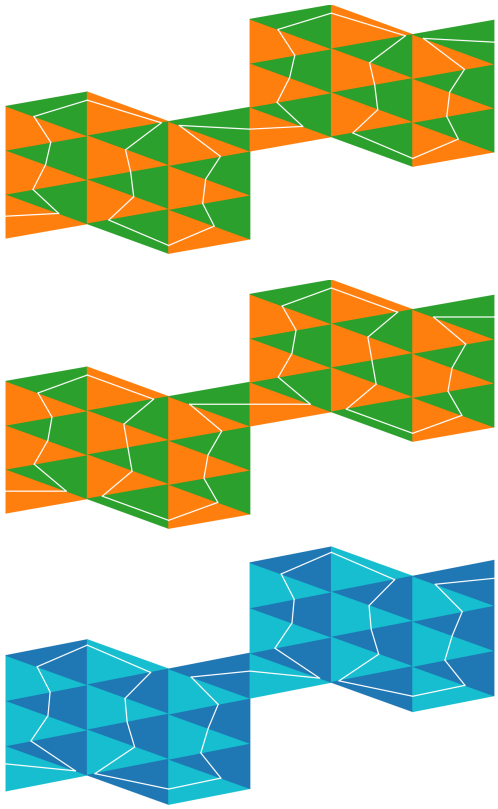

(b) Une trajectoire périodique à décalage près et deux perturbations de celle-ci

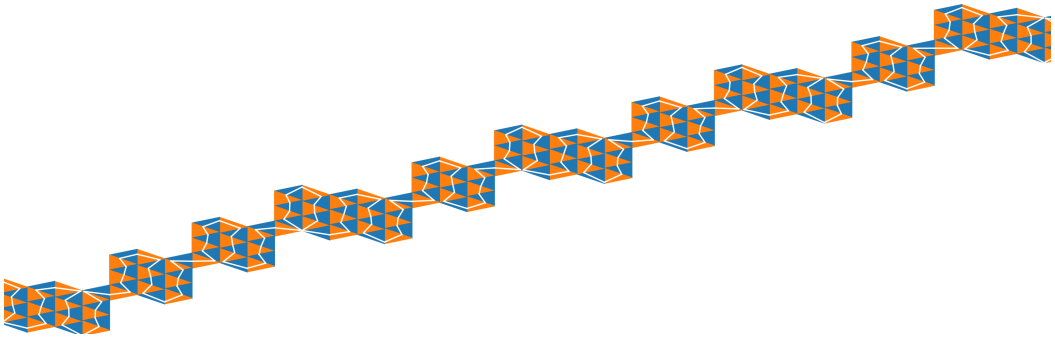

(c) Une trajectoire à échappement linéaire

FIGURE 1.3. – Exemples de trajectoires de billards dans un pavage triangulaire



(a) Une trajectoire périodique



(b) Une trajectoire à échappement linéaire

FIGURE 1.4. – Trajectoires génériques pour un billard de pavage quadrilatéral

Dans ces deux cas, le système dynamique admet une *intégrale première*, c'est-à-dire une quantité préservée au cours du temps. Il s'agit de la longueur d'une corde particulière, représentée en bleu et en gras dans la Figure 1.5. Baird-Smith, Davis,

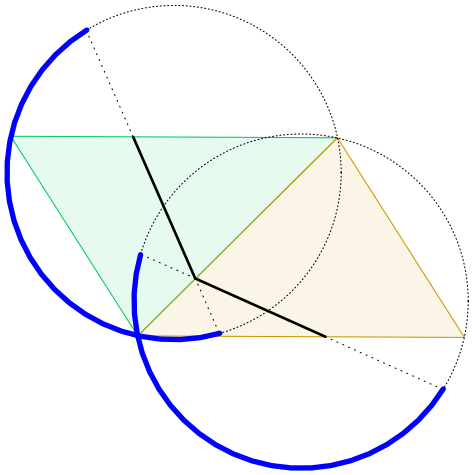

FIGURE 1.5. – La grandeur conservée au cours de la trajectoire
Toutes les cordes définies de la sorte le long de la trajectoire ont la même longueur.

Fromm et Iyer expliquent cela pour des triangles dans [BDFI24] (Lemme 3.2), avec le bel argument de pliage. Paris-Romaskevich [Par19] le présente pour tout pavage *localement pliable*, c'est-à-dire dont la somme alternée des angles autour d'un sommet est nulle, comme dans la Figure 1.6. Dans le chapitre 3, nous verrons que

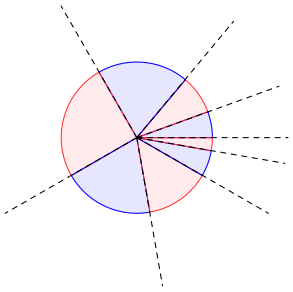

FIGURE 1.6. – Sommet pliable : la somme des angles bleus et celle des angles rouges sont égales

c'est vrai aussi pour un pavage dont toutes les tuiles sont inscrites dans un cercle de même rayon. J'appellerai *cocycliques* de telles tuiles. Le fait que cette quantité soit conservée nous permet d'étudier les billards de pavages à l'aide d'échanges d'intervalles avec retournements (EIR). La section 3.2.2 explique en détail le lien entre billards de pavages et EIR.

1.1.2.b. Pavage trihexagonal

Davis et Hooper se sont intéressés au billard dans le pavage fait d'hexagones réguliers et de triangles équilatéraux. Ils l'ont étudié via une certaine surface de translation S. Ils ont montré qu'à chaque trajectoire du billard dans le pavage trihexagonal correspond une trajectoire sur S. Ils ont ainsi prouvé le résultat suivant.

Théorème 2 (Davis–Hooper [DH18]). *Pour presque tout $(x, \theta) \in \mathbb{R}^2 \times \mathbb{S}^1$, il existe un ouvert $\mathcal{O} \subset \mathbb{R}^2$ qui est invariant par un réseau, tel que la trajectoire du billard de pavage trihexagonal partant de x et dans la direction θ est dense dans $\mathbb{R}^2 \setminus \mathcal{O}$.*

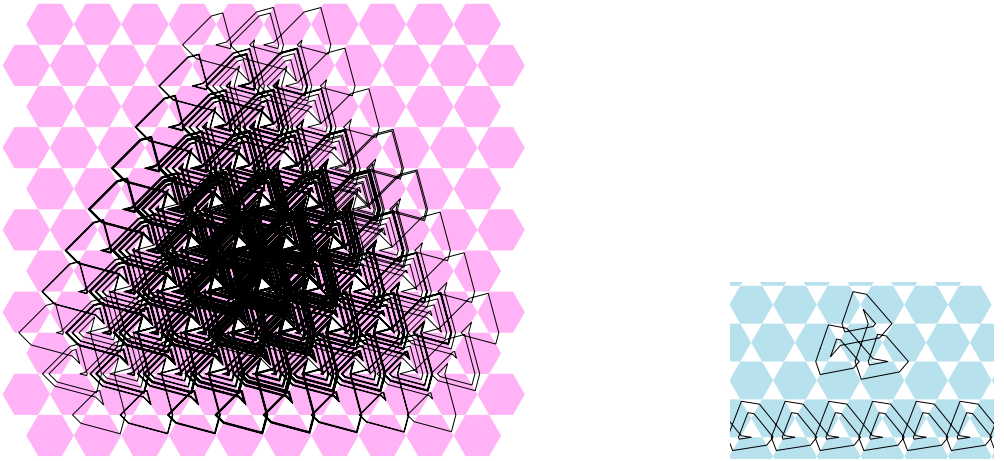

(a) Une trajectoire générique (b) Deux trajectoires exceptionnelles

FIGURE 1.7. – Exemples de trajectoires du billard dans le pavage trihexagonal. Source : [DH18]

Dans la Figure 1.7a, seul le début de la trajectoire est tracé. Plus on avance, plus elle remplit le plan, à l'exception de petits triangles positionnés régulièrement (ils se détachent en blanc sur le noir de la trajectoire au centre de la figure). Cet ensemble de triangles constitue l'ouvert $\mathcal{O}$.

1.1.3. Situations étudiées dans cette thèse

Au cours de cette thèse, j'étudie différentes configurations de billards de pavages. Chacune sera l'objet d'un chapitre.

1.1.3.a. Billards de pavages généralisés

Les pavages triangulaires et les pavages quadrilatéraux cycliques présentent des comportements similaires : presque toutes leurs trajectoires sont périodiques

ou à distance bornée d'une droite. En est-il de même pour des polygones avec plus de côtés ? Deux remarques s'imposent. Première remarque : comme pour les quadrilatères, on ne considère que des polygones inscrits dans un cercle. Seconde remarque : on ne peut pas paver le plan avec des polygones à cinq côtés ou plus par un pavage où chaque tuile est image de ses voisines par une symétrie centrale, comme on le faisait pour les triangles et les quadrilatères. La généralisation des billards dans les pavages triangulaires et quadrilatéraux demande donc de généraliser le contexte des pavages.

On fixe un polygone cyclique P. On trace les copies de P au fur et à mesure de la trajectoire : dès que la trajectoire touche le bord b_i d'une copie P_i de P, on trace l'image P_{i+1} de P_i par la symétrie de centre le milieu de b_i, la trajectoire continue son chemin, réfractée, dans P_{i+1}. L'ensemble des polygones obtenus peut ne pas remplir le plan et les polygones peuvent se superposer. J'appellerai *billard de pavage généralisé* un tel système, noté $\mathcal{B}(P)$. Je les étudie au chapitre 3 où j'exhibe une famille de trajectoires qui ne restent pas à distance bornée d'une droite. C'est l'objet du théorème suivant.

Théorème A. *Soit P un polygone inscrit dans un demi-cercle. Il existe un ouvert $\mathcal{O}(P) \subset \mathbb{R}^2 \times \mathbb{S}^1$ tel que pour tout $(x, \theta) \in \mathcal{O}$, la trajectoire de $\mathcal{B}(P)$ partant de x dans la direction θ admet une direction asymptotique et en dévie de façon sous-linéaire.*

Je donne l'expression de cette direction asymptotique et j'établis le taux de croissance des déviations de la trajectoire par rapport à une droite dans la direction asymptotique, dans le cas générique.

Théorème B. *Soit $N \in \mathbb{N}, N \geqslant 5$. Il existe $\theta_1 > \theta_2 > \theta_3 > 0$ tels que pour presque tout polygone P à N côtés inscrit dans un demi-cercle et toute condition initiale $(x, \theta) \in \mathcal{O}(P)$, la trajectoire de $\mathcal{B}(P)$ partant de x dans la direction θ admet le taux de déviation suivant :*

$$\limsup_{n\to\infty} \frac{\log |p_n - nm|}{\log n} = \begin{cases} \frac{\theta_2}{\theta_1} > 0 & \text{si } N \text{ est impair} \\ \frac{\theta_2}{\theta_1} \text{ ou } \frac{\theta_3}{\theta_1} > 0 & \text{si } N \text{ est pair} \end{cases}$$

où p_n est n'importe quel point du n-ième segment de la trajectoire et $m = \lim_{n\to\infty} \frac{p_n}{n}$ est la direction asymptotique de la trajectoire.

Pour certains cas non génériques importants (ce sont les équivalents des pseudo-Anosov), je peux calculer de façon plus précise ces déviations. Dans le théorème suivant, $P(a_1, \ldots, a_N)$ désigne un polygone cyclique à N cotés où la corde sous-tendue par le côté i de P, et sur le cercle circonscrit de P, est de longueur a_i.

Théorème C. *Soit $N \in \mathbb{N}, N \geqslant 5$. Il existe $\nu \in]0, 1[$ et un sous-ensemble $\mathcal{V} \subset \Delta_{N-1}$ du simplexe de dimension $N-1$, tel que pour tout $(a_1, \ldots, a_N) \in \mathcal{V}$, il existe deux constantes C_1, C_2, un ensemble infini $\mathcal{S} \subset \mathbb{N}$, et un ouvert $\mathcal{O} \subset \mathbb{R}^2 \times \mathbb{S}^1$ tels*

que toute trajectoire dans $\mathcal{B}(P(a_1,\dots,a_N))$ de condition initiale dans $\mathcal{O}$ admet une direction asymptotique m et en dévie de la façon suivante :

$$\begin{cases} \forall n \in \mathbb{N} & |p_n - nm| < C_1 n^\nu \\ \forall n \in \mathcal{S} & |p_n - nm| > C_2 n^\nu \end{cases},$$

où p_n désigne n'importe quel point du n-ième segment de la trajectoire.

1.1.3.b. Billards de pavages bi-triangulaires

Pavons le plan $\mathbb{R}^2$ avec deux triangles δ_1 et δ_2 cocycliques, ayant un côté de même longueur (i.e. un angle de même mesure), cf. Figure 1.8. Si δ_1 « ressemble » à δ_2, on peut voir ce pavage comme une perturbation du pavage triangulaire $\mathcal{P}(\delta_1)$ présenté dans la partie 1.1.2.a. Que peut-on dire du billard dans ce pavage ? Ses trajectoires ont-elles le même comportement que celles du billard dans $\mathcal{P}(\delta_1)$? Au chapitre 4, j'introduis une classe d'EIR $\mathcal{F}$ pour étudier ce nouveau billard

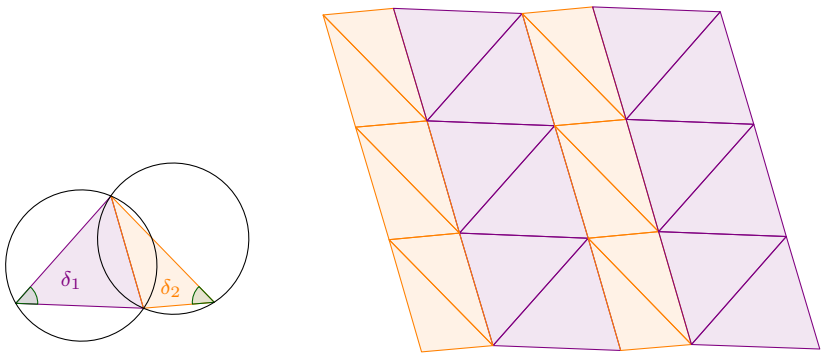

FIGURE 1.8. – Pavage bi-triangulaire du plan

de pavage. L'apport principal de ce chapitre est la définition d'une induction (cf. partie 1.2.2) sur cette classe d'EIR, bien que son étude complète ne soit pas encore terminée. La poursuite de ce travail devrait permettre d'obtenir des résultats relatifs aux trajectoires. Le but est de trouver des trajectoires vagabondes – ou alors de montrer qu'il n'en existe pas si δ et δ' ne sont pas isométriques. Les trajectoires vagabondes des billards de pavages triangulaires et quadrilatéraux cycliques sont associés à des EIR minimaux. Ce n'est *a priori* plus le cas pour les billards de pavages bi-triangulaires : un EIR minimal fournit des trajectoires vagabondes mais un EIR non minimal avec un seul cylindre de points périodiques pourrait aussi, *a priori*, fournir des trajectoires vagabondes. Je commence donc par chercher des EIR minimaux au sein de la classe $\mathcal{F}$. Si j'en trouve, c'est gagné ! S'il n'y en a pas, il faudra continuer plus précisément l'étude des EIR de $\mathcal{F}$, en particulier ceux avec peu de cylindres de points périodiques. Je montre en particulier le théorème suivant.

Théorème D. *Il existe un ensemble V_0 de sommets du diagramme de Rauzy tel que si T est un EIR de la famille $\mathcal{F}$ dont l'orbite $(\mathcal{R}^k(T))_{k\in\mathbb{N}}$ par l'induction est infinie, ne passant que par les sommets de V_0, alors les deux triangles δ et δ' sont isométriques.*

Pour conclure à propos des trajectoires de billards de pavages bi-triangulaires, il faut finir le parcours du diagramme de Rauzy et la description des EIR dont l'orbite par l'induction est infinie. Si tous correspondent au cas où δ et δ' sont isométriques, il faudra préciser la description des EIR dont l'orbite par l'induction est finie.

1.1.3.c. Billard de pavage dans le modèle du vent dans les arbres

Le modèle du vent dans les arbres est la troisième configuration dans laquelle j'ai étudié les billards de pavages. Le modèle du vent dans les arbres fut introduit au début du XXe siècle par Paul et Tatiana Ehrenfest [EE12] pour modéliser le mouvement d'une molécule légère de gaz (« le vent ») au sein d'un ensemble de molécules lourdes (« les arbres »), disposées aléatoirement dans l'espace. Lors d'une collision, la molécule légère rebondit sur la molécule lourde statique (*choc élastique*), comme dans la Figure 1.9a. Ce modèle a été largement étudié dans le plan, où les molécules lourdes sont des rectangles disposés selon un réseau, et la molécule légère est un point. En particulier, le flot d'un tel billard dans le plan privé d'obstacles rectangulaires est récurrent dans presque toute direction [AH20], le taux de diffusion est de $\frac{2}{3}$ pour les temps d'éloignement maximal [DHL14] ainsi qu'en moyenne [Bar23].

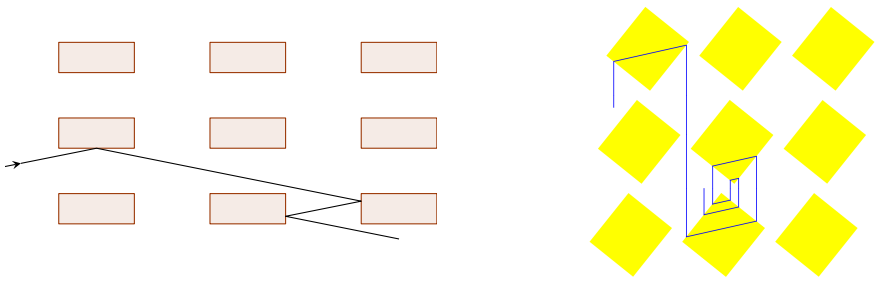

(a) Chocs élastiques (b) Une trajectoire de billard de pavage

FIGURE 1.9. – Le modèle du vent dans les arbres

Que se passe-t-il si les trajectoires ne rebondissent pas sur les obstacles mais les traversent, en étant réfractées ? J'étudie ce système au chapitre 5, cf. Figure 1.9b. Il se trouve que le résultat que je démontre (une trajectoire générique évolue dans une bande du plan) est similaire au résultat montré par Frączek et Schmoll [FS14] pour les systèmes de lentilles d'Eaton, que je présente maintenant.

Une lentille est un dispositif optique classique, dont l'indice de réfraction indique à quel point les rayons lumineux qui la traversent sont déviés. Moins connues,

certaines lentilles ont un indice de réfraction variable, ce qui a pour effet de courber la trajectoire de la lumière. Luneberg a cherché un indice variable pour une lentille sphérique au travers de laquelle l'image d'une sphère serait une sphère. Il a donné une solution simple à ce problème dans [LH64] (l'indice ne dépend que de la distance au centre). Les lentilles d'Eaton [Eat52] sont une généralisation des lentilles de Luneberg. Elles sont sphériques et leur indice de réfraction n dépend de la distance r au centre :

$$n(r) = \begin{cases} \sqrt{\frac{2R}{r} - 1} & \text{si } r_0 \leqslant r \leqslant R \\ \sqrt{\frac{2Rr_0 - r^2}{r_0^2}} & \text{si } 0 \leqslant r \leqslant r_0 \end{cases},$$

où R désigne le rayon de la lentille et $r_0 \in]0, R[$ un rayon fixé. On s'intéresse à un cas simplifié, $n(r) = \sqrt{\frac{2R}{r} - 1}$, avec une singularité au centre, cf. Figure 1.10.

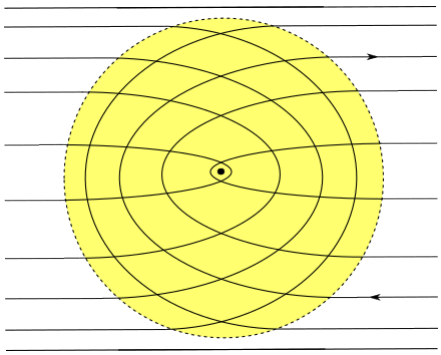

FIGURE 1.10. – Une lentille d'Eaton et des rayons lumineux déviés. Source : [FS14]

Plusieurs auteurs se sont intéressés au trajet d'un rayon lumineux au sein d'une disposition périodique de lentilles d'Eaton, cf. Figure 1.11.

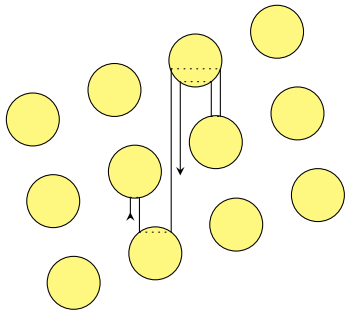

FIGURE 1.11. – Trajet d'un rayon lumineux dans un arrangement de lentilles d'Eaton

Notons $L(\Lambda, R)$ la configuration de lentilles de rayon R disposées sur les points du réseau Λ. On dit que $L(\Lambda, R)$ est admissible si les lentilles sont disjointes. On se limitera à l'étude du flot vertical (on peut toujours se ramener à cette situation en tournant l'obstacle et le réseau). Frączek et Schmoll ont montré que :

Théorème 3 (Frączek, Schmoll [FS14]). *Pour presque toute configuration admissible $L(\Lambda, R)$, il existe une direction $\theta \in \mathbb{S}^1$ et une constante $C > 0$ telles que tout rayon vertical est confiné dans une bande de largeur C et de direction θ.*

Frączek, Shi et Ulcigrai renforcent ce résultat en montrant qu'il est vrai pour n'importe quelle configuration et presque toute direction du rayon lumineux.

Théorème 4 (Frączek, Shi, Ulcigrai [FSU18]). *Soit $L(\Lambda, R)$ une configuration admissible. Pour presque toute direction initiale du rayon lumineux, il existe une direction $\theta \in \mathbb{S}^1$ et une constante $C > 0$ telles que tout rayon vertical est confiné dans une bande de largeur C et de direction θ.*

Notons maintenant $W(\Lambda, a, b, \theta)$ le système de billard de pavage dans le modèle du vent dans les arbres dont les obstacles sont de taille $a \times b$, inclinés de $\theta \in [0, \frac{\pi}{2}[$ par rapport à l'horizontale et placés sur les points du réseau Λ, cf. Figure 1.12. Je montrerai dans le chapitre 5 que :

Théorème E. *Pour presque tout réseau Λ, pour presque tout $a, b > 0$, pour presque toute inclinaison θ des obstacles rectangulaires de taille $a \times b$, il existe une constante C telle que toute trajectoire de direction verticale dans $W(\Lambda, a, b, \theta)$ est piégée dans une bande du plan de largeur C.*

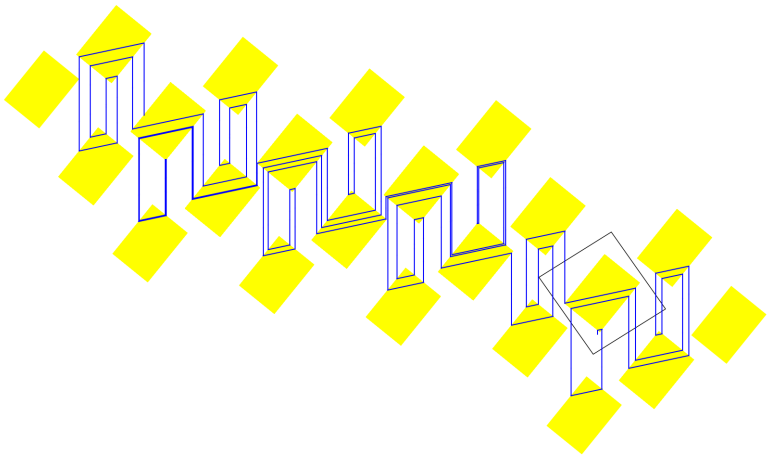

FIGURE 1.12. – Exemple de trajectoire dans le système $W(\Lambda, 0.7, 0.5, \frac{17\pi}{60})$
Le parallélogramme tracé en gris correspond à un domaine fondamental de
$\Lambda = \{(0.8, 0.5)\mathbb{Z} + (-0.6, 0.85)\mathbb{Z}\}$

1.2. Objets mathématiques associés

Les questions que nous nous posons font intervenir plusieurs objets – liés entre eux bien-sûr. Ainsi, nous rencontrerons des *échanges d'intervalles* avec ou sans

retournements (abrégé en EI ou EIR), des *involutions linéaires* (IL), des *surfaces de translation* (ST) et *surfaces de demi-translation* (SDT). Cette section les présente brièvement.

1.2.1. Aperçu historique et motivations

De façon informelle, un échange d'intervalles est une application définie sur un intervalle dans lui-même, qui coupe l'intervalle en un nombre fini de morceaux et les réordonne. L'histoire des échanges d'intervalles commence avec la fonction de premier retour d'un flot, définie par Poincaré au début du XXe siècle pour étudier des systèmes dynamiques. S'il n'étudie pas directement les échanges d'intervalles, son travail ouvre la voie à leur étude. Il s'intéresse notamment aux difféomorphismes du cercle et montre que tout difféomorphisme du cercle est semi-conjugué à une rotation [Poi90]. Ainsi, les rotations du cercle sont des objets simples et pourtant centraux dans l'étude dynamique d'applications plus complexes. Nous verrons au chapitre suivant que les échanges d'intervalles généralisent les rotations du cercle.

Dans les années 60, les mathématiciens russes s'intéressent aux EI en termes de formes différentielles. La première formalisation écrite des échanges d'intervalles (à trois intervalles) date de 1967, par Katok et Stepin [KS67]. Ils fournissent des exemples de systèmes dynamiques minimaux mais non uniquement ergodiques : Sataev [Sat76] montre qu'il existe des EI minimaux admettant g mesures ergodiques, et ce pour tout entier g. Keynes-Newton [KN76], Keane [Kea77] et ensuite Coffey [Cof88] ont donné d'autres exemples d'EI minimaux non uniquement ergodiques. Veech le fait dans [Vee82], sans utiliser le terme d'échanges d'intervalles. Plus tard, les EI ont notamment suscité de l'intérêt car ils interviennent dans l'étude des billards polygonaux à angles rationnels et dans celle du flot sur une surface plate.

Une *surface de translation* est définie de façon équivalente comme :

(1) un polygone dont on a identifié les côtés (parallèles et de même longueur) par des translations ;

(2) une surface topologique M compacte orientable avec un nombre fini de singularités Σ d'angles coniques multiples de 2π, et telle que les changements de carte d'un atlas maximal $M \setminus \Sigma \to \mathbb{C}$ sont des translations ;

(3) une surface de Riemann compacte, munie d'une 1-forme holomorphe.

Une surface de translation est naturellement munie d'une structure plate. Le feuilletage obtenu par le flot géodésique est orientable et l'application de premier retour sur un intervalle transverse au flot est un échange d'intervalles. Inversement, on peut associer à un échange d'intervalles une famille de surfaces de translation, appelées *suspensions* de l'EI, telles que l'application de premier retour sur un intervalle bien choisi est l'EI en question.

Une *surface de demi-translation* est la généralisation d'une surface de translation : l'identification des côtés du polygone peut se faire par translation ou rotation d'un

demi-tour ; les angles coniques sont multiples de π (et pas nécessairement 2π) ; la 1-forme sur la surface de Riemann peut avoir des pôles simples. On obtient une surface orientable, mais dont le feuilletage obtenu par le flot géodésique est non orientable : il admet des feuilles singulières. Danthony et Nogueira [DN90] introduisent les *involutions linéaires* comme une généralisation des échanges d'intervalles. En effet, elles constituent les applications de premier retour du flot géodésique d'une surface de demi-translation [1]. De même que pour les EI, on peut construire les suspensions d'une involution linéaire. Ces suspensions sont des surfaces de demi-translation.

Enfin, on peut généraliser les échanges d'intervalles d'une autre façon : on autorise l'application à retourner certains morceaux. On appelle ces fonctions des *échanges d'intervalles avec retournements*. Dans l'article [Nog89], Nogueira montre que, à l'opposé du comportement des échanges d'intervalles sans retournements, les échanges d'intervalles *avec* retournements ont presque tous une orbite périodique. A la fin de l'article, il propose d'étudier les *billards avec retournements* dans des polygones rationnels. Ces objets sont aux billards dans les polygones rationnels ce que les EIR sont aux EI. Un billard avec retournements dans lequel tous les côtés sont retournés correspond à un billard de pavage. Certains EIR admettent aussi des suspensions. Ce sont alors des surfaces non orientables admettant un feuilletage orientable.

Le tableau suivant résume les liens entre ces différents objets.

	EI	IL	EIR
feuilletage	orientable	non orientable	orientable
surface	orientable (ST)	orientable (SDT)	non orientable

À un billard dans un pavage localement pliable, on peut associer une surface appelée *hélicoïde de Dynnikov* [Par21]. C'est une surface orientable, plongée dans $\mathbb{R}^3$ et périodique dans les trois directions. Une trajectoire du billard de pavage correspond à l'intersection entre cette surface et un plan horizontal. Cette construction relie élégamment notre problème de billard à un problème de topologie posé par Novikov [Nov82], et motivé par des questions de physique concernant le déplacement des électrons dans un métal soumis à un faible champ magnétique. Le problème est le suivant : soit M une surface plongée dans $\mathbb{R}^3$, et invariante par un réseau de $\mathbb{R}^3$. Soit $\mathcal{P}$ un plan affine de $\mathbb{R}^3$. Que peut-on dire de l'intersection $M \cap \mathcal{P}$? Zorich [Zor84], Dynnikov [Dyn92 ; Dyn97 ; Dyn99] et De Leo [Leo03 ; Leo05 ; Leo06 ; DD09] ont fait des avancées dans ce problème. Pour plus de détails, le lecteur intéressé pourra aussi consulter la partie 2.2 du survol de Zorich [Zor06], et l'article [DHMPS] à venir. Je n'aborderai pas davantage cet aspect du problème dans la suite de ma thèse.

1. Plus précisément, c'est l'application de premier retour sur $\mathcal{I}$ du flot géodésique dans le fibré unitaire tangent $T^1(S)$ de la surface, où $\mathcal{I} = I \times \{+\frac{\pi}{2}\} \cup I \times \{-\frac{\pi}{2}\} \subset T^1S$ et $I \subset S$ est transverse au flot.

1.2.2. De l'importance de l'induction

Pour étudier un certain système dynamique $(\mathtt{X}, \Phi, \mu)$ – par exemple le flot géodésique sur une surface de translation S – il est très souvent fructueux de considérer un ensemble $\mathcal{X}$ plus grand qui le contient – par exemple l'ensemble [2] des surfaces de translation, chacune munie de leur flot géodésique – puis d'étudier un *autre* système dynamique sur cet ensemble $\mathcal{X}$. Dans plusieurs contextes, les propriétés du système dynamique sur $\mathcal{X}$ nous donnent des informations sur le système dynamique de départ. On appelle ce procédé une *renormalisation*, ou une *induction* selon le contexte. Le texte d'Avila [Avi10] donne un aperçu de plusieurs utilisations de la renormalisation.

Détaillons l'exemple des surfaces et de leur flot géodésique. On souhaite étudier le flot géodésique d'une surface de translation S, en particulier comprendre sa trajectoire γ_t entre les temps 0 et t grand. On transforme la surface S en une surface $g_T(S)$, qui constitue le futur de S par le flot géodésique g_T dans l'espace des modules. La transformation g_T est aussi appelée *flot de Teichmüller*. Via la matrice suivante, elle déforme les polygones qui permettent de définir S :

$$g_T = \begin{pmatrix} e^T & 0 \\ 0 & e^{-T} \end{pmatrix}.$$

Dans la surface $g_T(S)$ la trajectoire γ_t est contractée par un facteur e^{-T}. Si la surface $g_T(S)$ est proche de la surface S dans l'espace des modules, on a transformé S en une surface $g_T(S)$ qui lui ressemble, et la trajectoire γ_t en une trajectoire beaucoup plus courte, donc plus simple à comprendre. *Regarder le futur de la surface S permet d'avancer plus vite dans la trajectoire γ_t.* Citons le critère de Masur, qui illustre l'intérêt de ce paradigme.

Théorème 5 (Critère de Masur). *Soit S une surface de translation. Si $g_T(S)$ ne diverge [3] pas dans l'espace des modules, alors le flot géodésique sur S (dans la direction verticale) est uniquement ergodique.*

Pour étudier un échange d'intervalles T, on *induit* T sur $J \subset I$ un sous intervalle (bien choisi) de son domaine de définition I. Cela signifie que l'on considère l'application de premier retour de T sur J. L'orbite d'un point $x \in J$ par l'application induite $\mathcal{R}(T)$ correspond à une *accélération* de l'orbite $(T^k(x))_{k\in\mathbb{N}}$ de x par T : on a enlevé les points de l'orbite qui n'appartiennent pas à J, c'est-à-dire

$$\{(\mathcal{R}(T))^k(x) \,|\, k \in \mathbb{N}\} = \{(T)^k(x) \,|\, k \in \mathbb{N},\, T^k(x) \notin J\}.$$

Toute la difficulté pour définir une *bonne* induction réside dans le fait que l'on

2. c'est-à-dire l'espace des modules

3. la topologie dont on munit l'espace des modules provient de la topologie naturelle de $\mathbb{R}^n$: deux surfaces de translation sont *proches* si elles admettent une présentation par deux polygones P_1 et P_2 tels que le k-ième sommet de P_2 est dans un petit voisinage du k-ième sommet de P_1.

souhaite obtenir un EI $\mathcal{R}(T)$ de même « type » que celui de départ. Rauzy a défini une induction $\mathcal{R}$ telle que T et $\mathcal{R}(T)$ ont le même nombre d'intervalles de continuité. Grâce à cette induction, Keane [Kea75] a démontré que presque tout EI (relativement à la mesure de Lebesgue) est minimal, puis Masur [Mas82] et Veech [Vee82], ont montré que presque tout EI est uniquement ergodique. À l'inverse, Nogueira [Nog89] en adaptant l'induction de Rauzy pour le cas des EIR, a démontré que presque tout EIR admet une orbite périodique.

Pour T un EI fixé, et f une fonction définie sur le domaine $\mathcal{D}$ de T, nous nous intéresserons aux *sommes de Birkhoff* en $x \in \mathcal{D}$:

$$\frac{1}{n} S_n f(x) = \sum_{k=0}^{n-1} f(T^k(x)).$$

Si T est ergodique (par rapport à une mesure μ sur $\mathcal{D}$), et si f est intégrable sur $\mathcal{D}$ par rapport à μ, le théorème ergodique, dû à Birkhoff [Bir31], établit la convergence suivante

$$\mu - \text{p.p.t.} x \in \mathcal{D}, \quad S_n f(x) \underset{n\to\infty}{\longrightarrow} \int_{\mathcal{D}} f \mathrm{d}\mu.$$

Peut-on dire quelque chose du second terme du développement asymptotique $S_n f(x) \underset{n\to\infty}{=} n \int_{\mathcal{D}} f \mathrm{d}\mu + o(n)$? En utilisant l'induction de Rauzy, Zorich répond à cette question dans le cas où T est un EI et $f = \chi_I$ est la fonction indicatrice d'un intervalle de continuité I de T.

Théorème 6 (Zorich [Zor97]). *Soit T un EI sur $\mathcal{D}$, et $\mathcal{I}$ l'ensemble de ses intervalles de continuité. Alors :*

$$\max_{\substack{x\in\mathcal{D}\\ I\in\mathcal{I}}} \limsup_{n\to\infty} \frac{\log |S_n \chi_I(x) - \lambda_I n|}{\log n} = \frac{\theta_2}{\theta_1} \in (0,1)$$

où λ_I est la longueur de l'intervalle I, χ_I la fonction indicatrice de I et θ_1 et θ_2 sont des exposants de Lyapounov, qui ne dépendent que de la permutation $\pi(T)$ sous-jacente à T.

1.2.3. Dans cette thèse

L'induction est au cœur de mon travail.

Dans le chapitre 3, elle est essentielle bien qu'en coulisse : j'utilise un résultat prouvé par Zorich [Zor99] avec l'induction de Rauzy. La difficulté de ce chapitre se situe ailleurs : il s'agit de montrer que l'on peut effectivement appliquer ce résultat ! Pour cela, il faut montrer qu'un certain vecteur $H(e)$, dépendant d'un paramètre e, n'est pas dans un sous-espace vectoriel E fixé par le théorème ergodique multiplicatif d'Oseledets [Ose68]. Je donne une expression du vecteur H mais on ne connaît pas, en général, d'équation définissant le sous-espace vectoriel E. J'ai donc montré que *pour tout* sous-espace vectoriel de même dimension que E, *pour toute valeur* du

paramètre e *sauf un nombre fini*, le vecteur $H(e)$ n'est pas dans E.

L'idée de renormalisation a la vedette dans le chapitre 4, où je définis une nouvelle induction, adaptée au cas des billards de pavages bi-triangulaires. Cette induction est inspirée de l'induction définie par Arnoux–Rauzy [AR91] pour étudier la famille d'EI qui porte leurs noms, et de son adaptation au cas des billards triangulaires [Par19]. La description du diagramme de Rauzy associé à l'induction définie au chapitre 4 est encore partielle. Avec ce travail encore en cours, j'espère classifier les différents comportements des trajectoires de billards de pavages bi-triangulaires.

Dans le chapitre 5, l'élément principal est une surface de demi-translation associée au système de billard de pavage dans le wind-tree. Je transforme la question sur les trajectoires (en lignes brisées) du billard de pavage dans le modèle du vent dans les arbres en une question sur les géodésiques de cette surface de demi-translation. L'induction reste aussi sur le devant de la scène : je l'utilise pour comprendre le comportement des trajectoires en temps long, grâce à des techniques adaptées du travail de Forni [For02] et de Delecroix–Hubert–Lelièvre [DHL14]. À l'instar de l'amélioration apportée par Frączek–Shi–Ulcigrai [FSU18] au résultat de Frączek–Schmoll [FS14], la prochaine étape de mon travail sera de montrer que *pour tout* arrangement d'obstacles, les trajectoires de billard de pavage dans le modèle du vent dans les arbres sont confinées dans une bande du plan, *pour presque toute* direction initiale.

2. Background

2.1. Interval exchange transformations

2.1.1. Definition

Definition 2.1 (IET). *An* interval exchange transformation *(IET) on* $[0;1)$ *is a bijection from* $[0;1)$ *onto itself which is everywhere continuous on the right, continuous except on a finite number of points and differentiable where it is continuous with differential equal to 1.*

One denotes by $\Delta(T)$ *the set of discontinuities of* T*.*

One defines analogously an IET on another interval, a circle or a union of intervals and circles. Roughly speaking, an IET on $[0;1)$ cuts the interval $[0;1)$ into finitely many intervals and shuffles them. Let us introduce some examples.

Example 2.2. *Let* $\theta \in]0;1)$ *and define* R *by:*

$$\forall x \in [0;1),\ R(x) = \begin{cases} x+1-\theta & \text{if } 0 \leqslant x < \theta \\ x-\theta & \text{if } \theta \leqslant x < 1 \end{cases}.$$

Then R *is an IET. One can think of it as the rotation of angle* $1-\theta$ *on the circle* $\mathbb{R}/\mathbb{Z}$*. See Figure 2.1.*

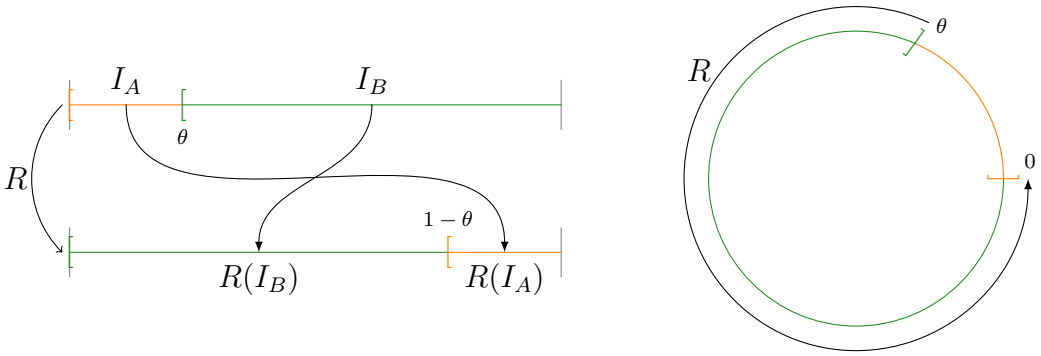

Figure 2.1. – Example of an IET which is a rotation

We can also see it as the first recurrence map of the flow of angle $\frac{1}{1-\theta}$ *on the two dimensional torus. See Figure 2.2.*

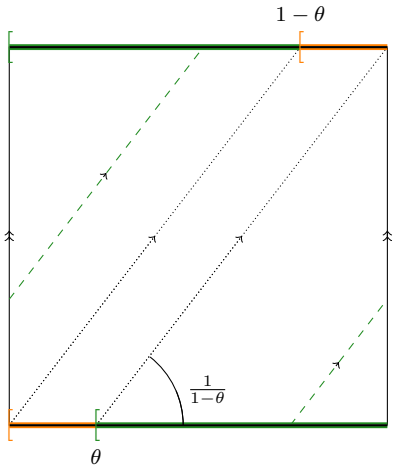

Figure 2.2. – The IET R seen as a first recurrence map on the torus

Example 2.3. *Let T defined by:*

$$\forall x \in [0;1),\ T(x) = \begin{cases} x + \frac{4}{5} & \text{if } x \in A = \left[0; \frac{2}{10}\right) \\ x + \frac{1}{2} & \text{if } x \in B = \left[\frac{2}{10}; \frac{3}{10}\right) \\ x + \frac{1}{10} & \text{if } x \in C = \left[\frac{3}{10}; \frac{6}{10}\right) \\ x - \frac{3}{5} & \text{if } x \in D = \left[\frac{6}{10}; 1\right) \end{cases}.$$

A, B, C and D are the intervals of continuity of T. Figure 2.3 illustrates T and the composition of T with the rotation R.

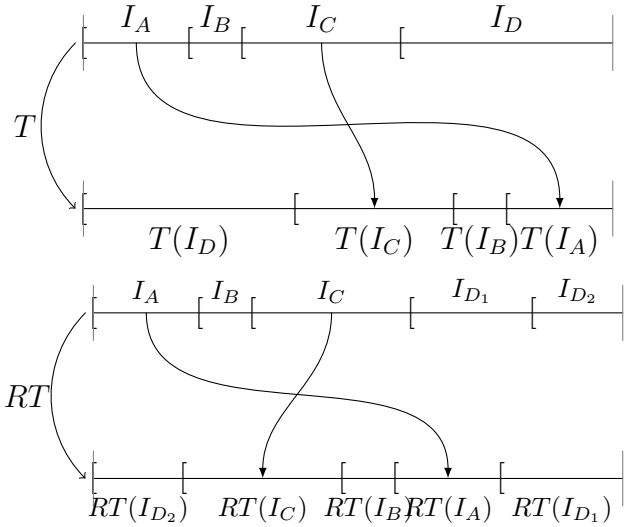

Figure 2.3. – Composition of IETs

Proposition 2.4. *The set of IETs on a domain $\mathcal{D}$, endowed with the law of composition, is a group.*

2.1.2. Description of an IET

We use the formalism introduced by Marmi, Moussa and Yoccoz [MMY05] to describe IETs. Let T be an IET on $[0;1)$. Let $\mathcal{A}$ be a finite alphabet (of cardinal n) and $[0;1) = \bigcup_{a\in\mathcal{A}} I_a$ be a partition of $[0;1)$ such that T is continuous on each interval I_a. For every $a \in \mathcal{A}$, let $\lambda_a = |I_a|$ be the length of I_a. Let $\pi_0 : \mathcal{A} \to \{1, ..., n\}$ be the one-to-one map sending a to i if and only if a is the letter of the i-th interval (from the left to the right) of $[0;1)$ with regard to the partition $[0;1) = \bigcup_{a\in\mathcal{A}} I_a$. Let $\pi_1 : \mathcal{A} \to \{1, ..., n\}$ be the one-to-one map sending a to i if and only if a is the letter of the i-th interval (from the left to the right) of $[0;1)$ with regard to the partition $[0;1) = \bigcup_{a\in\mathcal{A}} T(I_a)$. Then $\pi = \pi_1 \circ \pi_0^{-1} \in \mathfrak{S}_n$ describes the action of T on the set $(I_a)_{a\in\mathcal{A}}$.

We represent π by the table $\begin{pmatrix} \pi_0^{-1}(1) & \pi_0^{-1}(2) & ... & \pi_0^{-1}(n) \\ \pi_1^{-1}(1) & \pi_1^{-1}(2) & ... & \pi_1^{-1}(n) \end{pmatrix}$.

Remark 2.5. *Given a permutation π, there are many pairs (π_0, π_1) such that $\pi = \pi_1 \circ \pi_0^{-1}$, each one corresponding to a different labeling of the intervals. In most examples in this thesis, we take the Latin alphabet for $\mathcal{A}$ and π_0 such that $\pi_0(A) = 1$, $\pi_0(B) = 2$, $\pi_0(C) = 3$, etc. We sometimes denote the intervals by their label in bold:* $\mathbf{A}, \mathbf{B}, \mathbf{C}$*,etc.*

Remark 2.6. *If there exists $i \in \{1, ..., n\}$ such that $\pi(i+1) = \pi(i) + 1$, then T is continuous on the union $I_{\pi_0^{-1}(i)} \cup I_{\pi_0^{-1}(i+1)}$ of the i-th and the $(i+1)$-th intervals. The converse also holds. In other words, the intervals $(I_a)_{a\in\mathcal{A}}$ are exactly the intervals of continuity of T if and only if $\forall i \in [1; n[,\ \pi(i+1) \neq \pi(i) + 1$. In this case we call π the* underlying permutation *of T.*

Proposition 2.7. *An IET T is defined by the set $\lambda(T)$ of the lengths of its intervals of continuity, and the underlying permutation $\pi(T)$.*

Example 2.8. *For the IET T of the previous example, we have*

$$\lambda(T) = \left(\lambda_A = \frac{2}{10}, \lambda_B = \frac{1}{10}, \lambda_C = \frac{3}{10}, \lambda_D = \frac{4}{10}\right)$$

and the underlying permutation is $\pi(T) = \begin{pmatrix} A & B & C & D \\ D & C & B & A \end{pmatrix}$.

Remark 2.9. *Given $\lambda(T) = (\lambda_a(T))_{a\in\mathcal{A}}$ and $\pi(T) = \pi_1 \circ \pi_0^{-1}$, one easily computes $\lambda(T^{-1}) = \lambda(T)$ and $\pi(T^{-1}) = \pi_0 \circ \pi_1^{-1}$. In our example, it gives* $\pi(T^{-1}) = \begin{pmatrix} D & C & B & A \\ A & B & C & D \end{pmatrix}$.

See Figure 2.4. If S is another IET, the data $\lambda(S \circ T)$ and $\pi(S \circ T)$ are less straightforward to compute.

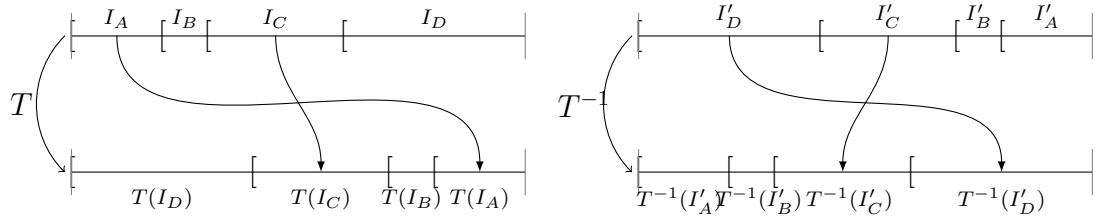

Figure 2.4. – Example of an IET and its inverse

There are other ways to describe T: one can replace the data of the lengths of the intervals of continuity by the data of the points of discontinuity, or replace the data of the underlying permutation by the data of the translation lengths.

The relation between the lengths and the translations on each subinterval is the following:

$$\forall i \in \{1, ..., n\},\ t_i = -\sum_{j=1}^{i-1} l_j + \sum_{j=i}^{\pi(i)-1} l_{\pi^{-1}(j)}.$$

If we denote by $0 < b_1 < \cdots < b_{n-1} < 1$ the set of discontinuities of T, and $b_0 = 0, b_n = 1$, then

$$\forall i \in \{1, ..., n\},\ \forall x \in [b_{i-1}; b_i[,\ T(x) = x + t_i.$$

Definition 2.10 (irreducible permutation). *A permutation $\sigma \in \mathfrak{S}_n$ is said to be* irreducible *if for all $k < n$, the set $\{1, ..., k\}$ is not σ-invariant.*

If the underlying permutation π of an IET T is reducible, say $\{1, ..., k\}$ is π-invariant, then T preserves $I_1 \cup ... \cup I_k$ (hence $I_{k+1} \cup ... \cup I_n$ too). We can study the dynamics of both restrictions instead of studying the dynamics of T.

2.1.3. Topology and measure

Fix a combinatorial data π. The set $\mathrm{IET}_\pi([0;1))$ of IETs on $[0,1)$ with combinatorial data π is endowed with the following distance:

$$\begin{array}{rccc} d: & \mathrm{IET}_\pi([0;1)) \times \mathrm{IET}_\pi([0;1)) & \longrightarrow & \mathbb{R}_+ \\ & (S,T) & \longmapsto & ||\lambda(S) - \lambda(T)|| \end{array}.$$

The set IET_π is a simplex of dimension $n-1$ (with n such that $\pi_0, \pi_1 \in \mathfrak{S}_n$).

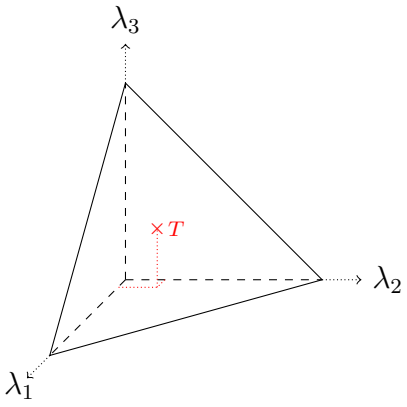

Figure 2.5. – The simplex representing IET_π and $T = (\pi, \lambda(T))$ from examples 2.3 and 2.8

2.1.4. The Rauzy induction

The Rauzy induction $\mathfrak{R}(T)$ of an IET T defined on I is the first return map of T to a well chosen subinterval $J \subset I$. Let T be an IET on an interval I, with permutation $\pi = \begin{pmatrix} \alpha_1^0 & \alpha_2^0 & \dots & \alpha_d^0 \\ \alpha_1^1 & \alpha_2^1 & \dots & \alpha_d^1 \end{pmatrix}$ and lengths $\lambda = (\lambda_{\alpha_1^0}, ..., \lambda_{\alpha_d^0})$. We denote by $\alpha(\epsilon) = \alpha_d^\epsilon$ the label of the last subinterval of the top ($\epsilon = 0$) or bottom ($\epsilon = 1$) interval. The Rauzy-Veech induction of T is an IET, denoted here by $\mathfrak{R}(T)$, defined on $J \subset I$, where

$$J = \begin{cases} I \setminus I_{\alpha(1)} & \text{if } \lambda_{\alpha(0)} > \lambda_{\alpha(1)} \qquad \text{case (top)} \\ I \setminus I_{\alpha(0)} & \text{if } \lambda_{\alpha(0)} < \lambda_{\alpha(1)} \qquad \text{case (bot)} \end{cases}$$

and $\mathfrak{R}(T)$ is the first return map of T on J. The smallest interval between $I_{\alpha(0)}$ and $I_{\alpha(1)}$ is called the loser, the biggest is called the winner. The length of the interval on which $\mathfrak{R}^k(T)$ is defined is shrinking as k grows up. To avoid this problem, we consider the renormalized Rauzy induction $\mathcal{R}$ that consists to remormalise J to the size of I. See Figure 2.6.

Following Veech, Zorich [Zor96] showed that one can speed up the Rauzy induction so that the induction is ergodic with respect to an absolutely continuous invariant probability measure μ_Z.

2.1.5. The Rokhlin towers

When we cut off $I' = I \setminus J$ from I, we can think of it being stacked over its preimage by T. The choice of J ensures that the subinterval on which I' is being stacked corresponds exactly to an interval of continuity of $\mathfrak{R}(T)$. We can do that at each iteration of Rauzy induction. We obtain a stack of subintervals of I, that

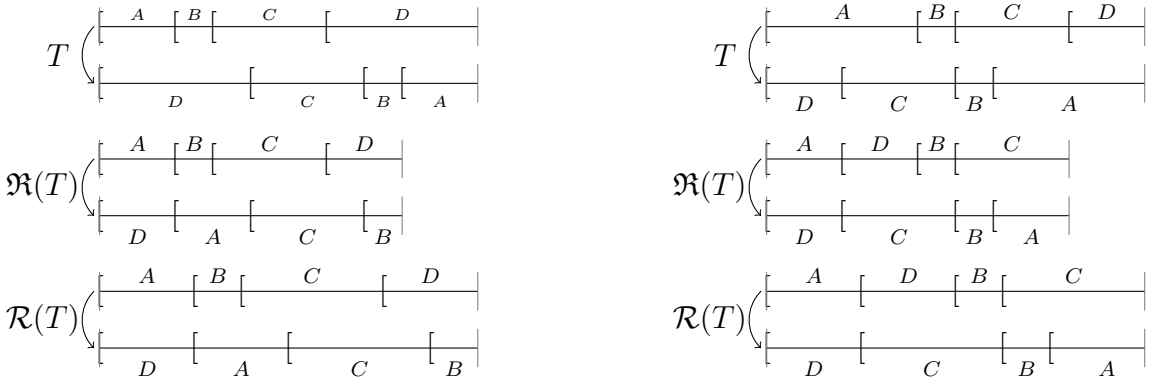

(a) Rauzy induction in case (top)

(b) Rauzy induction in case (bot)

Figure 2.6. – Rauzy induction

we call a *Rokhlin tower*. Let $J^{(k)}$ be the subinterval on which $\mathfrak{R}^k(T)$ is defined and $x \in J^{(k)}$. The subintervals stacked over x allow to keep track of the orbit of x under T. Their number corresponds to the time of first return of x to $J^{(k)}$. See Figure 2.7. We call *towers of order* l the ones obtained when applying l times the induction [1].

2.1.6. The Kontsevich–Zorich cocycle (combinatorial point of view)

We denote by $A_{i,j}^{(l)}$ the number of subintervals stacked over the interval of continuity $I_j^{(l)}$ of $\mathfrak{R}^l(T)$ that were initially in the interval of continuity I_i of T. It corresponds to the number of times that the orbit of $x \in I_j^{(l)}$ lies in the *old* interval I_i before first return to $I_j^{(l)}$. This number does not depend on $x \in I_j^{(l)}$ thanks to the choice of subintervals on which we induce. We denote by $A_T = \left(A_{i,j}^{(1)}\right)_{1 \leqslant i,j \leqslant d}$ the matrix whose entries are these numbers. It is a transvection. This defines a cocycle $T \in \mathrm{IET}(I) \mapsto A_T \in \mathrm{SL}_d(\mathbb{R})$.

Analogously we denote by B the cocycle associated to Zorich induction. We underline the fact that the time related to cocycle B is not the same as the one related to cycle A, there is a speeding up factor. Moreover there is an exponential factor between the time of cocycle B and the time of the iteration of T, see Lemma 4 in [Zor99].

2.1.7. The Rauzy diagram

The Rauzy induction acts both on the vector lengths of the IET and on the underlying permutation of the IET. The Rauzy diagram gives the action of the

1. Note that this notion depends on the induction we apply, the Rauzy or Zorich one.

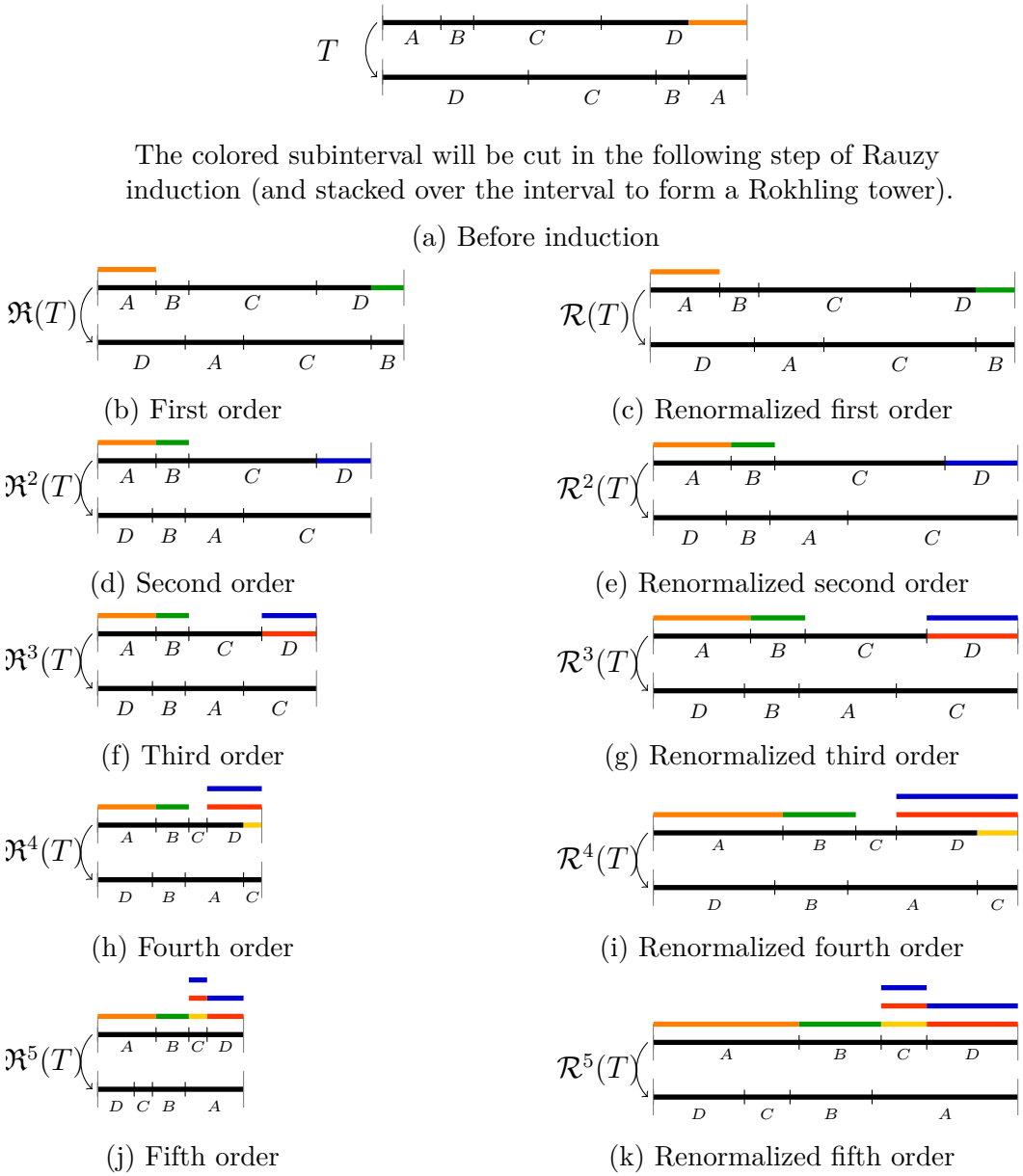

The colored subinterval will be cut in the following step of Rauzy induction (and stacked over the interval to form a Rokhling tower).

(a) Before induction

(b) First order

(c) Renormalized first order

(d) Second order

(e) Renormalized second order

(f) Third order

(g) Renormalized third order

(h) Fourth order

(i) Renormalized fourth order

(j) Fifth order

(k) Renormalized fifth order

Figure 2.7. – Rokhlin towers of orders 1 to 5 for the Rauzy induction of an IET

induction on the combinatorial data. It is a graph whose vertices are combinatorial data and edges are steps of induction, labeled by the case (top or bottom). We call the *Rauzy class of the permutation* π the permutations in the orbit of π by the Rauzy induction. The Rauzy class of a permutation π consists in the set of vertices of the Rauzy diagram that belong to the connected component of the permutation π.

2.1.8. Associated substitution

Definition 2.11 (Symbolic coding). *Let T be an IET on an interval I, with n intervals of continuity $I_1, I_2, ...I_n$. Let $\mathcal{A} = \{1, 2, ..., n\}$. The* symbolic coding *of $x \in I$ under T is the infinite word $\omega \in \mathcal{A}^*$ such that for every $k \in \mathbb{N}, T^k(x) \in I_{\omega_k}$.*

Remark 2.12. *When an orbit hits a boundary point of an interval of continuity, then its symbolic coding is not defined.*

Definition 2.13 (Substitution). *Let $\mathcal{A}$ be an alphabet. A* substitution *is a morphism on the set of (finite or infinite) words $\mathcal{A}^*$ to itself.*

Remark 2.14. *It is enough to define a substitution on every single letter of the alphabet.*

Definition 2.15 (Primitive substitution). *A* primitive *substitution on an alphabet $\mathcal{A}$ is a substitution such that there exists $k \in \mathbb{N}$ such that for every letter $a \in \mathcal{A}$, the word $\sigma^k(a)$ contains all letters of $\mathcal{A}$.*

Definition 2.16 (Matrix of a substitution). *Let σ be a substitution on a finite alphabet. We call* matrix of σ *the matrix of the abelianisation of the action of σ on $\mathcal{A}^*$.*

Example 2.17. *The matrix of the substitution* $\sigma : \begin{cases} a & \mapsto & ab \\ b & & bbcb \\ c & & aaa \end{cases}$ *is*

$$M = \begin{pmatrix} 1 & 0 & 3 \\ 1 & 3 & 0 \\ 0 & 1 & 0 \end{pmatrix}.$$

Proposition 2.18. *A substitution is primitive if and only if its matrix is.*

Lemma 2.19. *Let σ be a primitive substitution. There exist $k_0, L \in \mathbb{N}$ such that for every $u \in \mathcal{A}$ and $k \geqslant k_0$, every subword of $\sigma^k(u)$ of length at least L contains all letters of the alphabet $\mathcal{A}$.*

For a proof of this lemma, see [Que10b].

Definition 2.20 (Substitution associated to the Rauzy induction). *At each step of renormalized Rauzy induction, we associate a substitution ζ over the alphabet $\mathcal{A}$ of labels of intervals such that:*

$$\forall a \in \mathcal{A} \setminus \{l\}, \zeta(a) = a \qquad \text{and} \qquad \zeta(l) = \begin{cases} lw & \text{in top case} \\ wl & \text{in bottom case} \end{cases}$$

where l and w denote respectively the loser and winner intervals.

This substitution describes the induction in the following way. Denote by $I_\alpha^{(1)}$ the interval of continuity of $\mathfrak{R}(T)$ labeled with the letter $\alpha \in \mathcal{A}$. Let x be a point in the interval $J^{(1)}$ on which we induce. Let α be the label of the interval of continuity in which x lies: $x \in I_\alpha^{(1)}$. Then, $\sigma(\alpha)$ gives the first letters of the symbolic coding of x. If we consider many iterations of the Rauzy induction, we get many substitutions and their product gives more letters of the symbolic coding of x.

For example, the substitutions associated to the examples of Figure 2.7 are:

$$\sigma_1 : \begin{cases} a & ad \\ b & b \\ c & c \\ d & d \end{cases} \quad \sigma_2 : \begin{cases} a & a \\ b & bd \\ c & c \\ d & d \end{cases} \quad \sigma_3 = \sigma_4 : \begin{cases} a & a \\ b & b \\ c & c \\ d & cd \end{cases} \quad \sigma_5 : \begin{cases} a & a \\ b & b \\ c & cd \\ d & d \end{cases} .$$

The composition of the substitutions gives the substitution associated to $\mathfrak{R}^5$:

$$\sigma = \sigma_5 \circ \sigma_4 \circ \sigma_3 \circ \sigma_2 \circ \sigma_1 : \begin{cases} a & ad \\ b & bd \\ c & cccd \\ d & ccd \end{cases} .$$

Its associated matrix is

$$M_\sigma = \begin{pmatrix} 1 & 0 & 0 & 0 \\ 0 & 1 & 0 & 0 \\ 0 & 0 & 3 & 2 \\ 1 & 1 & 1 & 1 \end{pmatrix}.$$

Denote by $\sigma^{(k)} = \sigma_k \circ \dots \sigma_1$ the substitution corresponding to the path of length k followed by T under the induction. The matrix M_σ gives information on the lengths of the interval of continuity of $\mathfrak{R}^k(T)$. If λ is the lengths vector of T and $\lambda^{(k)}$ that of $\mathfrak{R}^k(T)$, then

$$\lambda = {}^t M_\sigma \lambda^{(k)}.$$

See [Del16] for more details about the substitution associated to the Rauzy induction. We mention also that Definition 8 of [AI01] proposes a more general framework. For more details about the matrix of a substitution we refer to [Que10a].

2.1.9. Decomposition of the symbolic coding

Proposition 2.21. *Let T be a self-similar IET on an interval I. Let q be the minimal integer such that $\mathcal{R}^q(T) = T$. Let σ be the substitution associated to $\mathfrak{R}^q$ applied to T. We define $K = \max_{a \in \mathcal{A}} |\sigma(a)|$. Let $x \in I$. Let $\overline{x} = x_0 x_1 x_2 \dots$ be the symbolic coding of x under T. Let $n \in \mathbb{N}$. We can decompose the prefix of $\overline{x}$ of length n as*

$$\overline{x}_n = s_0 \sigma(s_1) \dots \sigma^{l-1}(s_{l-1}) \sigma^l(m_l) \sigma^{l-1}(p_{l-1}) \dots \sigma(p_1) p_0$$

where each word s_i or p_i is of length at most $K-1$ and the length of m_l is between 1 and $2K-2$.

Remark 2.22. *In this decomposition, the integer l is as big as possible, the words s_i (resp. p_i) are suffixes (resp. prefixes) of words of $\sigma(\mathcal{A})$.*

For a proof of Proposition 2.21, see Lemma 5.5 in [Que10a].

In terms of Rokhlin towers, Proposition 2.21 means that we consider towers of order l. If the point x (whose symbolic coding begins with $\overline{x}_n$) belongs to the interval on which we induce, then all s_i are empty words. The orbit of x under T can be read on the Rokhlin towers, starting at the bottom of one tower. If not, it starts in the middle of some tower, goes up until the top of this tower and then returns at the bottom of another (or maybe the same) tower (of order l). The length of the word m_l corresponds to the number (with multiplicity) of towers totally wandered by the first n steps of the orbit of x. If the orbit stops on the top of a tower, all p_i are empty words. Otherwise, the orbit continues to wander a part of a tower of rank l, and this part is the concatenation of $|p_{l-1}|$ towers of rank $l-1$, $|p_{l-2}|$ towers of rank $l-2$, ..., $|p_1|$ towers of rank 1 and finally $|p_0|$ towers of rank 0 (i.e. non-towers). See Figure 2.8

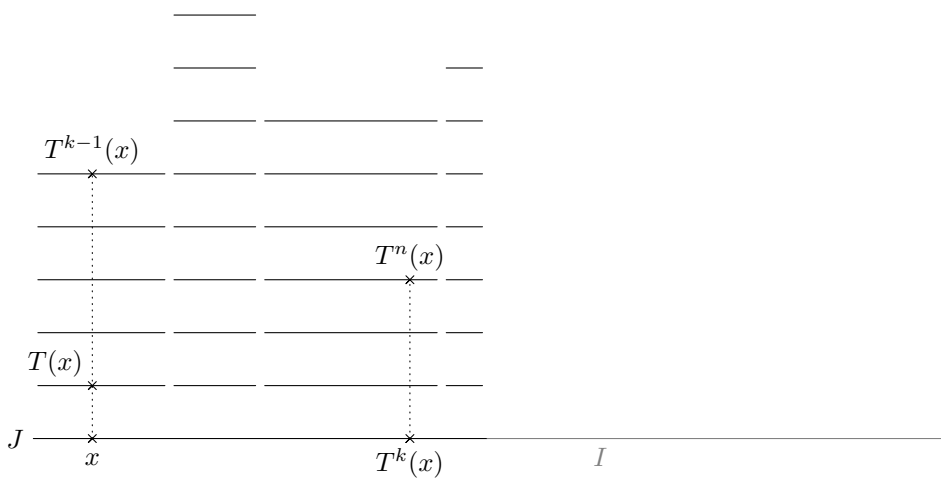

Figure 2.8. – The link between the orbit of x and the Rokhlin towers

2.1.9.a. Bounding the number l of induction steps in terms of the size n of the orbit

Lemma 2.23. *Let σ be a primitive substitution on an alphabet $\mathcal{A}$ and λ the Perron-Frobenius eigenvalue for the matrix M_σ of the substitution. There exist constants*

$A, B > 0$ such that for every letter x in $\mathcal{A}$ and every $n \in \mathbb{N}$, $A\lambda^n < |\sigma^n(x)| < B\lambda^n$.

This lemma results from basic properties of primitive substitution that are explained in [Que10a].

Corollary 2.24. *Let T be an IET on an interval I and $x \in I$. Let $\overline{x}$ be the symbolic coding of x under T. Assume that $\mathcal{R}^q(T) = T$. Denote by λ the Perron-Frobenius eigenvalue of M_σ where σ is the substitution associated to $\mathfrak{R}^q$ applied to T. There exists a constant $\kappa > 0$ such that the decomposition*

$$\overline{x}_n = s_0\sigma(s_1)...\sigma^{l-1}(s_{l-1})\sigma^l(m_l)\sigma^{l-1}(p_{l-1})...\sigma(p_1)p_0$$

verifies

$$\forall l \in \mathbb{N}, \left| l - \frac{\log(n)}{\log(\lambda)} \right| \leqslant \kappa.$$

Proof. — Let A, B be the constants of Lemma 2.23, and $K = \max_{a\in\mathcal{A}} |\sigma(a)|$. We set $C = \max\left(A, \frac{(2K-2)B\lambda}{\lambda-1}\right)$ and $\kappa = \frac{\log C}{\log \lambda}$. Lemma 2.23 gives upper and lower bounds for $n = \sum_{k=0}^{l-1}(|\sigma^k(s_k)| + |\sigma^k(p_k)|) + |\sigma^l(m_l)|$, which permits to show the corollary.■

2.2. Translation surfaces

2.2.1. Definition

There are three equivalent definitions for a translation surface :

(1) It is a finite collection of polygons, with sides identified by translation.

(2) It is a topological orientable surface M of genus $g \geqslant 1$ where
- there exists a finite set of points $\Sigma = \{s_1, \ldots, s_n\} \subset M$, called the *singularities*,
- there exists a tuple $k = (k_1, \ldots, k_n)$ of integers,
- the surface $M \setminus \Sigma$ is a manifold, and the maximal atlas contains only charts $M \setminus \Sigma \to \mathbb{C}$ that are translations,
- for every singularity s_i, there exists a neighborhood $\mathcal{U}_i$ and a ramified covering $\pi_i : \mathbb{D} \to \mathcal{U}_i$ of degree k_i such that the restriction of π_i on a sheet is a chart.

(3) It is a pair (X, ω) where X is a compact Riemann surface and ω a holomorphic 1-form on X.

A translation is a map $z \mapsto z + c$ with $c \in \mathbb{C}$. If we replace the condition "by translation" in the first definition with the condition "by a map of the form $z \mapsto \pm z + c$", then we get a half-translation surface. It changes in the same way the second point. In the third point, it is equivalent to replace "holomorphic 1-form" with "meromorphic quadratic form with simple poles". Many properties of the translation surfaces hold for half-translation as well.

2.2.2. Suspensions of an IET

If T is an IET, one can defined a translation surface M such that there exists a segment $I \subset M$ such that the first return map on I of the vertical flow on M is T.

Let $T = (\pi, \lambda)$ be an IET with n intervals of continuity. Following Marmi, Moussa, and Yoccoz [MMY05], we call *suspension data* for $T = (\pi, \lambda)$ a tuple of complex numbers $(\zeta_i)_{1 \leqslant i \leqslant n}$ such that:

- $\forall i \in \{1, \dots, n\}$, $Re(\zeta_i) = \lambda_i$,
- $\forall k \in \{1, \dots, n-1\}, Im(\sum_{\pi_0(i) \leqslant k} \zeta_i) > 0$,
- $\forall k \in \{1, \dots, n-1\}, Im(\sum_{\pi_1(i) \leqslant k} \zeta_i) < 0$.

Figure 2.9 illustrates a suspension data.

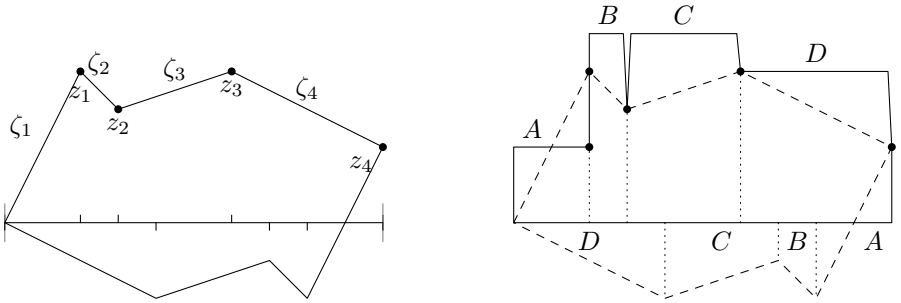

(a) The broken line gives a polygon (b) The zippered rectangles

Figure 2.9. – Suspensions data for the example of Figure 2.6

For $k \in \{0, \dots, n\}$, we set $z_k = \sum_{\pi_0(i) \leqslant k} \zeta_i$ and $z'_k = \sum_{\pi_1(i) \leqslant k} \zeta_i$. If the broken line that joins the points $z_0, z_1 \dots, z_n = z'_n, z'_{n-1} \dots, z'_0 = z_0$ does not intersect itself, we get a translation surface. This broken line may intersects itself (see Figure 2.10), but we can always consider the so-called *zippered rectangles* introduced by Veech [Vee82]. We give an example in Figure 2.9b.

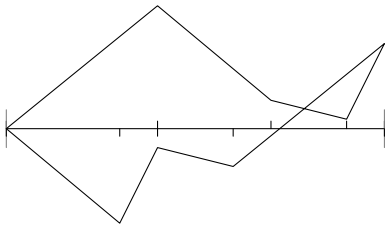

Figure 2.10. – The suspension data may not give a polygon

For more detail, we refer to Chapter 2 of [Via06].

2.2.3. Teichmüller space and moduli space

Let S be a topological surface of genus $g \geqslant 1$. The *Teichmüller space of Riemann surfaces* of genus g is

$$\mathscr{T}_g = \mathscr{T}(S) = \{(X, f) \,|\, X \text{ a Riemann surface}, f : S \to X \text{ an homeomorphism}\}/\backsim$$

where two pairs (X_1, f_1) and (X_2, f_2) are equivalent if there exists a biholomorphic map $h : X_1 \to X_2$ such that $f_2^{-1} \circ h \circ f_1$ is homotopic to the identity.

The *mapping class group* is the group of the orientation-preserving diffeomorphisms on S quotiented by the group of those which are homotopic to the identity.

$$\Gamma(S) = \mathrm{Diff}^+(S)/\mathrm{Diff}_0^+(S).$$

The group $\Gamma(S)$ is discrete and finitely generated. It acts on $\mathscr{T}(S)$ properly discontinuously. The *moduli space of Riemann surfaces* of genus g is the quotient

$$\mathscr{M}_g = \mathscr{T}_g/\Gamma(S).$$

A translation surface is a Riemann surface together with a holomorphic 1-form. Thus, the Teichmüller and moduli spaces of translation surfaces contains also the data of the 1-form. The Teichmüller space $\mathscr{T}_g$ admits a vector bundle, denoted by $\mathscr{T}\Omega_g$, whose fiber in point X is the set

$$\Omega(X) = \{(X, \omega) \,|\, \omega \text{ a holomorphic 1-form defined on } X\}$$

of pairs of X and a holomorphic 1-form ω defined on X. The group $\Gamma(S)$ acts on $\mathscr{T}\Omega_g$ as well. The *Teichmüller space of translation surfaces* $\mathscr{T}\Omega_g$ and the *moduli space of translation surfaces* is the quotient

$$\Omega_g = \mathscr{T}\Omega_g/\Gamma(S)$$

which is a vector bundle over $\mathscr{M}_g$ whose fiber in point X is $\Omega(X)$. In the point of view of the first given definition of translation surfaces, the moduli space Ω_g is the set of polygons with identificated sides, modulo cut and paste operations.

The group $SL_2(\mathbb{R})$ acts naturally on the moduli space as follows. Let M be a translation surface given by a polygon P with sides identified by translation. Let $g \in SL_2(\mathbb{R})$. Then, $g.P$ is a polygon and the identifications are still by translation, since $SL_2(\mathbb{R})$ preserves the parallelism. Thus $g.P$ defines a translation surface, which is $g.M$. The *Teichmüller flow* is defined as the restriction of the action of $SL_2(\mathbb{R})$ to the diagonal subgroup:

$$g_t = \begin{pmatrix} e^t & 0 \\ 0 & e^{-t} \end{pmatrix}.$$

It corresponds to the geodesic flow on the moduli space.

2.2.4. The Kontsevich-Zorich cocycle (geometric point of view)

The Kontsevich-Zorich defined in Section 2.1.6 can also be defined with a geometric point of view. To avoid confusion between the genus and the Teichmüller flow, we now simply write $\mathscr{T}$ and $\mathscr{M}$ for the Teichmüller space and the moduli space of translation surfaces of genus g, g being fixed. Take a translation surface M (of genus g), defined by a polygon P with identified sides. Take also a tuple of closed curves $(\zeta_1, \dots, \zeta_d)$ such that the tuple of the cycles $([\zeta_1], \dots, [\zeta_d])$ forms a basis of the homology $H_1(M, \mathbb{R})$. Consider the orbit $(g_t.M)_{t\in\mathbb{R}}$ of M along the Teichmüller flow. For a time $t > 0$, the polygon $g_t.P$ that defines the surface $g_t.M$ is stretched in the horizontal direction. We can cut and paste it into another polygon that still defines $g_t.M$. For some[2] well chosen time t, we can obtain a polygon whose shape is approximately the one of P, which allows to identify $H_1(g_t.M, \mathbb{R})$ and $H_1(M, \mathbb{R})$. The Kontsevich–Zorich cocycle expresses the cycles $([g_t.\zeta_1], \dots, [g_t.\zeta_d])$ in the basis $([\zeta_1], \dots, [\zeta_d])$.

We now give a more formal definition, following the nice presentation given in [FSU18]. Let $\pi : \mathscr{T} \to \mathscr{M}$ and $\Delta \subset \mathscr{T}$ a fundamental domain for the action of Γ. Let $t \in \mathbb{R}$, $x \in \mathscr{M}$, and $\tilde{x}$ be any point in the fiber $\pi^{-1}(x)$ of x. There is an only element $\psi \in \Gamma$ such that $\psi(g_t.\tilde{x}) \in \Delta$. The Kontsevich–Zorich cocycle is

$$A^{KZ} : \begin{array}{ccc} \mathbb{R} \times \mathscr{M}(M) & \to & GL(H_1(M, \mathbb{R}) \\ (t, x) & \mapsto & (\psi_{g_t, \tilde{x}})_* \end{array} .$$

2.3. The Oseledets theorem

The Oseledets theorem is a multiplicative version of the ergodic theorem. We consider a dynamical system (X, μ, φ), and A a cocycle $A : \begin{array}{ccc} X & \longrightarrow & \mathcal{M}_d(\mathbb{R}) \\ x & \mapsto & A_x \end{array}$. We are interested in the growth of vectors under the action of $A_x^{(n)} = A_{\varphi^{n-1}(x)} \dots A_{\varphi(x)} A_x$.

Theorem 2.25 (Oseledets). *Let X be a topological space, endowed with a probability measure μ. Let $\varphi : X \longrightarrow X$ be an ergodic function. Let $A : \begin{array}{ccc} X & \longrightarrow & \mathcal{M}_d(\mathbb{R}) \\ x & \mapsto & A_x \end{array}$ be a cocycle. Assume that the cocycle is log-integrable: $\int_X \log |||A_x||| d\mu < \infty$.*

There exist $\theta_1 > \theta_2 > \dots > \theta_k$, called Lyapunov exponents*, such that for almost every $x \in X$, there exists a flag $\mathbb{R}^d = \mathcal{H}_k^{(x)} \supset \mathcal{H}_{k-1}^{(x)} \supset \dots \supset \mathcal{H}_1^{(x)}$ such that:*

$$A_x \mathcal{H}_j^{(x)} = \mathcal{H}_j^{(\varphi(x))}$$

and

2. the time t can be arbitrarily large by ergodicity of the Teichmüller flow in $\mathscr{M}$

$$\forall v \in \mathcal{H}_j \setminus \mathcal{H}_{j-1},\ \frac{1}{n} \log ||A_x^{(n)} v|| \underset{n\to\infty}{\longrightarrow} \theta_j$$

where $A_x^{(n)} = A_{\varphi^{n-1}(x)} ... A_{\varphi(x)} A_x$.

Consider the set

$$X = \bigsqcup_{\sigma \in [\pi(T)]} \Delta_{N-1} \times \{\sigma\}$$

of all IETs whose underlying permutation is in the Rauzy class $[\pi(T)]$ of

$$\pi(T) = \begin{pmatrix} I_1 & I_2 & ... & I_{N-1} \\ I_{N-1} & ... & I_2 & I_1 \end{pmatrix}.$$

The space X is equipped with μ_Z, which is an ergodic $\mathfrak{R}$-invariant probability measure [Zor96]. The cocycle $A = A^{KZ}$ introduced in Sections 2.1.6 and 2.2.4 is invertible, A and A^{-1} are log-integrable. We consider here A^{-1}. This is used in [Zor99] to prove Proposition 3.11 that we will use in Chapter 3.

3. Deviations for generalized tiling billiards in cyclic polygons

3.1. Introduction

Tiling billiards in triangle or in cyclic quadrilaterals tiling are now well understood thanks to the work of many mathematicians [Par19; Par21; HP22; BDFI24; DHMPS]. In this chapter, we will handle all N-gons with $N \geqslant 5$, that are inscribed in a half-circle, although they will not tile the plane. All polygons will be drawn as pentagons. The results are true for polygons with more than five sides but the reader can think of pentagons in a first reading.

3.1.1. The generalized tiling

We first define how we build the generalized tiling. Let P be an N-gon with $N \geqslant 5$. Each tile of the generalized tiling is congruent to P. Moreover if T and T' are two neighboring tiles then T' is the image of T under a central symmetry with respect to the middle of their shared side. This does not define a proper tiling: polygons will either overlap each other or not fill the entire plane. Indeed when turning around a vertex, all the angles of the N-gon appear and sum up to $(N-2)\pi$, which is not a divisor of 2π, see Figure 3.1. But we can still define a billiard trajectory in the plane, generalizing tiling billiards for any polygon.

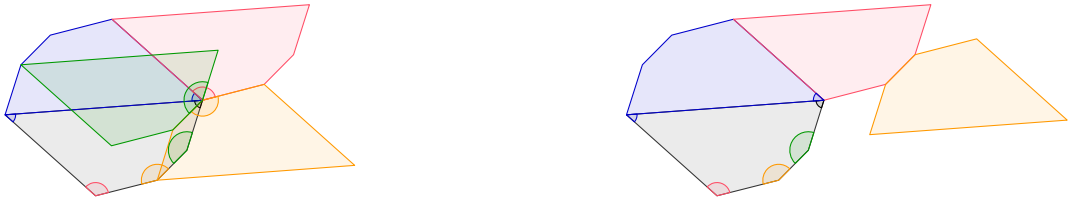

(a) Polygons either overlap... (b) ... or leave empty space

Figure 3.1. – The way we put polygons together to play tiling billiards will not tile the plane with N-gons, $N \geqslant 5$.

Fix a copy of P in the plane, a point inside it and a direction (see Figure 3.2a). Follow the direction until reaching a side. Then draw a second centrally symmetric polygon, so that the two polygons share the crossed side (see Figure 3.2b). The trajectory is refracted through the side and continues in a straight line in the second

polygon (see Figure 3.2c). Each time the trajectory reaches a side s, we draw the next polygon, which is the image of the current one under the central symmetry with respect to the middle of the crossed side s. The new polygon may overlap a previous one. The trajectory takes into account only the last drawn polygon (see Figure 3.2e and 3.2f). A trajectory that hits a corner stops. We call this system a P-generalized tiling billiard.

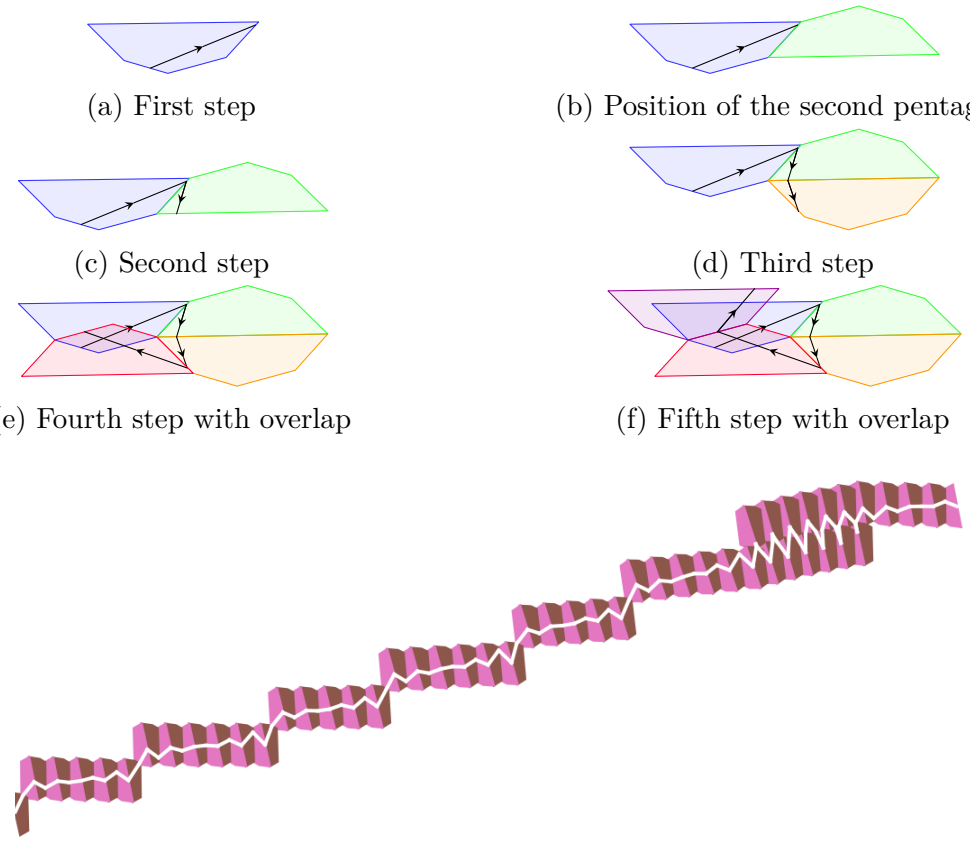

(a) First step

(b) Position of the second pentagon

(c) Second step

(d) Third step

(e) Fourth step with overlap

(f) Fifth step with overlap

(g) A part of a trajectory in a generalized pentagonal tiling billiard satisfying condition (C)

Figure 3.2. – Examples of trajectories in generalized pentagonal tiling billiards

3.1.2. Assumptions

Let P be a polygon inscribed in a circle. We name such polygons *cyclic*. We will denote by $\mathbf{a_1}, ..., \mathbf{a_N}$ the sides of P, clockwise labeled and $\mathbf{a_N}$ being its longest side. We denote by $a_1, ..., a_N$ the lengths of the arcs subtended by each side (see Figure 3.3a). Conversely, if $a_1, \ldots, a_N > 0$, with a_N being maximal, we denote by

$P(a_1, \dots, a_N)$ the cyclic polygon whose arcs subtended by its sides have lengths $a_1, \dots, a_N$.

Each trajectory of the P-generalized tiling billiard follows a *conservation law*: if we fold the plan according to the k-th crossed side, the $(k+1)$-step of the trajectory folds on the k-th step, and the circumcircle of the $(k+1)$-th drawn copy of P folds on the k-th one. This beautiful argument was developed in [BDFI24]. It implies that the oriented distance d_k between the circumcenter and the (oriented) line supporting the k-th step of the trajectory is a constant: $\forall k \in \mathbb{N}$, $d_k = d_0$. We give another formulation for this conservation law. We call x_k and y_k the intersection points between the circumcircle of the k-th polygon and the line supporting the k-th step of the trajectory, the trajectory going in the direction from x_k to y_k. We denote by τ_k the length of the chord between y_k and x_k (counter-clockwise). This length is a constant, that we will call the parameter τ of the trajectory, see Figure 3.3b. We will restrict ourselves to the study of trajectories of tiling billiards

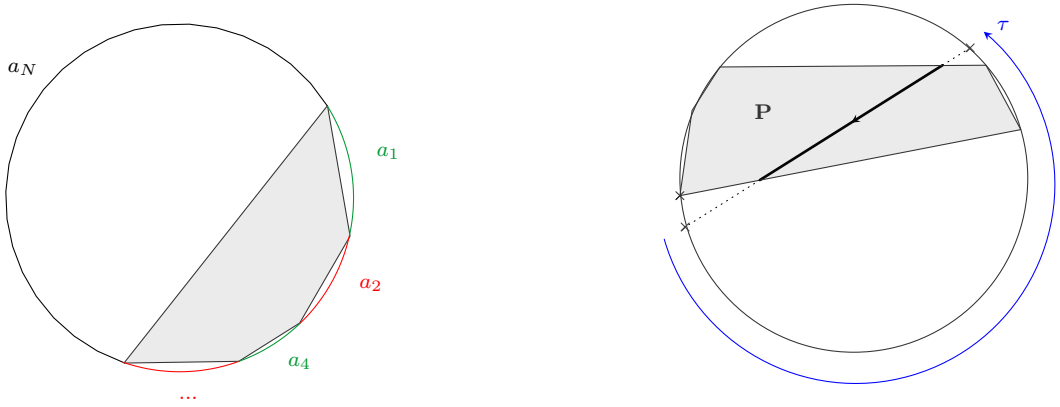

(a) Sides

(b) Parameter τ of the trajectory

Figure 3.3. – Notations for cyclic polygons and assumption (C)

satisfying the following conditions:

$$(\mathrm{C}) \begin{cases} P \text{ is inscribed in a circle} & (\mathrm{C0}) \\ a_1 + .. + a_{N-1} < \tau < a_N & (\mathrm{C1}) \end{cases}$$

We highlight the fact that (C) is a condition on both the N-gon P *and* the initial point and initial direction of the trajectory. Condition (C0) ensures that a certain parameter τ (see Figure 3.3b and Definition 3.6) is preserved all along the trajectory and hence allows us to use IETFs to study the system (see Sections 3.2.2 and 3.2.3), as in [BDFI24], [HP22], [Par19], [Par21] and [DHMPS]. This is a crucial fact and we know nothing for tiling billiards made with non-cyclic polygons. Condition (C1) means both that P is inscribed in a half-circle and that the trajectory is close to the circumcenter. It is crucial for the following since it allows to reduce the system to a standard IET without flips with N intervals of

continuity, which permits to use ergodic theory tools (see Sections 3.2.2 and 3.2.3).

3.1.3. Results

Let us identify the real plane with $\mathbb{C}$. Let $p_n \in \mathbb{C}$ be the point of the trajectory on the n-th side crossing. The following lemma and theorem state that the trajectory has an asymptotic direction but does not stay at a bounded distance from it.

Lemma 3.1. *For every $a_1, \dots, a_{N-1}$, almost every $a_N > \sum_{i=1}^{N-1} a_i$, and every $\tau \in \left(\sum_{i=1}^{N-1} a_i, a_N\right)$, the cyclic N-gon $P(a_1, \dots, a_N)$ defines a generalized tiling billiard whose trajectories having parameter τ all admit a mean displacement $m = \lim_{n\to\infty} \frac{p_n}{n}$ that does not vanish.*

Theorem A. *For almost every parameters $a_1, ..., a_{N+1}, \tau$ satisfying (C), the trajectories with parameter τ in the $P(a_1, ..., a_{N+1})$-generalized tiling billiard do not stay at a bounded distance from any line.*

Remark 3.2. *The limit m depends on $a_1, \dots, a_N$ but not on $\tau \in \left(\sum_{i=1}^{k} a_i, a_N\right)$.*

We quantify the order of magnitude of deviations from the asymptotic direction with the following two theorems. They are linked to the behavior of the Teichmüller flow on the moduli space of translation surfaces.

Theorem B. *Let $N \in \mathbb{N}, N \geqslant 5$. There exist $\theta_1 > \theta_2 > \theta_3 > 0$ such that for almost every N-gon P and every τ, satisfying condition (C), for any initial direction having parameter τ in a P-tiling billiard, the sequence of points $(p_n)_{n\in\mathbb{N}}$ satisfies:*

$$\limsup_{n\to\infty} \frac{\log|p_n - nm|}{\log n} = \begin{cases} \frac{\theta_2}{\theta_1} > 0 & \text{if } N \text{ is odd} \\ \frac{\theta_2}{\theta_1} \text{ or } \frac{\theta_3}{\theta_1} > 0 & \text{if } N \text{ is even} \end{cases}$$

where $m = \lim_{n\to\infty} \frac{p_n}{n}$ is the asymptotic direction of the trajectory.

Remark 3.3. *The numbers θ_1, θ_2 and θ_3 depend only on the number of sides of the polygon! The $1 + \frac{\theta_i}{\theta_1}$ are the first three Lyapounov exponents of Teichmüller flow in the hyperelliptic component of the stratum $\mathcal{H}(N-3)$ if N is odd, and $\mathcal{H}(\frac{N}{2} - 2, \frac{N}{2} - 2)$ if N is even.*

When $N = 5$, a result of Eskin, Kontsevich and Zorich [EKZ11] states that $\frac{\theta_2}{\theta_1} = \frac{1}{3}$. The fact that θ_1, θ_2 and θ_3 are distinct comes from [For02].

We prove these results with interval exchange transformations (IETs) and their generic properties. The *Rauzy induction* $\mathfrak{R}$ (see Section 2.1.4) is a powerful tool to study orbits of an IET. If T is an IET on I, $\mathfrak{R}(T)$ is the first return map of T on a well chosen subinterval $J \subset I$, which gives once again an IET with the same number of intervals of continuity. To track the orbit of T through Rauzy induction,

we need to know both the sequence of combinatorial data of the induced IETs $(\mathfrak{R}^n(T))_{n\in\mathbb{N}}$ and the lengths of their intervals of continuity. This information can be encoded in an infinite path in a finite graph, called the Rauzy diagram. The lengths of intervals of continuity of $\mathfrak{R}^n(T)$ linearly depend on those of T. A corresponding matrix cocycle (see Section 2.1.6) is important for the study of our dynamical system. The Rauzy induction for IETs corresponds to the Teichmüller flow for their suspensions (that are translation surfaces). See [Via06], [MMY05],[Yoc10].

When the path in the Rauzy diagram corresponding to some IET is a loop, which is the same as to say that the orbit of the IET through the Rauzy induction is periodic, we say that this IET is *self-similar*. The matrix associated to this loop allows us to study the symbolic coding of a point by the IET T. When the loop is complex enough, the matrix is primitive. This case is not generic but important. Indeed it corresponds to the case when the vertical flow on a suspension of the IET is the foliation of a pseudo-Anosov map. In this case, one can give a more precise estimate of the deviations.

Theorem C. *Let $N \in \mathbb{N}, N \geqslant 5$ and $a = (a_1, a_2, ..., a_{N-1})$ be the (normalized) Perron eigenvector (with eigenvalue λ_1) of a primitive matrix $M \in \mathcal{M}_{N-1}(\mathbb{R})$ that corresponds to a loop in the Rauzy diagram. Assume that the second eigenvalue λ_2 of M is such that $|\lambda_2| > 1$ and that no other eigenvalue has the same modulus as λ_2. For almost every $a_N > \sum_{i=1}^{N-1} a_i$, there exist C_1 and C_2 and an infinite set $\mathcal{S} \subset \mathbb{N}$ such that for every $\tau \in (\sum_{i=1}^{N-1} a_i, a_N)$ and any trajectory having parameter τ in a $P(a_1, ..., a_N)$-tiling billiard, the sequence of points $(p_n)_{n\in\mathbb{N}}$ satisfies:*

$$\begin{cases} \forall n \in \mathbb{N} & |p_n - nm| < C_1 n^{\frac{\log \lambda_2}{\log \lambda_1}} \\ \forall n \in \mathcal{S} & |p_n - nm| > C_2 n^{\frac{\log \lambda_2}{\log \lambda_1}} \end{cases}.$$

This theorem quantify the second term of the asymptotic expansion of some Birkhoff's sums for a fixed point. Figure 3.4 illustrates the deviations established in Theorem C. Another related problem is to study the uniform speed of convergence of these Birkhoff's sums, i.e. to study the *discrepancy*. This was done by Adamczewski in [Ada04].

To summarize, this chapter shows that for almost every generalized tiling billiard satisfying condition (C):

(1) the trajectory has an asymptotic direction (Lemma 3.1), like for triangle or cyclic quadrilateral tiling billiards,

(2) the trajectory admits unbounded (sublinear) deviations from its asymptotic direction (Theorems A, B and C), unlike in triangles and cyclic quadrilaterals case.

3.1.4. Outline of the proof

The proofs of Theorems A, B and C are organized as follows:

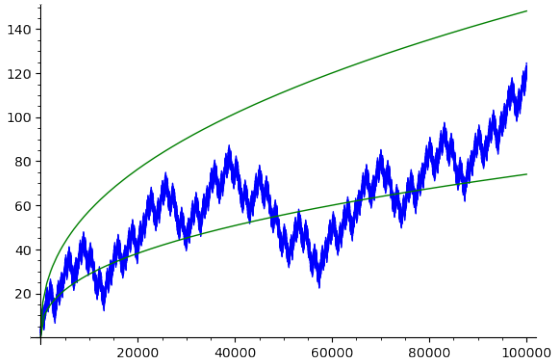

Figure 3.4. – The modulus of the deviations, depending on the number of steps of the trajectory, has a sublinear growth

(1) Define the IET that corresponds to our generalized tiling billiard.

(2) Define a piecewise constant function f (that depends on P) and approximates the trajectory. We show that f has almost always a non-zero mean, which means that the trajectory of the studied tiling billiard has an asymptotic direction.

(3) Study the function $h = \mathrm{Im}(\frac{1}{m}f - 1)$ linked to the deviations from the asymptotic direction. We show that for almost every a_N, h is not contained in a codimension 3 subspace (resp. 2 if N is odd).

(4) Zorich's results [Zor99] on deviations for IETs give the rate given in Theorem B

IETs are generically uniquely ergodic [Mas82] [Vee82]. Hence we know that the orbit of a point equidistributes in the different intervals of continuity. Zorich [Zor99] establishes how much an orbit can deviate from this equidistribution. To prove this, Zorich studies Teichmüller flow of suspension surfaces (that are translation surfaces) of IETs and how it behaves with respect to Oseledets flag decomposition.

The main contribution of this chapter is to prove that one can apply Zorich results to the case of the generalized tiling billiards we study. This is not a straightforward verification. We have to show where some specific vector lies in the flag given by the Oseledets theorem (see Section 2.3). The difficult point is that we know the expression of the vector but, in general, not of the subspaces of the flag. We can think of them as random subspaces. We can still conclude for almost every parameter because the vector has one more degree of freedom than the flag. Moreover the vector's coordinates depend analytically on the parameter which is independent of the flag. This corresponds to step (3) in the previous decomposition of the proof.

The most technical parts of the proof of Theorem B are done first for pentagons and then generalized. We prove Theorem C by direct computation.

We explain step (1) in Section 3.2. We introduce functions f and g in Section 3.3. Section 3.4 studies the function g and establishes the properties that allow us to apply Zorich's results.

3.2. The studied system

3.2.1. Definition of a generalized tiling billiard

Definition 3.4 (Generalized tiling billiard). *Let P be a polygon and v a vertex of P. We call a* generalized tiling billiard trajectory *the triplet $(\mathbf{T}, (P_i)_{i\in\mathbb{N}}, (v_i)_{i\in\mathbb{N}})$ where $\mathbf{T}$ is a piecewise linear curve in the real plane such that for every integer i:*

- *(P_i, v_i) is an isometric copy of (P, v) in the plane,*
- *$\mathbf{T}$ crosses P_i in a segment,*
- *P_i and P_{i+1} share a side, crossed by $\mathbf{T}$,*
- *P_{i+1} is the image of P_i through a central symmetry,*
- *the common side of P_i and P_{i+1} is the bisector of the angle made by $\mathbf{T} \cap P_i$ and $\mathbf{T} \cap P_{i+1}$.*

This defines a P-generalized tiling billiard as a dynamical system. See Figure 3.5 for an illustration.

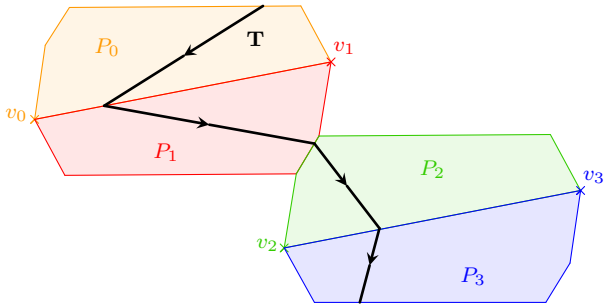

Figure 3.5. – Notations for generalized tiling billiards

Remark 3.5. *When we think of a generalized tiling billiard trajectory, we mostly think of $\mathbf{T}$ although defining it as a triplet with crossed polygons and vertices v_i is much more convenient for the study of the trajectory. The definition requires no property of P although we will restrict in the following to the case where P is cyclic. We denote by $\mathcal{C}_i$ the circumcircle of P_i.*

3.2.2. A system of coordinates

Here we describe a convenient frame of reference to study a tiling billiard trajectory. It is the one of an ant that would follow this trajectory. At each step, the ant can see the polygon it is crossing and its circumcircle. We need the following data to determine the position of P_i with respect to the ant (in other words, the position of the ant in P):

(1) On which chord of the circumcircle $\mathcal{C}_i$ of P_i the ant is traveling,

(2) Where v_i is on $\mathcal{C}_i$ (this determines how P_i is placed in $\mathcal{C}_i$).

The data (1) is a parameter of the trajectory since the refraction law implies that it is preserved along the trajectory. For example if the ant is traveling on a diameter of $\mathcal{C}_i$, then it will also travel on a diameter of any $\mathcal{C}_j$. Therefore we will need only the position of v_i on $\mathcal{C}_i$ to determine the position of P with respect to the ant.

Definition 3.6. *We say that the trajectory has parameter τ if the arc between the two endpoints of the chord supporting a step of the trajectory $\mathbf{T}$ has length τ (see Figure 3.3b).*

Let $(\mathbf{T}, (P_i)_{i\in\mathbb{N}}, (v_i)_{i\in\mathbb{N}})$ be a tiling billiard. We normalize the situation to $a_1 + \cdots + a_{N-1} = 1$. We identify the circumcircle $\mathcal{C}_i$ of P_i with the interval $[0, \sum_{k=1}^{N} a_k) = [0, 1 + a_N)$ by identifying 0 to the point $o_i \in \mathcal{C}_i$ where the line containing $T_i = \mathbf{T} \cap P_i$ would meet $\mathcal{C}_i$ if going on in straight line after the side crossing. Then we locate the vertex v_i of P_i in the frame of $\mathcal{C}_i$. Let $x_i \in [0, 1+a_N)$ be the point with which v_i is identified. See Figure 3.6 for an illustration of notations.

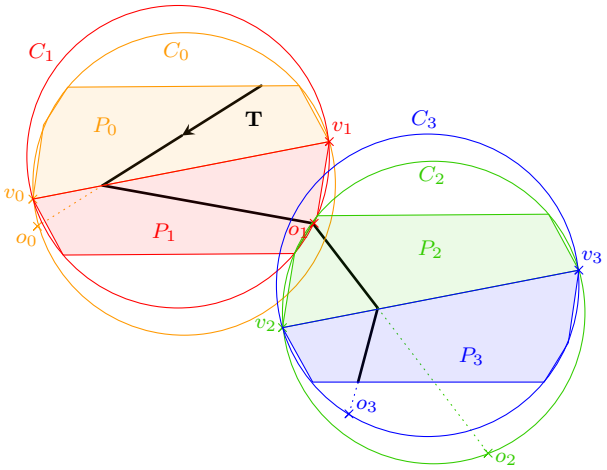

(a) Notations

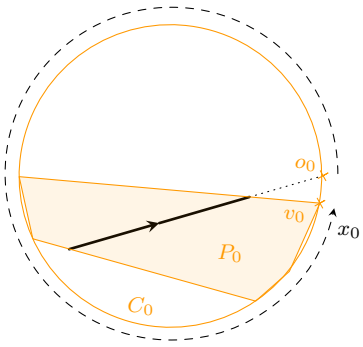

(b) First crossed polygon

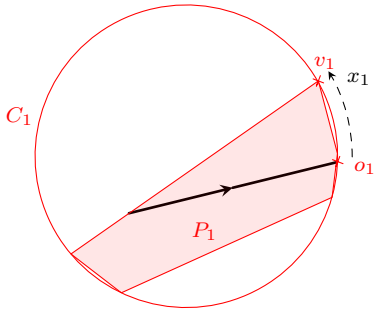

(c) Second crossed polygon

Figure 3.6. – Moving frame of reference

3.2.3. The obtained Interval Exchange Transformation

The following Theorem is proved in [BDFI24] for triangles but can be extended to any cyclic polygon.

Theorem 3.7 (Theorem 3.3 of [BDFI24]). *There is an IET with flips (IETF) Φ such that $x_{i+1} = \Phi(x_i)$ for every i (see Figure 3.8a).*

Proof. — We consider the frame of reference described in Section 3.2.2 and compute the coordinates x_{i+1} depending on x_i, $a_1, \dots, a_N$ and τ. We illustrate the situation with Figure 3.7.

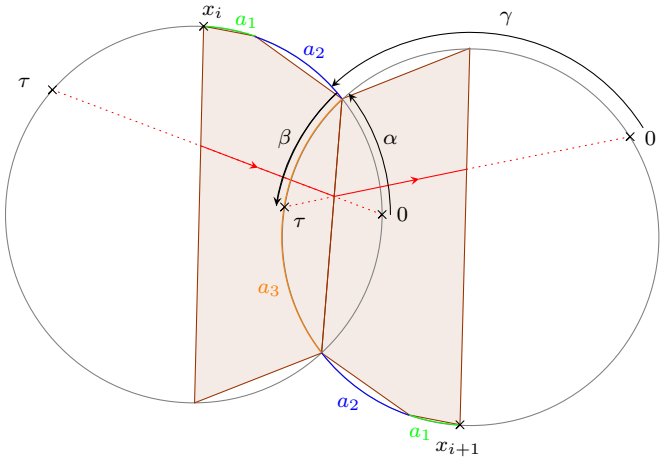

Figure 3.7. – Coordinates x_i and x_{i+1} are related by a a linear equation

Because of the refraction law, the lengths α and β on the Figure 3.7 are equal. Let $j \in \{1, \dots, N\}$ be such that $x_i \in \left(\sum_{k=1}^{j} a_k, \sum_{k=1}^{j+1} a_k\right)$. In Figure 3.7, $j = 2$. We have $\alpha = x_i - \sum_{k=1}^{j-1} a_k$, which leads to $\gamma = \tau - \beta = \tau - x_i + \sum_{k=1}^{j} a_k$. We conclude the expression of x_{i+1} depending on x_i, $a_1, \dots, a_N$ and τ:

$$\begin{aligned} x_{i+1} &= \gamma + \sum_{k=1}^{j+1} a_k \\ &= \tau + \sum_{k=1}^{j+1} a_k - (x_i - \sum_{k=1}^{j} a_k) \end{aligned}$$

which corresponds to the expression of a fully flipped IET (the points of discontinuity are exactly the a_k's). ■

If we add the hypothesis (C1), the IETF Φ of Theorem 3.7 has permutation

$$\pi(\Phi) = \begin{pmatrix} \overline{I_1} & \overline{I_2} & \dots & \overline{I_{N-1}} & \overline{I_N^+} & \overline{I_N^-} \\ \overline{I_N^+} & \overline{I_1} & \overline{I_2} & \dots & \overline{I_{N-1}} & \overline{I_N^-} \end{pmatrix}$$

where we overlined flipped intervals (here, the IET flips every interval). The intervals of continuity of the IET have lengths

$$\lambda(\Phi) = \begin{pmatrix} a_1 & a_2 & \dots & a_{N-1} & a_N - \tau & \tau \end{pmatrix}.$$

Remark 3.8. *Here we consider Φ as an IET on an interval, it has $N+1$ intervals of continuity. If we define it on a circle it has only N intervals of continuity.*

The choice of v ensures that the trajectory crosses the side $\boldsymbol{a}_k$ if and only if $x \in I_k$.

The condition (C1) implies that the trajectory crosses the longest side every other crossing. It is hence enough to study the squared map Φ^2, which is an IET without flip, see Figure 3.8. We consider $T = \Phi^2_{|I}$ the square of Φ, restricted on $I = I_1 \cup \dots \cup I_{N-1}$. Recall that we have normalized the situation so that $a_1 + \dots + a_{N-1} = 1$ so T is defined on $(0,1)$. It is an IET (without flip) with permutation

$$\pi(T) = \begin{pmatrix} I_1 & I_2 & \dots & I_{N-1} \\ I_{N-1} & \dots & I_2 & I_1 \end{pmatrix}$$

and lengths

$$\lambda(T) = \begin{pmatrix} a_1 & a_2 & \dots & a_{N-1} \end{pmatrix}.$$

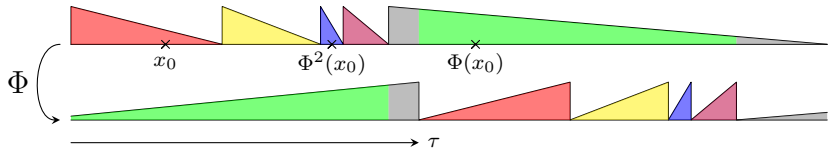

(a) The IETF Φ

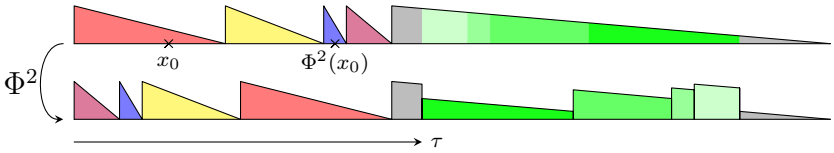

(b) The IET Φ^2 without flip

Orbits of points inside grey parts do not correspond to a trajectory of a tiling billiard.

Figure 3.8. – Example of the IETs Φ and Φ^2, corresponding to a tiling billiard.

3.3. To approximate the trajectory

3.3.1. Lengths of shifts

The assumption (C1) implies that one out of two crossed sides is the side a_N (the biggest one). Let us remark that every other polygon along the trajectory is a

translation of the first one. Therefore we can approach two steps (i and $i+1$) of the trajectory by a translation: the one that sends the polygon P_i to the polygon P_{i+2}.

We identify the space of translation with $\mathbb{C}$. Let us denote by f_i the translation induced by crossing the side $\mathbf{a_i}$ and then the side $\mathbf{a_N}$ (see Figure 3.9). We recall that x_0 denotes the position of the vertex v_0 of P_0 in $\mathcal{C}_0$. One has:

$$\forall k \in \{1, .., N-1\},\ f_k = r\left(e^{X_k} - e^{X_N} + e^{X_{k-1}} - e^{X_0}\right)$$

where

$$X_k = -\frac{i}{r}\left(x_0 + \sum_{j=1}^{k} a_j\right) \quad \text{and} \quad r = \frac{1+a_N}{2\pi} \text{ is the radius of the circumcircle of } P.$$

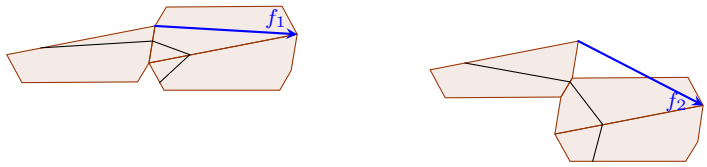

(a) f_1 (b) f_2

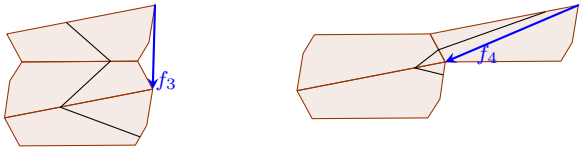

(c) f_3 (d) f_4

Figure 3.9. – Translations f_i when crossing sides a_i followed by side a_5

3.3.2. Estimate the trajectory

Let us define the piecewise constant complex function f on the interval $[0, 1)$ by:

$$\forall i \in \{1, \ldots, N-1\}, \quad f(x) = f_i \quad \text{if } \sum_{k=1}^{i-1} a_k \leqslant x < \sum_{k=1}^{i} a_k.$$

After $2n$ steps in the plane, the trajectory is in the polygon P_{2n}, polygon which is equal to the first one (P_0) translated by

$$S_n f(x_0) = \sum_{k=0}^{n-1} f(T^k(x_0)).$$

This sum is the *Birkhoff sum* of f with respect to T and x_0. We approach the trajectory with this value. We highlight that we only need to know how many times the orbit $(T^k x)_{k\leqslant n}$ goes into each interval $I_i \subset (0,1)$ to compute Birkhoff sum. The sequence $(S_n f(x_0))_{n\in\mathbb{N}}$ of Birkhoff sums gives us (with uniformly bounded error) an estimate of the position p_{2n} (of the $2n$-th side crossing of the trajectory) and hence also of p_{2n+1}.

Note that f depends on x_0. However, a change of x_0 will only multiply f by a complex number. Therefore all the translations f_i depend on x_0 (i.e. on the position of P_0) only up to the same rotation. Whether the trajectory has a limit or not hence does not depend on x_0. Nor the fact that the trajectory stays at bounded distance of a line. Only the asymptotic direction (if it exists) depends on x_0.

3.3.3. Average shift

We first show that our trajectory has almost always an asymptotic direction.

Lemma 3.1. *For every $a_1, \dots, a_{N-1}$, almost every $a_N > \sum_{i=1}^{N-1} a_i$, and every $\tau \in \left(\sum_{i=1}^{N-1} a_i, a_N\right)$, the cyclic N-gon $P(a_1, \dots, a_N)$ defines a generalized tiling billiard whose trajectories having parameter τ all admit a mean displacement $m = \lim_{n\to\infty} \frac{p_n}{n}$ that does not vanish.*

Proof. — As soon as T is uniquely ergodic (which is the generic case [Mas82], [Vee82]), Birkhoff's theorem tells us that the main part of this sum will be n times the mean value $m = \sum_{k=1}^{N-1} a_k f_k$ of f:

$$\forall x_0 \quad S_n f(x_0) \underset{n\to\infty}{=} n \sum_{k=1}^{N-1} a_k f_k + o(n).$$

Hence, in terms of the trajectory, m corresponds to the asymptotic direction of the trajectory, as soon as it does not vanish. Let us show that this is almost always the case.

We have:

$$\begin{aligned} m &= \sum_{k=1}^{N-1} a_k f_k \\ &= r e^{\frac{i}{r} x_0} \left[\sum_{k=1}^{N-2} (a_k + a_{k+1}) e^{\frac{i}{r}\sum_{j=1}^{k} a_j} - \left(\sum_{k=1}^{N-2} a_k \right) e^{\frac{i}{r}\sum_{j=1}^{N-1} a_j} - \left(\sum_{k=2}^{N-1} a_k \right) \right]. \end{aligned}$$

Let us write $s = \frac{2\pi}{1+a_N} = \frac{1}{r}$ the inverse of the radius of the circumcircles $\mathcal{C}_i$. If $a_1, ..., a_{N-1}$ are fixed, the map $s \in [0, \pi] \mapsto sm$ is analytic. As a non-trivial sum of linearly independent functions ($s \mapsto e^{is\sum_{j=1}^{k} a_j}$ for $1 \leqslant k \leqslant N$), it cannot be everywhere equal to zero. Therefore the map has a finite number of zeros in the compact set $[0, \pi]$. We conclude that only a finite number of values of $a_N \in (1, +\infty)$ could make m vanish. ■

3.3.4. Normalized deviations

Our goal is to study the deviations from the mean displacement. We want to estimate their size and their direction, in particular we want to show that they are not bounded in the direction orthogonal to m. To do so, we renormalize the situation so that the trajectory goes asymptotically in the horizontal direction at unit speed, namely we rotate and contract (or expand) the plane by the complex coefficient $\frac{1}{m}$. Now we have to show that the deviations have an unbounded imaginary part. In the following, an IET is said *Oseledets generic* if the Oseledets theorem (see Section 2.3) holds for this IET.

Lemma 3.9. *We set* $G = \frac{1}{m}\begin{pmatrix} f_1 \\ \vdots \\ f_{N-1} \end{pmatrix} - \begin{pmatrix} 1 \\ \vdots \\ 1 \end{pmatrix}$ *and* $H = \mathrm{Im}(G)$. *Let* $h : (0,1) \longrightarrow \mathbb{R}$ *be the map that is piecewise constant and equal to* H_i, *the* i*-th coordinate of* H, *on the subinterval* $(\sum_{j=1}^{i} a_j, \sum_{j=1}^{i+1} a_j)$ *for every* $0 \leqslant i \leqslant N-1$. *The following statements are equivalent:*

(1) The trajectory in the plane admits unbounded deviations in the direction orthogonal to the asymptotic one.

(2) The trajectory does not stay at a bounded distance from a line.

(3) The sequence $(S_n(h))_{n\in\mathbb{N}}$ *is not bounded.*

Moreover, if T *is Osseledets generic they are also equivalent to:*

(4) The vector H *is not in the contracted plane of the flag decomposition of* $\mathbb{R}^{N-1}$ *given by the Oseledets theorem.*

Proof. — The first two statements are clearly equivalent.

Quantifying deviations consists in computing the second term of the asymptotic expansion of $S_n f(x_0)$, namely studying $S_n f(x_0) - nm$. We renormalize the situation by dividing by m: $\frac{1}{m} S_n f(x_0) - n$. This corresponds to contract the plane by a factor of $\frac{1}{m}$, the renormalized trajectory admits the real line as an asymptotic direction. Since we are interested in its deviations from this asymptotic line, we want to compute the imaginary part of the second term in the asymptotic expansion of $S_n f(x_0)$:

$$\mathrm{Im}\left(\frac{1}{m} S_n f(x_0) - n\right) = S_n h(x_0).$$

The function h corresponds to the deviations from the renormalized mean displacement (equal to $(1,0) \in \mathbb{R}^2$).

If H is in the contracted plane of the Oseledets flag, then the sum converges (as a geometric sum), i.e. $S_n h(x_0)$ is bounded, and the trajectory stays at a bounded distance from the asymptotic line. On the contrary, if H is not in the contracted plane of the Oseledets flag, then the sum diverges (see Proposition 3.11), i.e. $S_n h(x_0)$ is not bounded, and the trajectory does not stay at a bounded distance from the asymptotic line. ■

The following property of vector G will be useful.

Lemma 3.10. *The vector G is normal to the vector $V = \begin{pmatrix} a_1 \\ \vdots \\ a_{N-1} \end{pmatrix}$.*

Proof. — This is a direct computation:

$$ {}^tVG = \frac{1}{m} \underbrace{\sum_{k=1}^{N-1} a_k f_k}_{=m} - \underbrace{\sum_{k=1}^{N-1} a_k}_{=1} = 0. $$

We show in the next section that in the generic case we can apply Zorich's result on deviations for IETs. This gives Theorem B . We handle the non-generic case of a self-similar IET in Section 3.5. The Kontsevich-Zorich cocycle $A = A^{KZ}$ is in this case such that $A^{(nq)} = \left(A^{(q)}\right)^n$. Direct computations on H and $M = (A^{(q)})$ allow to prove Theorem C.

3.4. The generic case

We assume here that T is Oseledets generic, which means (see Subsection 2.3) that there exists a flag depending on T

$$ \mathcal{H}_1 \subset \mathcal{H}_2 \subset ... \subset \mathcal{H}_{\mathbf{g}(T)} \subset \mathbb{R}^{N-1} $$

with $2\mathbf{g}(T) = \begin{cases} N-1 & \text{if } N \text{ is odd} \\ N-2 & \text{if } N \text{ is even} \end{cases}$, such that

$$ \forall v \in \mathcal{H}_k \setminus \mathcal{H}_{k-1}, \frac{1}{n} \log ||B_T^{(n)}(v)|| \underset{n\to\infty}{\longrightarrow} \theta_k $$

where the numbers $\theta_1 > \cdots > \theta_{\mathbf{g}(T)}$ do not depend on T. The $1 + \frac{\theta_i}{\theta_1}$ are the Lyapunov exponents of the Teichmüller flow on the hyperelliptic stratum $\mathcal{H}(N-3)$ if N is odd, (resp. $\mathcal{H}(\frac{N}{2}-2, \frac{N}{2}-2)$ if N is even) of the moduli space of abelian differentials. We will apply Proposition 3 of [Zor99]:

Proposition 3.11 (Zorich). *For a generic IET on $(0,1)$, any point $x \in (0,1)$, and any function $\varphi \in Ann(\mathcal{H}_p) \setminus Ann(\mathcal{H}_{p+1})$, $1 \leqslant p \leqslant \mathbf{g}(T) - 1$, the following holds:*

$$\limsup_{n\to+\infty} \frac{\log|S_n(\varphi(x))|}{\log n} = \frac{\theta_{p+1}}{\theta_1}.$$

We already know that the function h is in $Ann(\mathcal{H}_1)$ (because it has 0 mean). In this section we will show that it is not in $Ann(\mathcal{H}_3)$ for almost every choice of parameters (see Proposition 3.16). This will establish Theorems A and B.

To do that, we give an expression of H. It involves a matrix Q whose size increases with N: $Q \in \mathcal{M}_{\frac{(N-1)N}{2},N-1}(\mathbb{R})$. This is why we do the proof first for $N = 5$ (in Sections 3.4.1 and 3.4.2) and then for $N > 5$ (in Section 3.4.3), with the very same idea of proof but with more coefficients to handle,

3.4.1. Expression of H, when $N = 5$

Let us compute

$$H = Im\left(\frac{1}{m}\begin{pmatrix} f_1 \\ f_2 \\ f_3 \\ f_4 \end{pmatrix} - \begin{pmatrix} 1 \\ 1 \\ 1 \\ 1 \end{pmatrix}\right) = \frac{1}{|m|^2} Im\left(\overline{m}\begin{pmatrix} f_1 \\ f_2 \\ f_3 \\ f_4 \end{pmatrix}\right)$$

where $\overline{m}$ denotes the complex conjugate of m. One can check that, with $s = \frac{2\pi}{1+a_5}$,

$$H = \frac{1}{|m|^2} Q \begin{pmatrix} \sin(a_1 s) \\ \sin(a_2 s) \\ \sin(a_3 s) \\ \sin(a_4 s) \\ \sin((a_1+a_2)s) \\ \sin((a_2+a_3)s) \\ \sin((a_3+a_4)s) \\ \sin((a_1+a_2+a_3)s) \\ \sin((a_2+a_3+a_4)s) \\ \sin((a_1+a_2+a_3+a_4)s) \end{pmatrix} = H(a_1, a_2, a_3, a_4, s)$$

where

$$ {}^tQ = \begin{pmatrix} a_2+a_3+a_4 & -a_1+a_3+a_4 & -(a_1+a_2) & -(a_1+a_2) \\ a_2+a_3 & -a_1+a_3 & -(a_1+a_2) & 0 \\ 0 & a_3+a_4 & -a_2+a_4 & -(a_2+a_3) \\ a_3+a_4 & a_3+a_4 & -(a_1+a_2)+a_4 & -(a_1+a_2+a_3) \\ 0 & a_4 & a_4 & -(a_2+a_3) \\ a_3+a_4 & a_3+a_4 & -(a_1+a_2) & -(a_1+a_2) \\ a_2+a_3 & -a_1 & -a_1 & 0 \\ 0 & -(a_3+a_4) & a_2 & a_2 \\ -a_3 & -a_3 & a_1+a_2 & 0 \\ -(a_2+a_3+a_4) & a_1-a_4 & a_1-a_4 & a_1+a_2+a_3 \end{pmatrix}. $$

3.4.2. The vector H is almost never in a fixed plane, when $N = 5$

We show that H does not stay in a fixed plane of $\mathbb{R}^4$ when s varies.

Proposition 3.12. *Let $\mathcal{P}$ be a plane in $\mathbb{R}^4$. Let $a_1, a_2, a_3, a_4 \in \mathbb{R}^+$ summing up to 1. Then the set $\{s \in (0,\pi) \mid H(a_1,a_2,a_3,a_4,s) \in \mathcal{P}\}$ is finite.*

We first show:

Lemma 3.13. *The matrix Q has rank 3.*

Proof. — Since the vector $V = {}^t(\ a_1 \quad a_2 \quad a_3 \quad a_4\ )$ is normal to G, and $H = Im(G)$, the relation $\sum_{i=1}^4 a_i R_i(Q) = 0$ holds, where $R_i(Q)$ denotes the i-th row of Q (i.e. the i-th column of ${}^tQ$). It means that Q has rank at most 3.

Moreover the minor of ${}^tQ$ formed by the first three columns and the fourth, fifth and eighth rows of ${}^tQ$ is:

$$ \begin{vmatrix} a_3+a_4 & a_3+a_4 & -(a_1+a_2)+a_4 \\ 0 & a_4 & a_4 \\ 0 & -(a_3+a_4) & a_2 \end{vmatrix} = (a_3+a_4)a_4(a_2+a_3+a_4) > 0. $$

The matrix Q has hence rank at least 3. ∎

Proof (Proof of Proposition 3.12). — The map

$$ \mathbf{H} : \begin{array}{ccc} [0,\pi] & \longrightarrow & \mathbb{R}^4 \\ s & \mapsto & H(a_1,a_2,a_3,a_4,s) \end{array} $$

is analytic. If $\mathbf{H}(s)$ were lying in $\mathcal{P}$ for all s in a subinterval J of $[0,\pi]$, then we would have two linearly independent relations

$$ \begin{cases} \sum_i \mu_i \sin(\theta_i s) = 0 \\ \sum_i \lambda_i \sin(\theta_i s) = 0 \end{cases} $$

where the numbers θ_i are sums of a_j with consecutive indices. Since G is normal to v, the first relation holds if $\mu = v$. But Q has rank 3 and $s \mapsto \sin((a_1 + a_2 + a_2 + a_3 + a_4)s) = sin(s)$ is linearly independent of all other maps $s \mapsto \sin(\theta s)$ for $\theta \neq \pm 1$. Therefore the second relation cannot hold for all $s \in J$.

Moreover, the zeros of the analytic map $s \in [0, \pi] \mapsto \sum_i \lambda \sin(\theta_i s)$ are discrete, and in finite number in the compact $[0, \pi]$. This proves Proposition 3.12

■

3.4.3. For $N > 5$

As in the case $N = 5$, we consider H the imaginary part of G:

$$H = Im\left(\frac{1}{m}\begin{pmatrix} f_1 \\ \vdots \\ f_{N-1}\end{pmatrix} - \begin{pmatrix} 1 \\ \vdots \\ 1\end{pmatrix}\right) = \frac{1}{|m|^2} Im\left(\overline{m}\begin{pmatrix} f_1 \\ \vdots \\ f_{N-1}\end{pmatrix}\right).$$

All coordinates of $|m|^2 H$ are of the form $\sum \lambda_i \sin(\theta_i s)$ where $s = \frac{1}{r}$, the numbers θ_i are sums of a_j with consecutive indices, and the coefficients λ_i are sums of $\pm a_j$. We can write $|m|^2 H$ as $|m|^2 H = Q\Theta$ where the matrix $Q \in \mathcal{M}_{\frac{(N-1)N}{2}, N-1}(\mathbb{R})$ has all of its coefficients in the set $\{0, \lambda_i\}$ and the vector $\Theta \in \mathcal{M}_{\frac{(N-1)N}{2}, 1}$ has all of its coordinates of the form $\sin(\theta_i s)$. We order this coordinates by lexical order on (number of terms a_j within the sum $\theta_i = \sum_j a_j$; number of the first index j), so that:

$$\Theta = \begin{pmatrix} \sin(a_1 s) \\ \vdots \\ \sin(a_{N-1} s) \\ \sin((a_1 + a_2)s) \\ \vdots \\ \sin((a_{N-2} + a_{N-1})s) \\ \sin((a_1 + a_2 + a_3)s) \\ \vdots \\ \sin((a_{N-3} + a_{N-2} + a_{N-1})s) \\ \vdots \\ \vdots \\ \sin((a_1 + a_2 + ... + a_{N-2})s) \\ \sin((a_2 + a_3 + ... + a_{N-1})s) \\ \sin((a_1 + a_2 + ... + a_{N-1})s) \end{pmatrix}.$$

One can check that lots of coordinates of Q are zero. In the following we only

need to consider a submatrix of Q.

Lemma 3.14. *The matrix $Q \in \mathcal{M}_{\frac{(N-1)N}{2},N-1}(\mathbb{R})$ has rank at least $N-3$, at most $N-2$, and exactly $N-2$ when N is odd.*

Remark 3.15. *I conjecture that Q has rank $N-2$ when N is even as well, but the expression of the determinant can not be simplified as for the case where N is odd.*

Proof. — As in the case $N=5$, G is normal to the vector $V = {}^t(\ a_1 \quad \dots \quad a_{N-1}\ )$, which implies that Q has rank at most $N-2$.

The submatrix of ${}^tQ$ made of the first $N-1$ rows and $N-2$ columns is:

$$\begin{pmatrix}
\sum_{k=2}^{N-1} a_k & -a_1+\sum_{k=3}^{N-1} a_k & -(a_1+a_2) & \cdots & -(a_1+a_2) \\
a_2+a_3 & -a_1+a_3 & -(a_1+a_2) & 0 & 0 \\
0 & a_3+a_4 & -a_2+a_4 & & 0 \\
 & & a_4+a_5 & & \\
 & & & -a_{N-4}+a_{N-2} & -a_{N-4}-a_{N-3} \\
0 & & & 0\ \ a_{N-2}+a_{N-1} & -a_{N-3}+a_{N-1} \\
a_{N-2}+a_{N-1} & & & a_{N-2}+a_{N-1} & -(\sum_{k=2}^{N-3} a_k)+a_{N-1}
\end{pmatrix}$$

Note that the framed submatrix formed by the rows $2,..,N-2$ and first $N-3$ columns of ${}^tQ$ is an invertible diagonal matrix, so Q has rank at least $N-3$.

We show now that if N is odd, Q has rank at least $N-2$. We replace the j-th column C_j of ${}^tQ$ by $C_j + \sum_{k=1}^{j-1}(-1)^{j-k}C_k$. The rows between 2 and $N-1$ and the first $N-2$ columns of this new matrix are equal to (changes are written in blue):

$$\begin{pmatrix}
a_2+a_3 & -a_1-a_2 & 0 & 0 & 0 \\
0 & a_3+a_4 & -a_2-a_3 & 0 & \\
 & & a_4+a_5 & -a_3-a_4 & \\
 & & & -a_{N-4}-a_{N-3} & 0 \\
0 & & & 0\ \ a_{N-2}+a_{N-1} & -a_{N-3}-a_{N-2} \\
a_{N-2}+a_{N-1} & 0 & a_{N-2}+a_{N-1} & 0 & -(\sum_{k=2}^{N-3} a_k)+a_{N-1}
\end{pmatrix}$$

We develop the determinant Δ with respect to the last row of this submatrix

and get:

$$\begin{aligned}\Delta =&(a_{N-2}+a_{N-1})[(-a_1-a_2)(-a_2-a_3)...(-a_{N-3}-a_{N-2})\\ &+(a_2+a_3)(a_3+a_4)(-a_3-a_4)...(-a_{N-3}-a_{N-2})\\ &+(a_2+a_3)(a_3+a_4)(a_4+a_5)(a_5+a_6)(-a_5-a_6)...(-a_{N-3}-a_{N-2})\\ &+(a_2+a_3)(a_3+a_4)...(a_7+a_8)(-a_7-a_8)...(-a_{N-3}-a_{N-2})\\ &\vdots\\ &+(a_2+a_3)(a_3+a_4)...(a_{N-4}+a_{N-3})(-a_{N-3}-a_{N-2})]\\ +&\left(-\sum_{k=1}^{N-3}a_k+a_{N-1}\right)(a_2+a_3)(a_3+a_4)...(a_{N-3}+a_{N-2})(a_{N-2}+a_{N-1}),\end{aligned}$$

that we rewrite in:

$$\begin{aligned}\Delta =&(a_{N-2}+a_{N-1})\left[(-1)^{N-3}\prod_{k=1}^{N-3}(a_k+a_{k+1})+\sum_{\substack{l=3\\ l\text{ odd}}}^{N-3}\left((a_l+a_{l+1})(-1)^{N-3-l+1}\prod_{k=2}^{N-3}(a_k+a_{k+1})\right)\right]\\ &+\left(-\sum_{k=1}^{N-3}a_k+a_{N-1}\right)\prod_{k=2}^{N-2}(a_k+a_{k+1}).\end{aligned}$$

Luckily, this long expression can be simplified:

$$\begin{aligned}\Delta &= \prod_{k=2}^{N-2}(a_k+a_{k+1})\left[\sum_{k=1}^{N-3}a_k-\sum_{k=1}^{N-3}a_k+a_{N-1}\right]\\ &= a_{N-1}\prod_{k=2}^{N-2}(a_k+a_{k+1})\neq 0.\end{aligned}$$

We conclude that if N is odd, then Q has rank exactly $N-2$. ■

As for the case $N=5$, the map

$$\mathbf{H}:\begin{array}{ccc}[0,\pi] & \longrightarrow & \mathbb{C}^{N-1}\\ s & \mapsto & H(a_1,...,a_{N-1},s)=Q\Theta\end{array}$$

is analytic. With Lemma 3.14, it allows us to prove the following proposition.

Proposition 3.16. *Let $\mathcal{P}$ be a subspace of dimension $N-3$ in $\mathbb{C}^{N-1}$. Let $a=(a_1,...,a_{N-1})\in(\mathbb{R}_+^*)^{N-1}$ summing up to 1 and Oseledets generic. The set $\{s\in(0,\pi)\mid H(a,s)\in\mathcal{P}\}$ is finite. Moreover, if N is odd, the statement holds also for $\mathcal{P}$ a subspace of dimension $N-2$ in $\mathbb{C}^{N-1}$.*

3.4.4. Conclusion

As a corollary we get Theorems A and B.

Theorem A. *For almost every parameters $a_1, ..., a_{N+1}, \tau$ satisfying (C), the trajectories with parameter τ in the $P(a_1, ..., a_{N+1})$-generalized tiling billiard do not stay at a bounded distance from any line.*

Theorem B. *Let $N \in \mathbb{N}, N \geqslant 5$. There exist $\theta_1 > \theta_2 > \theta_3 > 0$ such that for almost every N-gon P and every τ, satisfying condition (C), for any initial direction having parameter τ in a P-tiling billiard, the sequence of points $(p_n)_{n\in\mathbb{N}}$ satisfies:*

$$\limsup_{n\to\infty} \frac{\log|p_n - nm|}{\log n} = \begin{cases} \frac{\theta_2}{\theta_1} > 0 & \text{if } N \text{ is odd} \\ \frac{\theta_2}{\theta_1} \text{ or } \frac{\theta_3}{\theta_1} > 0 & \text{if } N \text{ is even} \end{cases}$$

where $m = \lim_{n\to\infty} \frac{p_n}{n}$ is the asymptotic direction of the trajectory.

Proof. — Recall that the function g is in $Ann(\mathcal{H}_1)$ (because it has 0 mean). Let $\mathcal{P} = Ann(\mathcal{H}_3)$ (or $Ann(\mathcal{H}_2)$ if Q has rank $N-2$). Proposition 3.16 tells that for almost every choice of parameters, h is not in $\mathcal{P}$. The proposition 3.11 applied to h hence establishes Theorem B:

$$\begin{aligned} |p_{2n} - 2nm| &= |S_n h(x_0)| + R_n \quad \text{where } R_n \text{ is uniformly bounded} \\ \limsup_{n\to+\infty} \frac{\log|p_{2n} - 2nm|}{\log(2n)} &= \limsup_{n\to+\infty} \frac{\log|S_n h(x_0)|}{\log(n)} \\ &= \frac{\theta}{\theta_2} \end{aligned}$$

where $\theta = \theta_2$ if N is odd, and $\theta \in \{\theta_2, \theta_3\}$ if N is even.

Moreover we have renormalized our problem to the case when the asymptotic direction is horizontal and we have studied the imaginary part of the deviations, this hence proves also Theorem A. ∎

3.5. A special case

The previous theorems tells nothing when our IET T is not Oseledets generic. The goal of this section is to study a non-generic but important case for which we manage to do explicit computations, and prove Theorem C.

Let M be the matrix associated to a loop in the Rauzy diagram. Then M is positive. We assume that the loop is complex enough so that M is primitive. We assume that the second eigenvalue λ_2 of M is simple, that M has no other eigenvalue of the same modulus than λ_2, and $|\lambda_2| > 1$. The article [Ham23] implies that this is the generic behavior. It follows that $\lambda \in \mathbb{R}$. We denote by V the Perron Frobenius vector for M, normalized so that its coordinates sum up to 1 and set $(a_1, ..., a_{N-1}) = V$. The IET with lengths $(a_1, ..., a_{N-1})$ is self similar and uniquely ergodic. Section 3.3.3 applies: the mean m of f (corresponding to the asymptotic

direction) does not vanish for almost every choice of $a_N > \sum_{k=1}^{N-1} a_k$. We will now compute the order of magnitude of deviations.

We denote by W_1 the Perron Frobenius eigenvector for ${}^tM$ (normalized so that its coordinates sum up to 1) and by W_2 its (normalized) eigenvector associated to the second eigenvalue λ_2. Note that W_2 is a real vector since M and λ are real. We decompose $\mathbb{R}^{N-1} = \text{Vect}(W_1) \oplus \text{Vect}(W_2) \oplus E_3$ where E_3 is the direct sum of characteristic spaces of ${}^tM$ (associated to eigenvalues $\lambda_3, \dots, \lambda_d$). By assumption:

$$\forall v \in E_3, \frac{||{}^tMv||}{||v||} \leqslant |\lambda_3| < |\lambda_2|.$$

We consider cases where $a_N > \sum_{k=1}^{N-1} a_k$ is such that $H \notin E_3$. According to Proposition 3.16, this is all cases but finitely many ones.

3.5.1. Upper bound

If $w = w_0 w_1 ... w_{n-1}$ is a finite word over the alphabet $\{1, ..., N-1\}$, we set $e_w = \sum_{k=0}^{n-1} e_{w_k}$.

Let $x \in \mathbb{S}^1$ and let $\overline{x}_n = x_0 x_1 ... x_{n-1}$ be the prefix of length n of its symbolic coding $\overline{x}$ under T, decomposed as (see Proposition 2.21)

$$\overline{x}_n = s_0 \sigma(s_1) ... \sigma^{l-1}(s_{l-1}) \sigma^l(m_l) \sigma^{l-1}(p_{l-1}) ... \sigma(p_1) p_0.$$

One has:

$$e_{\overline{x}_n} = \sum_{k=0}^{l-1} M^k e_{s_k} + M^l e_{m_l} + \sum_{k=0}^{l-1} M^k e_{p_k}.$$

The deviations from the mean displacement (normalized to be horizontal at unit-speed) are approximated by:

$$\begin{aligned} S_n h(x) &= \sum_{k=0}^{n-1} h(T^k(x)) \\ &= < H, e_{\overline{x}_n} > \\ &= \sum_{k=0}^{l-1} < {}^tM^k H, e_{s_k} + e_{p_k} > + < {}^tM^l H, e_{m_l} > \end{aligned}$$

The vector $H = Im(G)$ is in the vector space $\text{Vect}(W_2) \oplus E_3$ because G is normal to the Perron-Frobenius vector V of M, and $H \notin E_3$. It can therefore be decomposed as $G_I = \alpha W_2 + U$ with $U \in E_3$ and $\alpha \in \mathbb{R}^*$. Then one has:

$$S_n h(x) = \alpha \left(\sum_{k=0}^{l-1} < {}^t M^k W_2, e_{s_k} + e_{p_k} > + < {}^t M^l W_2, e_{m_l} > \right) + \sum_{k=0}^{l-1} < {}^t M^k U, e_{s_k} + e_{p_k} > + < {}^t M^l U, e_{m_l} > .$$

We write

$$P_1 = \alpha \left(\sum_{k=0}^{l-1} < {}^t M^k W_2, e_{s_k} + e_{p_k} > + < {}^t M^l W_2, e_{m_l} > \right)$$

and

$$P_2 = \sum_{k=0}^{l-1} < {}^t M^k U, e_{s_k} + e_{p_k} > + < {}^t M^l U, e_{m_l} >.$$

The principal part of the deviations is given by:

$$P_1 = \alpha \left(\sum_{k=0}^{l-1} \lambda_2^k < W_2, e_{s_k} + e_{p_k} > + z\lambda_2^l < W_2, e_{m_l} > \right)$$

whose norm is dominated by:

$$|\alpha||\lambda_2|^l \frac{|\lambda_2|}{|\lambda_2| - 1} 2(K-1)||W_2||_\infty$$

where K is such that all s_k and p_k are at length at most $K-1$ and m_l at most $2K-2$ (see Proposition 2.21). The other part of the deviations, P_2, whose norm is dominated by $|\lambda_3|^l \frac{|\lambda_3|}{|\lambda_3|-1} 2(K-1)||U||_\infty$, has a smaller order. To sum up, we have, for l big enough:

$$|S_n g(x)| \leqslant D\lambda_2^l$$

with $D = \alpha \frac{\lambda_2}{\lambda_2 - 1} 2(K-1)||W_2||_\infty + 1$.

Finally, using Corollary 2.24, one gets, for n big enough:

$$|S_n g(x)| \leqslant D' n^{\frac{\log(\lambda_2)}{\log(\lambda_1)}}$$

with $D' = D \exp\left(\frac{\log(\lambda_2)\log(A)}{\log(\lambda_1)}\right)$. One can replace D' by a larger constant C_1 so that the inequality

$$|S_n g(x)| \leqslant C_1 n^{\frac{\log(\lambda_2)}{\log(\lambda_1)}}$$

is true for all $n \in \mathbb{N}$.

This shows the first inequality of Theorem C. We prove the second one in the following paragraph.

3.5.2. Lower bound

We want to build an increasing sequence $(n_l)_{l\in\mathbb{N}}$ of indices of "significant deviations", in other words such that

$$(\star) \qquad \exists C_2, \forall l \geqslant l_0, |S_{n_l}h(x)| > C_2 n_l^{\frac{\log\lambda_2}{\log\lambda_1}}.$$

Let l be an integer. We decompose the symbolic coding of x as

$$\overline{x} = s_0\sigma(s_1)...\sigma^{l-1}(s_{l-1})\sigma^l(w)$$

where the s_i are finite words of length at most $K-1$ (see Proposition 2.21) and w is an infinite word. This corresponds to decompose the orbit of x with Rokhlin towers of order l.

Let us denote by π_j (for $1 \leqslant j \leqslant 2$) the projection onto $\mathrm{Vect}(W_j)$ and π_3 the one onto E_3 with respect to the decomposition $\mathbb{R}^{N-1} = \mathrm{Vect}(W_1) \oplus \mathrm{Vect}(W_2) \oplus E_3$.

Let us set $m_l = |s_0\sigma(s_1)...\sigma^{l-1}(s_{l-1})|$, corresponding to the hight of the partial Rokhlin tower before the orbit of x_0 arrives at the bottom of a tower of order l.

If $|S_{m_l}h(x)| > |\lambda_2|^l$, then we define $n_l = m_l$ and we have:

$$|S_{m_l}h(x)| > |\lambda_2|^l \geqslant D|\lambda_2|^{\frac{\log(n_l)}{\log(\lambda_1)}} = Dn_l^{\frac{\log(|\lambda_2|)}{\log(\lambda_1)}}$$

with $D = exp(\frac{-C}{\log(\lambda_1)})$ (where C is the constant given by Corollary 2.24).

Else ($|S_{m_l}h(x)| \leqslant |\lambda_2|^l$). At least one vector e_k of the canonical basis of $\mathbb{R}^{N-1}$ is such that $\pi_2(e_k) \neq 0$. Let i be such that $\pi_2(e_{w_i}) \neq 0$ and for every index $j < i$, $\pi_2(e_{w_j}) = 0$. The matrix M is primitive, so is the substitution σ. Hence there exists L (which depends only on M, not on w) such that $i \leqslant L$. Let us set $m'_l = |\sigma^l(w_1...w_{i-1})|$ and $m''_l = |\sigma^l(w_i)|$. We define n_l as the length $|s_0\sigma(s_1)...\sigma^{l-1}(s_{l-1})\sigma^l(w_1...w_i)| = m_l + m'_l + m''_l$. Then we have:

$$\begin{aligned}|S_{n_l}h(x)| &= |S_{m_l}h(x) + S_{m'_l}h(T^{m_l}(x)) + S_{m''_l}h(T^{m_l+m'_l}(x))| \\ &\geqslant |S_{m''_l}h(T^{m_l+m'_l}(x))| - |S_{m_l}h(x)| - |S_{m'_l}h(T^{m_l}(x))|\end{aligned}$$

By hypothesis, one has

$$|S_{m_l}h(x)| \leqslant |\lambda_2|^l.$$

By definition of i, if we set $c = \max_{1\leqslant k\leqslant N-1} |\pi_3(e_k)|$, one has

$$|S_{m'_l}h(T^{m_l}(x))| \leqslant c|\lambda_3|^i \leqslant c|\lambda_3|^L.$$

Finally

$$\begin{aligned}\left|S_{m_l''}h\left(T^{m_l+m_l'}(x)\right)\right| &= \left|< {}^tM^lH, e_{w_i} >\right| \\ &\geqslant |\alpha|\left|\lambda_2^l < W_2, e_{w_i} >\right| - \left|< {}^tM^lU, e_{w_i} >\right| \\ &\geqslant |\alpha|\,|\lambda_2|^l - c|\lambda_3|^l||U||.\end{aligned}$$

Putting these inequalities together we conclude that, for l big enough:

$$|S_{n_l}h(x)| \geqslant \frac{|\alpha|}{2}|\lambda_2|^l \geqslant \frac{|\alpha|}{2}D|\lambda_2|^{\frac{\log(n_l)}{\log(\lambda_1)}} = \frac{|\alpha|}{2}Dn_l^{\frac{\log(|\lambda_2|)}{\log(\lambda_1)}}.$$

In the first case $|S_{m_l}h(x)| > |\lambda|^l$ so m_l goes to infinity as l increases and in the second case $n_l \geqslant m_l'' \geqslant A\lambda_1^l$ (Lemma 2.23). Therefore the sequence $(n_l)_{l\in\mathbb{N}}$ goes to infinity. If we set

$$C_2 = \frac{|\alpha|}{2}D = \frac{|\alpha|}{4}exp(\frac{-C}{\log(\lambda_1)}),$$

the inequality $(\star)$ holds for $l \in \mathbb{N}$ big enough, which gives the second inequality of Theorem C.

3.6. Concluding remarks

In this chapter we assumed that the N-gons are inscribed in a half-circle [1] and we studied trajectories passing near the circumcenter of the polygons. In this section, we discuss briefly the obstacles to remove such assumptions. We recall the key elements to prove Theorems A, B and C.

(1) We can study the trajectory via an IETF Φ because the N-gon is cyclic.

(2) The square Φ^2 of this map stabilizes a subinterval J, and $\Phi^2_{|J}$ is an IET with $N-1$ intervals of continuity. We do not need assumption to ensure that Φ^2 does not flip any interval, but we do need the assumption on the parameter τ of the trajectory to ensure that $\Phi^2_{|J}$ has only $N-1$ intervals of continuity.

(3) We can define a function f of displacement, that is piecewise constant and depends analytically on the lengths of the N-gon. As well as f, the function $h = Im(\frac{1}{m}f - 1)$ is piecewise constant and depends analytically on the lengths of the N-gon.

(4) We can show that for any fixed codimension 3 (or 2 if N is odd) subspace E of $\mathbb{R}^{N-1}$, for almost every lengths of the N-gon, the vector H, whose coordinates are the values of the function $h = Im(\frac{1}{m}f - 1)$, is not in E. This relies strongly on the fact that we have an explicit expression of H.

1. The parameters $(a_1, \ldots, a_N)$ corresponding to polygons inscribed in a half-circle occupy a proportion $\frac{N}{2^N}$ of set of parameters corresponding to any cyclic N-gons, i.e. the $N-1$ dimensional simplex.

We could overcome point (2) by studying the Rauzy-Nogueira diagram of the underlying permutation of Φ. We would get many open sets of parameters, each one associated to a new map, that is a renormalization of Φ. So far, we can again define a function f of displacement and even ensure that it is analytic. But if we want to conclude, we need to have an explicit expression of the function f for each open set of parameters. These open sets depend on paths in the Rauzy-Nogueira diagram in question. The trouble is that this diagram, for $N = 5$, has more than 1 million of vertices and more than 3 millions of edges! Hence establishing the apropriate open sets seems out of reach without another idea, either about how we cut the set of parameters, or about how we show that H is not in E for almost every lengths of the N-gon.

4. Bi-triangle tiling billiards

4.1. Introduction

4.1.1. The bi-triangle tiling

We are interested in a generalization of the usual triangle tiling billiard, presented in the introduction (Section 1.1.2.a). Let δ_1 and δ_2 be two triangles with an angle of the same measure such that their circumcircles have the same radius. The triangles δ_1 and δ_2 hence have a side of same length, see Figure 4.1a. We tile the plane with them as in Figure 4.1b. The condition on the common circumcircle is crucial so that we can translate our problem into the study of an IETF (see Section 3.2.2 for details of the association of an IETF to a tiling billiard). This chapter gives the first results of an ongoing project whose goal is to exhibit a family of exceptional trajectories, that are not linearly escaping (just as case (4) of the Theorem 1 stated in the introduction).

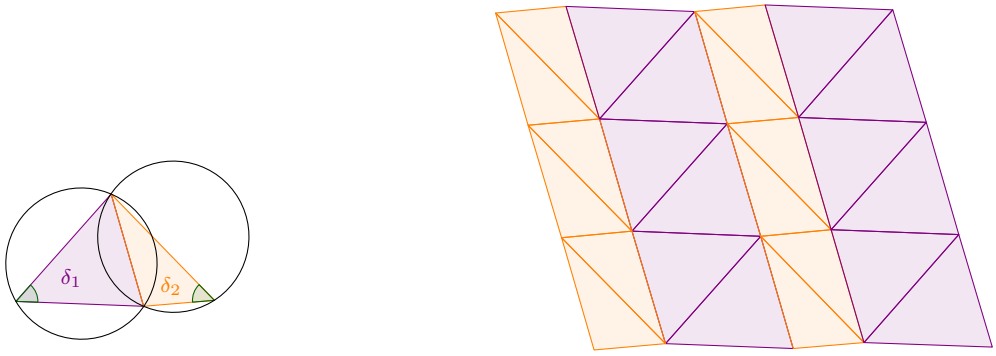

(a) The two triangles (b) The bi-triangle tiling

Figure 4.1. – Setting for bi-triangle tiling billiards

4.1.2. Motivations

We have many motivations to look at this system. Of course, it is a natural generalization of the triangle tiling billiard. This generalization is interesting for (at least) two reasons.

The bi-triangle tiling is *locally foldable*: there are an even number of tiles meeting at each vertex of the tiling, and the alternated sum of the angles around a vertex is always equal to 0. If $\mathcal{T}$ is a locally foldable tiling, then we can associate to the

$\mathcal{T}$-tiling billiard a one parameter family $\{\mathcal{D}_\tau\}_{\tau\in[0,2\pi)}$ of surfaces [Par21], each of them called *Dynnikov's helicoid*. A surface $\mathcal{D} = \mathcal{D}_\tau$ is an oriented surface in $\mathbb{R}^3$, periodic in three directions: there exist three independent vectors $u, v, w \in \mathbb{R}^3$ such that $\mathcal{D} + u = \mathcal{D} + v = \mathcal{D} + w = \mathcal{D}$. Moreover, each connected component of the intersection $\mathcal{P} \cap \mathcal{D}_\tau$ of a horizontal plane $\mathcal{P}$ with $\mathcal{D}_\tau$ is a trajectory with parameter τ (see Section 3.2.2) of the $\mathcal{T}$-tiling billiard. Since $\mathcal{D}$ is triply periodic, we can consider the quotient surface of $\mathcal{D}$ by the lattice spanned by u, v and w. In the case of mono-triangle and cyclic quadrilateral tiling billiards, the quotient surface $\mathcal{S}$ has genus 3 and is centrally symmetric. However, for bi-triangle tiling billiards, the surface $\mathcal{S}$ has genus 5.

Motivated by a question on the motion of electrons in metals, Novikov [Nov82] asked the following

Question 4.1 (Novikov problem). *Let $\Lambda \subset \mathbb{R}^3$ be a lattice, let $\mathcal{S} \subset \mathbb{R}^3$ be a Λ-invariant surface, and let $\mathcal{P}$ be an affine plane. How behaves the intersection $\mathcal{S} \cap \mathcal{P}$ in the quotient $\mathcal{S}/\Lambda$?*

The authors of [DHMPS] show that if $\mathcal{S}$ has genus 3, then Novikov problem reduces to the study of a triangle or cyclic quadrilateral tiling billiard. The bi-triangle tiling billiard gives a surface with higher genus for the Novikov's problem.

This work is also a step forward in the understanding of *admissible* tiling billiards (see Section 4.4.2). I think that these two directions of research are exciting, although I had not enough time to investigate them further. They are interesting future perspectives.

4.2. The associated IETFs

As for triangle tiling billiards, or generalized tiling billiard, one studies the bi-triangle tiling billiards via circle exchange transformations with flips. The relevant difference between the previous settings and the bi-triangle tiling is the number of distinct polygons. As we will see in Section 4.2.1, the bi-triangle tiling billiard leads to an interval exchange transformation defined on the union of two circles. Of course, we could decide to cut each circle and consider the IETF as defined on a union of intervals, with (in general) one more interval of continuity in each circle. We could also glue the intervals of the domain together so that we get an IETF defined on an interval. But we prefer not to, for two reasons. The first reason is that it is closer to our tiling billiards problem: each interval of continuity corresponds to a side of a polygon of the tiling. The second reason is that it simplifies the combinatorial data to consider, and decreases the (already important) number of cases to study in the induction.

Let us first introduce some notations, illustrated in Figure 4.2. For $i \in \{1, 2\}$:

- Label clockwise the side of δ_i by A_i, B_i, C_i such that each copy of A_1 in the tiling coincide with a copy of A_2. A_1 and A_2 denote the "common" side of δ_1 and δ_2.

- Denote by v_i the vertex between A_i and C_i.

We normalize the situation so that the circumcircles $\mathcal{C}_1$ of δ_1 and $\mathcal{C}_2$ of δ_2 have radius equal to $\frac{1}{2\pi}$. For $i \in \{1, 2\}$, denote by a_i (resp. b_1, c_i) the length of the arc of $\mathcal{C}_i$ which is subtended by the side A_i (resp. B_1, C_i). Then the renormalization is so that $a_1 + b_1 + c_1 = a_2 + b_2 + c_2 = 1$.

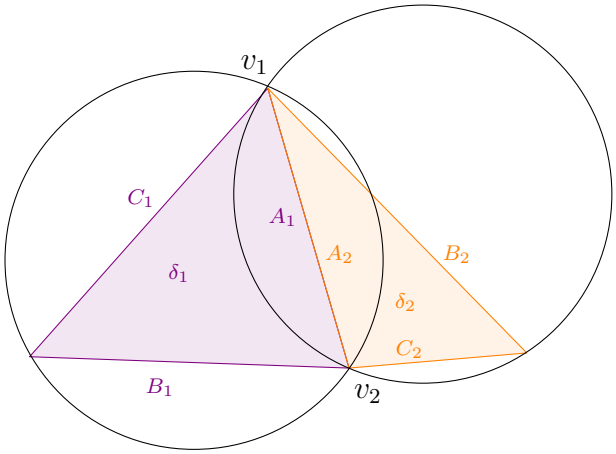

Figure 4.2. – Notation for the bi-triangle tiling billiard

4.2.1. How to associated an IETF to a bi-triangle tiling billiard

We consider the convenient frame of reference of Section 3.2.2, that is the one of an ant that would follow this trajectory. At each step, the ant can see the polygon it is crossing and its circumcircle. The ant can describe its trajectory by giving the following data, for each segment of the trajectory:

(1) whether it lies on a copy of δ_1 or δ_2,

(2) which chord of the circumcircle $\mathcal{C}$ of the crossed triangle the ant is following,

(3) where the copy of v_i lies on $\mathcal{C}$

We recall the beautiful argument of folding given in [BDFI24]. If we fold the plane along the k-th crossed side, then the $(k+1)$-th segment of the trajectory folds on the k-th segment of the trajectory, because of the refraction law. The circumcircles of the k-th and $(k+1)$-th triangles fold onto each other. This is why the data (2) is a parameter of the trajectory. We denote it τ. We consider the sequence $(x_k, i_k)_{k\in\mathbb{N}}$ where

- The k-th step of the trajectory lies in a copy of δ_{i_k}, say $\varphi(\delta_{i_k})$ with φ an isometry of $\mathbb{R}^2$.
- x_k is the length of the arc of $\varphi(\mathcal{C}_{i_k})$ between o and $\varphi(v_{i_k})$, where o is the point of $\varphi(\mathcal{C}_{i_k})$ where the k-th segment of the trajectory would arrive if going on in straight line after the side crossing.

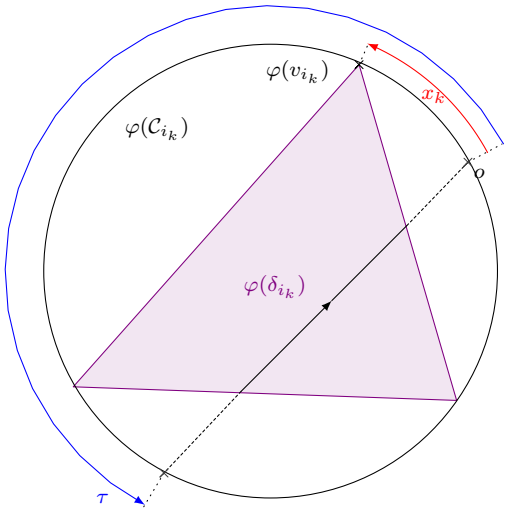

Figure 4.3. – Notations for the frame of reference to study the bi-triangle tiling billiard

See Figure 4.3 for an illustration of notations.

The sequence $(x_k, i_k)_{k\in\mathbb{N}}$ describes completely the bi-triangle tiling billiard's trajectory followed by the ant. The crucial point is that the map

$$T : (x_k, i_k) \mapsto (x_{k+1}, i_{k+1}) \tag{4.1}$$

is an IETF on a union of two circles $\mathcal{C}_1 \cup \mathcal{C}_2 \cong \mathcal{C} \times \{1, 2\}$. Before describing this map in Section 4.2.3, we explain how to describe an IETF defined on a union of several circles.

4.2.2. Description of an IETF defined on a union of d circles

As for IETs with or without flips defined on an interval, the transformation is determined by a combinatorial data and a vector of parameters (lengths data). The pair of permutations (π_0, π_1) is replaced by d pairs$\left(\left(\sigma_0^{(1)}, \sigma_1^{(1)}\right), \ldots, \left(\sigma_0^{(d)}, \sigma_1^{(d)}\right)\right)$ where:

$$\forall i \in \{0, 1\}, \forall k \in \{1, 2\},\ \sigma_i^{(k)} : \mathcal{A}_i^{(k)} \to \{1, 2, 3\} \text{ is a bijection,}$$

$$\begin{cases} \mathcal{A}_0^{(k)} & \text{is the set of labels of intervals of continuity of the circle } k \\ \mathcal{A}_1^{(k)} & \text{is the set of labels of intervals whose images are in the circle } k \end{cases}.$$

The lengths data consists of the lengths of all intervals of continuity (as in the usual setting), plus the *parameter of shift* τ_i on each circle (see Figure 4.5). The parameter of shift is defined in the following way. Let $x_0^{(i)}$ (resp. $x_1^{(i)}$) be the left

endpoint of the interval labeled $\left(\sigma_0^{(i)}\right)^{-1}(1)$ (resp. of the image of the interval labeled $\left(\sigma_1^{(i)}\right)^{-1}(1)$). We define

$$\tau_i = x_1^{(i)} - x_0^{(i)} \in \mathcal{C}_i. \tag{4.2}$$

Finally, the data of flipped intervals is as usual a subset of the set of labels: $F \subset \mathcal{A} = \sqcup \mathcal{A}_0^{(k)}$. In this entire chapter, all intervals are flipped: $F = \mathcal{A}$. In Chapter 3, we denoted the labels that are flipped with an overline in the permutation. Here, since all intervals are flipped, this data is not relevant and we decide to never put overline to simplify notations.

Say that two IETFs have the same combinatorial type if their d pairs of permutations $\left(\left(\sigma_0^{(1)}, \sigma_1^{(1)}\right), \ldots, \left(\sigma_0^{(d)}, \sigma_1^{(d)}\right)\right)$ and $\left(\left(\rho_0^{(1)}, \rho_1^{(1)}\right), \ldots, \left(\rho_0^{(d)}, \rho_1^{(d)}\right)\right)$ are equivalent, that is when there exist $\nu \in \mathfrak{S}_{|\mathcal{A}|}$, and $\zeta \in \mathfrak{S}_d$, such that $\forall i \in \{0,1\}, \forall k \in \{1,..,d\}$, there exists $l \in \{0,1,2\}$, such that:

$$\nu \circ \rho_i^{(\zeta(k))} = \nu \circ (1\,2\,3)^l \circ \sigma_i^{(k)}. \tag{4.3}$$

This equivalence corresponds to forgetting the order of the circles (with the permutation ζ), not to specify the origin 0 of the domain (resp. image) circle, and renaming the labels by the permutation ν.

4.2.3. The IETFs associated to the bi-triangle tiling billiards

The computations done in the proof of Theorem 3.7 give the expression of T in the case where the trajectory stay in the same triangle after refraction, i.e. whener the crossed side is B_i or C_i ($i \in \{1,2\}$):

$$\begin{array}{lll} x_{k+1} = \tau + a_i + b_i - (x_k - a_i) & \text{if } a_i < x_k < a_i + b_i & \text{(crossed side } B_i\text{)} \\ x_{k+1} = \tau + a_i + b_i + c_i - (x_k - a_i - b_i) & \text{if } a_i + b_i < x_k < a_i + b_i + c_i & \text{(crossed side } C_i\text{).} \end{array}$$

Moreover we have

$$i_{k+1} = i_k.$$

Figure 4.4 illustrates the configuration when the trajectory crosses the "common" side of the two triangle.

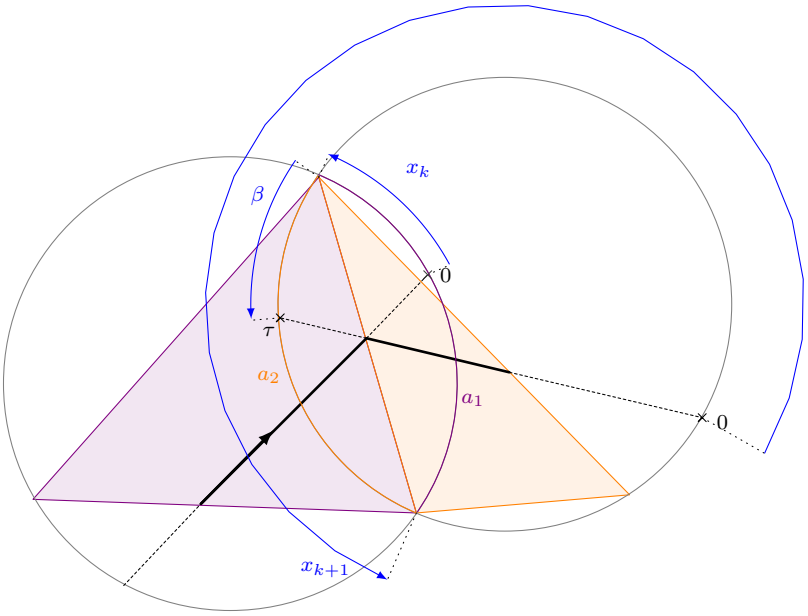

Figure 4.4. – Coordinates x_{k+1} and x_k are related by a linear equation

Because of the refraction law, we have $\beta = x_k$. Hence, $x_{k+1} = \tau - x_k + a_2$ whenever the trajectory crosses the side A_1 going from δ_1 to δ_2. Symmetrically, $x_{k+1} = \tau - x_k + a_1$ whenever the trajectory crosses the side A_2 going from δ_2 to δ_1. Since $a_1 = a_2$, writing $a = a_1 = a_2$, this reduces in both cases to

$$x_{k+1} = \tau - x_k + a.$$

Moreover, since the trajectory goes from a triangle to the other one, we have

$$i_{k+1} = i_k + 1 \mod 2.$$

To sum up in other words, the transformation cuts both circles into three intervals. One of the three intervals is sent on the other circle, whereas the two other ones stay on the same circle. All intervals are flipped. See Figure 4.5 (where each circle is pictured as a segment with identified endpoints).

4.2.3.a. Combinatorial data

The combinatorial data (up to combinatorial type equivalence) is the following pair of permutations

$$p_1 = \left\{ \circlearrowleft \begin{pmatrix} A_1 & B_1 & C_1 \\ A_2 & B_1 & C_1 \end{pmatrix} \circlearrowright, \circlearrowleft \begin{pmatrix} A_2 & B_2 & C_2 \\ A_1 & B_2 & C_2 \end{pmatrix} \circlearrowright \right\}.$$

We denote the fact that T acts on a circle and not on an interval with the parentheses $\oint$ and $\oint$. We highlight that in particular an IETF with combinatorial data $\oint \begin{pmatrix} A & B & C \\ A & B & C \end{pmatrix} \oint$ is not necessarily an involution, there is a parameter τ of shift (defined by 4.2).

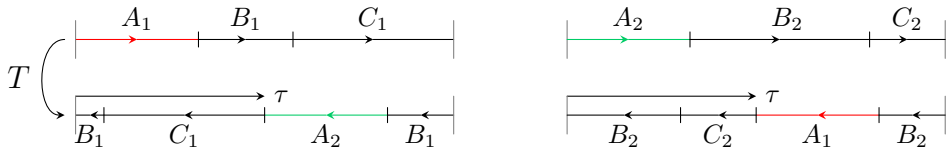

Figure 4.5. – The associated IETF

4.2.3.b. Lengths

For $i \in \{1, 2\}$, we denote by $\mathbf{A}_i$, $\mathbf{B}_i$, and $\mathbf{C}_i$ (in bold) the intervals of continuity. We denote by a_i, b_i, and c_i their respective lengths, and τ_i the parameter of shift in $\mathcal{C}_i$. Let T be a (totally flipping) IETF on two circles, with combinatorial data p_1 and lengths $\lambda = (a_1, b_1, c_1, \tau_1, a_2, b_2, c_2, \tau_2)$. The transformation T corresponds to our bi-triangle tiling billiard if and only if:

$$\begin{cases} a_1 + b_1 + c_1 = a_2 + b_2 + c_2 \\ a_1 = a_2 \\ \tau_1 = \tau_2 \end{cases} . \tag{4.4}$$

The relation $a_1 + b_1 + c_1 = a_2 + b_2 + c_2$ comes from the fact that triangles δ_1 and δ_2 are inscribed in a circle of the same radius, see Figure 4.1a. The $a_1 = a_2$ comes from the fact that triangles δ_1 and δ_2 share a side. Finally, $\tau_1 = \tau_2$ comes from the definition of the system and relies strongly on the fact that both triangles are inscribed in the same circle (see Section 4.2.1). We will restrict ourselves to this linear subspace of lengths. We define the hyperplanes

$$H_a = \left\{ (a_1, b_1, c_1, \tau_1, a_2, b_2, c_2, \tau_2) \in \mathbb{R}^8 \middle| \, a_1 = a_2 \right\},$$

and similarly H_b, H_c and H_τ, and

$$H_l = \left\{ (a_1, b_1, c_1, \tau_1, a_2, b_2, c_2, \tau_2) \in \mathbb{R}^8 \middle| \, a_1 + b_1 + c_1 = a_2 + b_2 + c_2 \right\},$$

The linear subspace in which we are interested is:

$$S_1 = H_a \cap H_l \cap H_\tau. \tag{4.5}$$

4.3. The induction

4.3.1. Presentation

We define an induction on the totally flipping IETFs with combinatorial data

$$p_1(A) = \left\{ \begin{pmatrix} A_1 & B_1 & C_1 \\ A_2 & B_1 & C_1 \end{pmatrix}, \begin{pmatrix} A_2 & B_2 & C_2 \\ A_1 & B_2 & C_2 \end{pmatrix} \right\}$$

or

$$p_2(A) = \left\{ \begin{pmatrix} A_1 & B_1 & C_1 \\ A_1 & B_2 & C_2 \end{pmatrix}, \begin{pmatrix} A_2 & B_2 & C_2 \\ A_2 & B_1 & C_1 \end{pmatrix} \right\}$$

or of the same combinatorial type (as defined in Section 4.2.2) as $p_1(A)$ or $p_2(A)$. We denote by p_1 (resp. p_2) the combinatorial type of $p_1(A)$ (resp. $p_2(A)$). It is defined on $d = 2$ circles, each divided into 3 intervals of continuity, such that one interval of continuity is sent to the other circle (resp. stays in the same circle) and the two other intervals of continuity stay in the same circle (resp. are sent to the other circle). For every letter $X \in \{A, B, C\}$, we denote by $p_1(X) = (\pi_0, \pi_1)$ (resp. $p_2(X)$) the element in the equivalence class p_1 (resp. p_2) obtained by the cyclic relabeling of $p_1(A)$ (resp. $p_2(A)$) that send the letter A to the letter X. Recall that τ_i is measured in the circle $\mathcal{C}_i$ between the top interval labeled with $\pi_0^{-1}(1) = X_i$ and the bottom interval labeled with $\pi_1^{-1}(1) = X_j$ ($j \neq i$ in case of p_1 whereas $j = i$ in case of p_2).

Let T be a (totally flipping) IETF on the union of two circles with combinatorial data p_1 or p_2 and parameters $(a_1, b_1, c_1, \tau_1, a_2, b_2, c_2, \tau_2)$. For every letter $X \in \{A, B, C\}$, we write $\mathbf{X} = \mathbf{X}_1 \cup \mathbf{X}_2$ the union of the two intervals of continuity $\mathbf{X}_1$ and $\mathbf{X}_2$ labeled with the same letter X. Let s be the total lengths of these unions of intervals: $s(\mathbf{A}) = a_1 + a_2$, $s(\mathbf{B}) = b_1 + b_2$, and $s(\mathbf{C}) = c_1 + c_2$. In the case when s attains its minimum with a unique argument, say X, we consider the first return map of T on

$$J = (\mathcal{C}_1 \cup \mathcal{C}_2) \setminus \left(\mathbf{X} \cup T^{-1}(\mathbf{X}) \right). \tag{4.6}$$

We denote this first return map by $\mathcal{R}(T)$, and call it the *induced* map.

4.3.2. Conditions

We consider three conditions.

- $(C0)$: s attains its minimum with a unique argument.
- $(C1)$: $\forall \{X, Y, Z\} = \{A, B, C\}$, $\begin{cases} T(\mathbf{X}) \subset \mathbf{Y} \cup \mathbf{Z} \\ T(\mathbf{X}) \cap \mathbf{Y} \neq \emptyset \\ T(\mathbf{X}) \cap \mathbf{Z} \neq \emptyset \end{cases}$.
- $(C2)$: $\exists M \in \{A, B, C\}, s(\mathbf{M}) = \min s$ and $T(\mathbf{M}) \cap T^{-1}(\mathbf{M}) = \emptyset$.

$(C0)$ means that there is no ambiguity in the definition of the induction. $(C1)$ means that the singularities are criss-crossed, which can be reformulated in terms of lengths as in the following lemma.

Lemma 4.2. *The assumption $(C1)$ is equivalent to*

$$\forall i \in \{1,2\},\ \max\{a_i, b_i, c_i\} < \tau_i < \min\{a_i + b_i, a_i + c_i, b_i + c_i\}$$

for the permutation p_1, and, to:

$$\forall i \in \{1,2\},\ \max\{a_i, b_i + a_{i+1} - a_i, c_{i+1}\} < \tau_i < \min\{a_i + b_i, a_i + c_{i+1}, b_i + c_i\},$$

in the case of permutation p_2 (where all the indices are given modulo 2).

Proof. — This is a direct computation, illustrated by Figure 4.6.

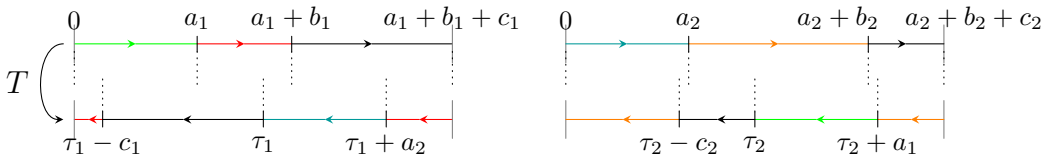

(a) with combinatorial data p_1

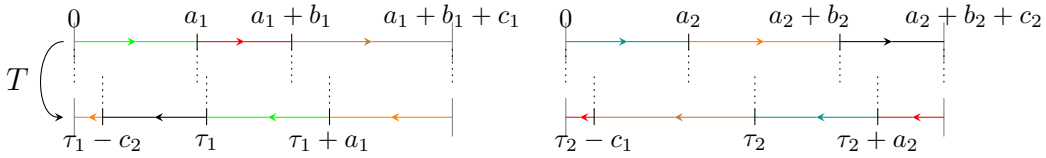

(b) with combinatorial data p_2

Figure 4.6. – "Criss-crossed" singularities

Remark 4.3. *The assumption $(C1)$ implies that the longest interval of continuity is less than the half the perimeter of the circle.*

Lemma 4.4. *Let T be an IETF with combinatorial data p_1 or p_2. If T satisfies $(C1)$, then $\frac{l}{3} < \tau_1 + \tau_2 < \frac{2l}{3}$, where $l = a_1 + b_1 + c_1 + a_2 + b_2 + c_2$.*

Proof. — Using Lemma 4.2, we have, if T has combinatorial data p_1:

$$l \leqslant 3(\max\{a_1, b_1, c_1\} + \max\{a_2, b_2, c_2\}) < 3(\tau_1 + \tau_2)$$

and

$$\tau_1 + \tau_2 < \min\{a_1 + b_1, b_1 + c_1, c_1 + a_1\} + \min\{a_2 + b_2, b_2 + c_2, c_2 + a_2\} \leqslant 2l.$$

Similarly, if T has combinatorial data p_2, then:

$$l \leqslant 3(\max\{a_1, b_1 + a_2 - a_1, c_2\} + \max\{a_2, b_2 + a_1 - a_2, c_2\}) < 3(\tau_1 + \tau_2)$$

and

$$\tau_1 + \tau_2 < \min\{a_1 + b_1, b_1 + c_1, c_2 + a_1\} + \min\{a_2 + b_2, b_2 + c_2, c_1 + a_2\} \leqslant 2l.$$

This proves the lemma. ■

Lemma 4.5. *If the conditions* $(C0)$ *and* $(C1)$ *are satisfied, then every point in the set* J *comes back in* J *with an odd return time.*

Note that the condition $(C0)$ is needed only to define the induction, but the results still hold without $(C0)$ if we choose to induce on the complementary of $X \cup T^{-1}(X)$ in $\mathcal{C}_1 \cup \mathcal{C}_2$, for any X such that $s(\mathbf{X}) = \min s$.

Proof. — Denote by $\mathbf{M}$ the loser union of intervals. Let $x \in J$. Denote by k the return time of x in J. We prove by induction that

$$\forall l < \frac{k}{2},\ T^{2l-1}(x) \in T^{-1}(\mathbf{M}) \text{ and } T^{2l}(x) \in \mathbf{M}.$$

If $k = 1$ there is nothing to do. If $k > 1$, $T(x) \notin J$ and since $x \in J$, we have $T(x) \notin \mathbf{M}$ so $T(x) \in T^{-1}(\mathbf{M})$ and hence $T^2(x) \in \mathbf{M}$. This establishes the property for $l = 1$. Moreover, if $T^{2l}(x) \in \mathbf{M}$, either $T^{2l+1} \in J$ and x has return time $2l + 1$ or $T^{2l+1}(x) \notin J$ and $T^{2l+1}(x) \in T^{-1}(\mathbf{M})$ since $\mathbf{M} \cap T^{-1}(\mathbf{M}) = \emptyset$ by $(C1)$. ■

Corollary 4.6. *If the conditions* $(C0)$ *and* $(C1)$ *are satisfied, the induced IET is fully flipped as the initial map.*

Lemma 4.7. *If* $(C0)$, $(C1)$, *and* $(C2)$ *hold, then every point in the set* J *has a return time in* J *that is equal to either* 1 *or* 3.

Proof. — Denote by $\mathbf{M}$ the loser union of intervals. Let $x \in J$. If $x \in T^{-2}(\mathbf{M})$, then $T(x) \in T^{-1}(\mathbf{M})$ so $T(x) \notin J$, and $T^2(x) \in \mathbf{M}$ so $T^2(x) \notin J$. But $T^3(x)$ is in $T(\mathbf{M})$, so $T^3(x)$ is neither in $\mathbf{M}$ (because of $(C1)$) nor in $T^{-1}(\mathbf{M})$ (because of condition $(C2)$), which means that $T^3(x)$ is in J. We conclude that x has return time 3.

Else, $x \in J \setminus T^{-2}(\mathbf{M})$, so $T(x)$ is neither in $T^{-1}(\mathbf{M})$ nor in $\mathbf{M}$, which means that x has return time 1. ■

More precisely, we will see that a non-loser interval is divided into exactly two subintervals: one that returns directly in J and another that comes back after three iterations of T. Moreover, the two subintervals of return time 3 form together a new interval of continuity. This is the key point that makes this induction work so well: the complexity of the combinatorial data does not increase. We can be more precise and give the combinatorial data of the induced IET. The computations of the induction, presented in Figures 4.8, 4.10, 4.12, 4.9, 4.11, and 4.13 prove the following lemma.

Lemma 4.8. *Let T be an IETF with combinatorial data p_1 (resp. p_2). If T satisfies $(C0)$, $(C1)$, and $(C2)$, then the induced IET $\mathcal{R}(T)$ is also a fully flipped IETF with combinatorial data p_1 or p_2. Moreover if T has lengths in the subspace S_1 (resp. S_2), then $\mathcal{R}(T)$ has lengths in the subspace S_i if it has combinatorial type p_i, for $i \in \{1, 2\}$.*

This lemma permits to study the IETFs for which the conditions $(C0)$, $(C1)$, and $(C2)$ are fulfilled at each step of the induction. But we will see later that these IETFs are very specific:

Theorem D. *Let T be an IETF with combinatorial data p_1, with lengths in the subspace S_1. If for every $k \in \mathbb{N}$, the induced map $\mathcal{R}^k(T)$ satisfies (C0), (C1), and (C2), then T is the skew-product over an IETF defined on a unique circle. In other words, its lengths lie in the linear subspace*

$$S = H_a \cap H_b \cap H_c \cap H_\tau.$$

Moreover, T is minimal, (a_1, b_1, c_1) are in the Rauzy gasket, and $\tau_1 = \tau_2 = \frac{1}{2}(a_1 + b_1 + c_1) = \frac{1}{2}(a_2 + b_2 + c_2)$.

The Rauzy gasket is a fractal subset of the 2 dimensional simplex. For a definition, we refer to [AS13], where the Rauzy gasket get its name.

Theorem D is the main result of this chapter. We postpone its proof to Section 4.3.3.e. This theorem leads to ask the question: what happens when $(C0)$, $(C1)$ or $(C2)$ is not fulfilled? We will investigate this issue in the Subsection 4.3.4.

Table 4.1 reformulates the condition (C2) in terms of lengths, under the assumption of (C0) and (C1), and in the linear subspace S_1 (defined in (4.5)) for the combinatorial data p_1 and

$$S_2 = H_a \cap H_l \cap H_{c+\tau}$$

respectively for the combinatorial data p_2, where

$$H_{c+\tau} = \left\{ (a_1, b_1, c_1, \tau_1, a_2, b_2, c_2, \tau_2) \in \mathbb{R}^8 \middle| \, c_1 + \tau_1 = c_2 + \tau_2 \right\}.$$

	on p_1, with $\lambda \in S_1$	on p_2, with $\lambda \in S_2$
argmin(s)=A	$b_1, c_1, b_2, c_2 > a_1 = a_2$	
argmin(s)=B	$a_1, c_2 > b_1$ and $a_2, c_1 > b_2$	
argmin(s)=C	$a_1, b_1 > c_2$ and $a_2, b_2 > c_1$	$a_1, b_1 > c_1$ and $a_2, b_2 > c_2$

Table 4.1. – Condition ($C2$) in terms of lengths

4.3.3. Computations under conditions (C0), (C1) and (C2)

In order to prove Lemma 4.8, we have to handle six cases (two possible combinatorial data and three possible loser union of intervals). First, in Subsection 4.3.3.a, we do the computation without relabeling, and get a (non-reduced) Rauzy diagram. By relabeling the intervals at each step of induction, we reduce the Rauzy diagram in Subsection 4.3.3.a. We also give (in both cases, with or without relabeling) the expression of the lengths of the "new" intervals, i.e. the intervals of continuity of the induced IETF, depending on the lengths of the "old" intervals. The relabeling simplifies the study of the induction: there are less vertices in the diagram, hence less matrices that describe the change of the lengths of the intervals. However, the expressions of the new lengths are easier to follow without relabeling, that is why we present first the induction without relabeling.

We assume nothing more than ($C0$), ($C1$), and ($C2$) on the lengths, in particular the lengths need not to be in the subspaces S_i. Note however that λ is necessarily in the space H_a when the combinatorial data is p_1 and in H_{b+c} when the combinatorial data is p_2.

4.3.3.a. Induction without relabeling

Rauzy diagram. The computations presented in Figures 4.8, 4.9, 4.10, 4.11, 4.12, and 4.13 give the following Rauzy diagram (Figure 4.7), which, together with Table 4.2, proves Lemme 4.8. The letters labeling the arrows correspond to the label of the loser union of intervals.

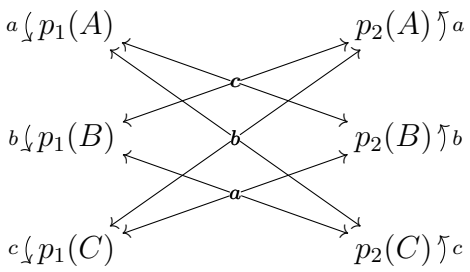

Figure 4.7. – Rauzy diagram for the induction without relabeling
The labels of the edges denote the loser union of intervals.

The following figures, that have a role of computation, should be read like this:

- The first row shows T, the IETF on which we apply the induction. Following the visual notation introduced in [BDFI24], we represent each interval of continuity as a triangle, so that we can easily follow the changes of the orientation under the IETF. Each triangle has its own color. The two endpoints of the top (resp. bottom) segment are identified to give the circle on which T is defined.
- The second row consists of the "computation" of the induction. It gives the proof of the formula given in Table 4.2. We remind also the action of T drawn in transparency.
- The shaded parts are the removed intervals, we induce on the complementary.
- Each interval of continuity I_{X_i} is cut into three intervals: a first one outside J, a second one with return time 1 (colored) and the last one, $I^3_{X_i}$, with return time 3 (hatched). We use the same color for them as for the interval I_{X_i} in the first row. We draw the images $T(I^3_{X_i})$ and $T^2(I^3_{X_i})$ that lie outside J (in the shaded part of the figure), so that we can keep track of them. The number 1 or 2 above these images indicates whether it is the image under T or T^2.
- The lengths are expressed without any assumption on them, even though their specific values chosen in the figures are in the subspace S_1 or S_2. In this way, on the one hand we have the generic expressions, and on the other hand, we have in mind the pictures we are interested in for our specific context.
- The last line gives the result of the induced IET, $\mathcal{R}(T)$.

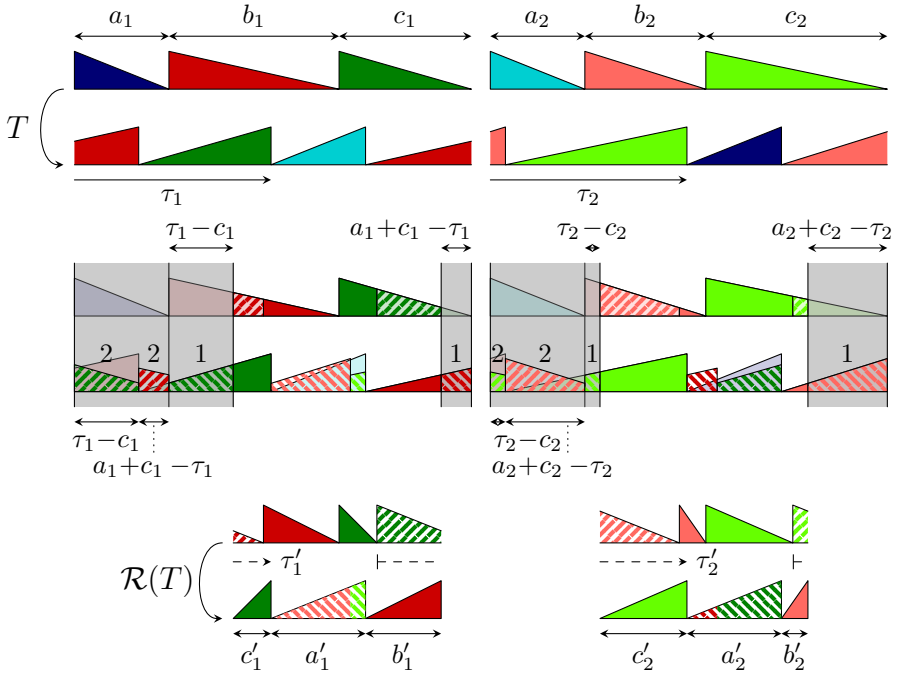

Figure 4.8. – Induction on $p_1(A)$ with loser A: we get $p_1(A)$

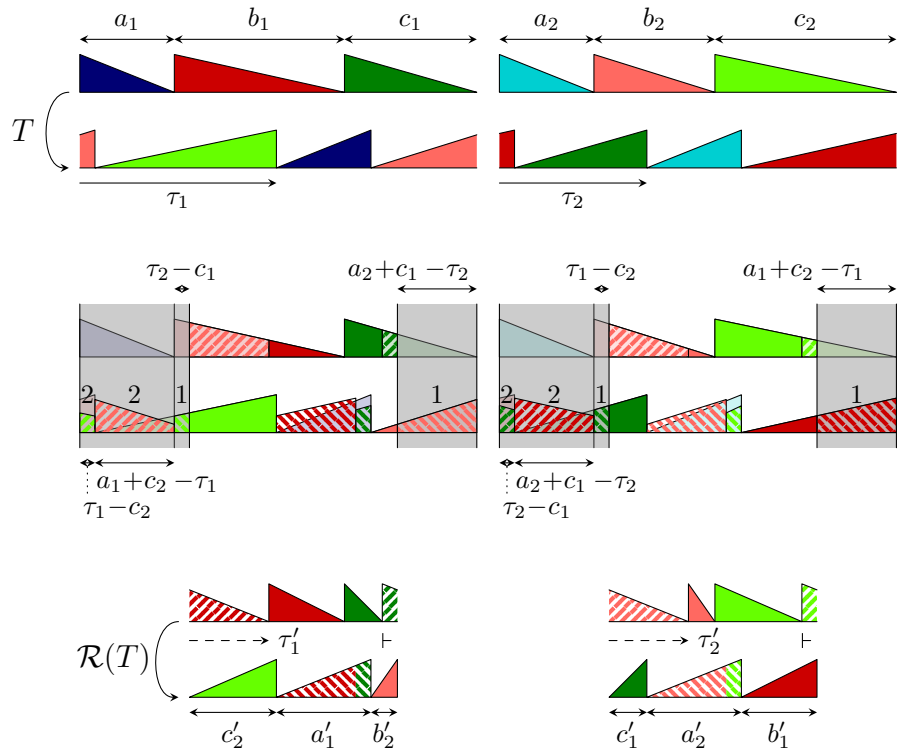

Figure 4.9. – Induction on $p_2(A)$ with loser A: we get $p_2(A)$

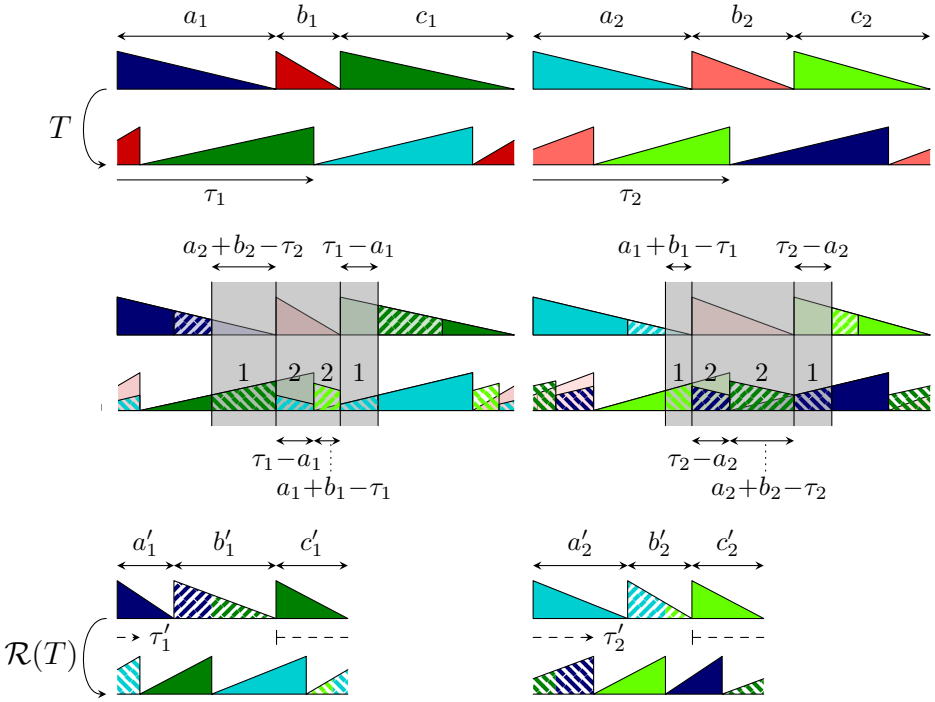

Figure 4.10. – Induction on $p_1(A)$ with loser B: we get $p_2(C)$

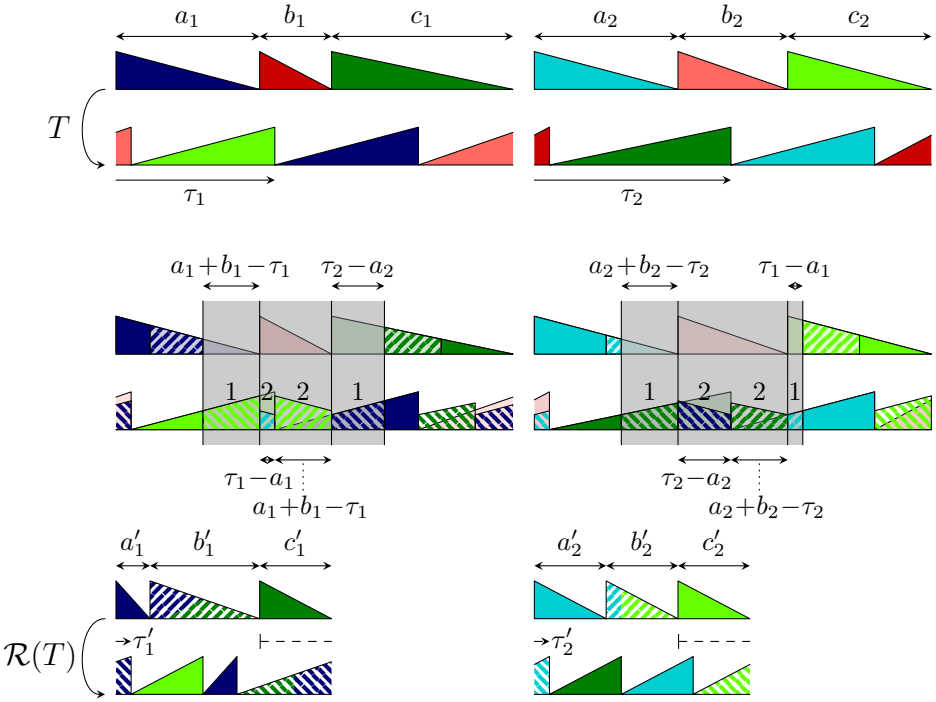

Figure 4.11. – Induction on $p_2(A)$ with loser B: we get $p_1(C)$

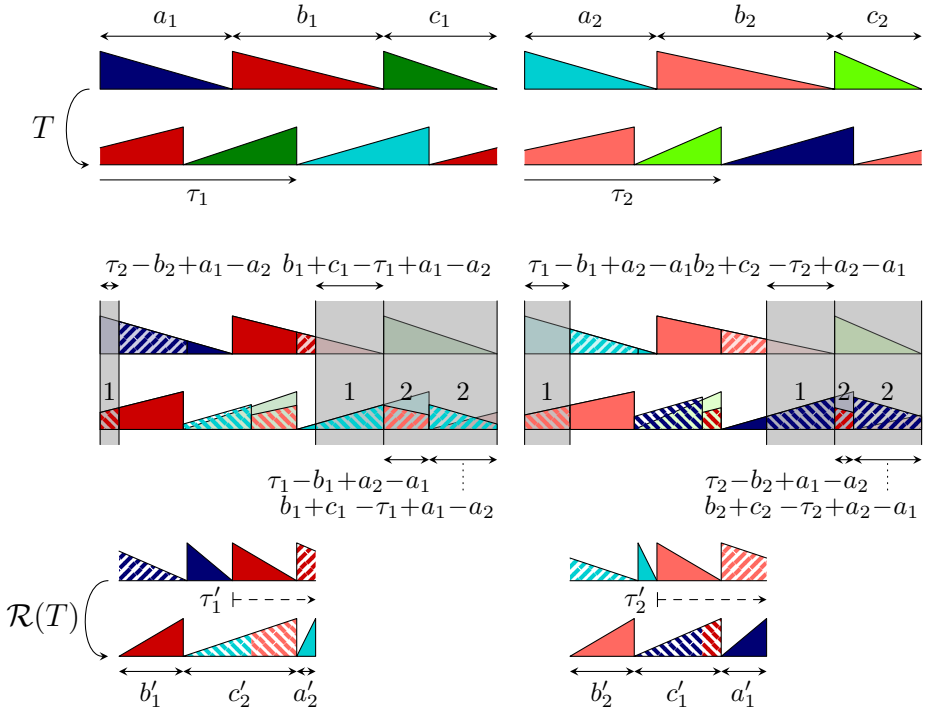

Figure 4.12. – Induction on $p_1(A)$ with loser C: we get $p_2(B)$

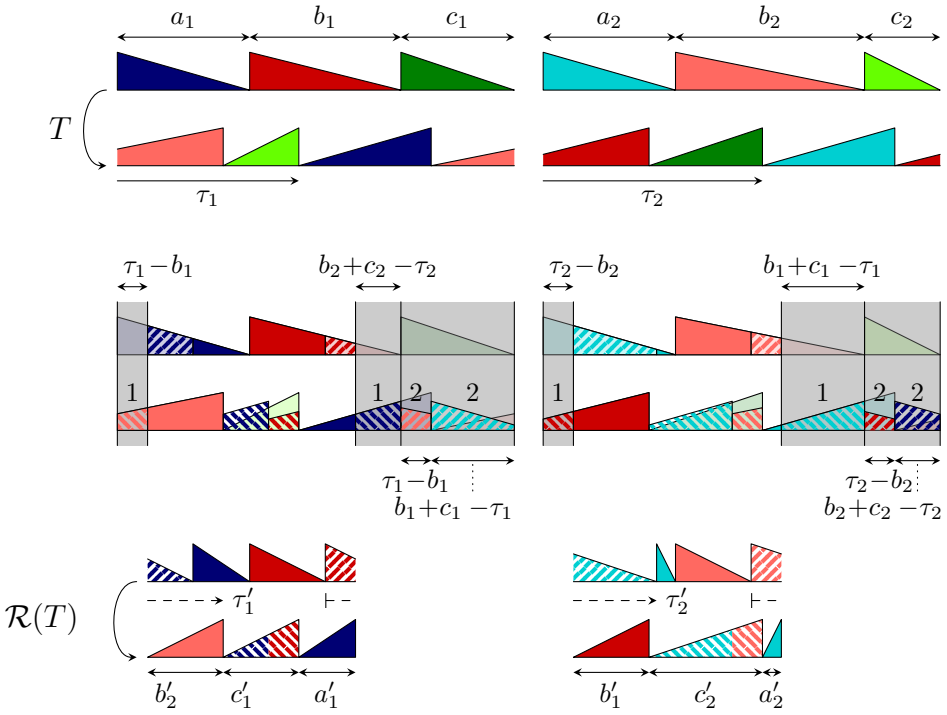

Figure 4.13. – Induction on $p_2(A)$ with loser C: we get $p_1(B)$

Lengths. We sum up the change of lengths in Table 4.2.The indices are given modulo 2.

induction on the combinatorial data	$p_1(A)$ (implies $a_1 = a_2$)	$p_2(A)$ (implies $b_1 + c_1 = b_2 + c_2$)
loser a	$a'_i = a_i$ $b'_i = b_i - a_i$ $c'_i = c_i - a_i$ $\tau'_i = \tau_i - a_i$	$a'_i = a_i$ $b'_i = b_{i+1} - a_i + \tau_i - \tau_{i+1}$ $c'_i = c_{i+1} - a_{i+1} + \tau_{i+1} - \tau_i$ $\tau'_i = 2\tau_i - \tau_{i+1} - a_i + c_i - c_{i+1}$
loser b	$a'_i = a_i - b_{i+1}$ $b'_i = b_{i+1}$ $c'_i = c_i - b_{i+1} + \tau_{i+1} - \tau_i$ $\tau'_i = \tau_{i+1} - b_{i+1}$	$a'_i = a_{i+1} - b_i + \tau_i - \tau_{i+1}$ $b'_i = b_{i+1}$ $c'_i = c_i - b_{i+1}$ $\tau'_i = \tau_i - b_i$
loser c	$a'_i = a_i - c_{i+1}$ $b'_i = b_{i+1} - c_i + \tau_i - \tau_{i+1}$ $c'_i = c_{i+1}$ $\tau'_i = \tau_i - c_i$	$a'_i = a_i - c_i + \tau_{i+1} - \tau_i$ $b'_i = b_i - c_{i+1}$ $c'_i = c_{i+1}$ $\tau'_i = \tau_{i+1} - c_i$

Table 4.2. – New lengths after induction without relabeling

Note that when the lengths are in the subspace S_1 (resp. S_2), the expressions can be simplified.

induction on permutation	$p_1(A)$ or $p_2(A)$
loser a	$a'_i = a_i$ $b'_i = b_i - a_{i+1}$ $c'_i = c_i - a_{i+1}$ $\tau'_i = \tau_i - a_i$
loser b	$a'_i = a_i - b_{i+1}$ $b'_i = b_{i+1}$ $c'_i = c_i - b_{i+1}$ $\tau'_i = \tau_{i+1} - b_{i+1}$
loser c	$a'_i = a_i - c_{i+1}$ $b'_i = b_i - c_{i+1}$ $c'_i = c_{i+1}$ $\tau'_i = \tau_{i+1} - c_i$

Table 4.3. – New lengths after induction without relabeling, on subspace S

Write L the label of the loser intervals, we can sum up these equations by: $x'_i = \begin{cases} l_{i+1} & \text{if } x = l \\ x_i - l_{i+1} & \text{otherwise} \end{cases}$ and the expression of τ' is more subtle.

4.3.3.b. Induction with relabeling

If we rename the label after each step so that we handle only the element $p_1(A)$ (resp. $p_2(A)$) of equivalence class p_1 (resp. p_2), we get a reduced Rauzy diagram, and the new lengths are permuted.

Reduced Rauzy diagram. The induction gives this Rauzy diagram, after relabeling (i.e. modulo equivalence of combinatorial type).

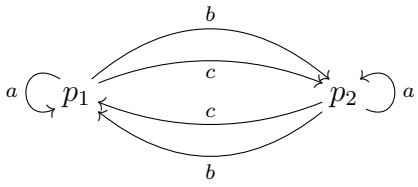

Figure 4.14. – Rauzy diagram for the induction with relabeling
Each edge is labeled with the loser union of intervals.

Lengths. Table 4.4 gives the new parameters after one step of induction. The indices are still given modulo 2.

induction on permutation	p_1	p_2
loser a	$a'_i = a_i$ $b'_i = b_i - a_i$ $c'_i = c_i - a_i$ $\tau'_i = \tau_i - a_i$	$a'_i = a_i$ $b'_i = b_{i+1} - a_i + \tau_i - \tau_{i+1}$ $c'_i = c_{i+1} - a_{i+1} + \tau_{i+1} - \tau_i$ $\tau'_i = 2\tau_i - \tau_{i+1} - a_i + c_i - c_{i+1}$
loser b	$a'_i = c_i - b_{i+1} + \tau_{i+1} - \tau_i$ $b'_i = a_i - b_{i+1}$ $c'_i = b_{i+1}$ $\tau'_i = \tau_{i+1} - b_{i+1}$	$a'_i = c_i - b_{i+1}$ $b'_i = a_{i+1} - b_i + \tau_i - \tau_{i+1}$ $c'_i = b_{i+1}$ $\tau'_i = \tau_i - b_i$
loser c	$a'_i = b_{i+1} - c_i + \tau_i - \tau_{i+1}$ $b'_i = c_{i+1}$ $c'_i = a_i - c_{i+1}$ $\tau'_i = \tau_i - c_i$	$a'_i = b_i - c_{i+1}$ $b'_i = c_{i+1}$ $c'_i = a_i - c_i + \tau_{i+1} - \tau_i$ $\tau'_i = \tau_{i+1} - c_i$

Table 4.4. – New lengths after induction with relabeling, on subspace S

We can express the formula of Table 4.4 with matrices M_x, where $x \in \{1a, 1b, 1c, 2a, 2b, 2c\}$ denotes the induction step: if $x = k\alpha$ with $k \in \{1, 2\}$ and $\alpha \in \{a, b, c\}$ then the step of induction x applies to combinatorial data p_k with loser union of intervals labeled with α.

The new vector of lengths $\lambda' = (a_1', b_1', c_1', \tau_1', a_2', b_2', c_2', \tau_2')$ is the product of M_x and the old vector of lengths $\lambda = (a_1, b_1, c_1, \tau_1, a_2, b_2, c_2, \tau_2)$: $\lambda' = M_x\lambda$. The corresponding matrices expressed in the bases

$$\mathcal{B}_1 = \mathcal{B}_2 = (a_1, b_1, c_1, \tau_1, a_2, b_2, c_2, \tau_2)$$

are:

$$M_{1a} = \begin{pmatrix} 1 & 0 & 0 & 0 & 0 & 0 & 0 & 0 \\ -1 & 1 & 0 & 0 & 0 & 0 & 0 & 0 \\ -1 & 0 & 1 & 0 & 0 & 0 & 0 & 0 \\ -1 & 0 & 0 & 1 & 0 & 0 & 0 & 0 \\ 0 & 0 & 0 & 0 & 1 & 0 & 0 & 0 \\ 0 & 0 & 0 & 0 & -1 & 1 & 0 & 0 \\ 0 & 0 & 0 & 0 & -1 & 0 & 1 & 0 \\ 0 & 0 & 0 & 0 & -1 & 0 & 0 & 1 \end{pmatrix}, M_{2a} = \begin{pmatrix} 1 & 0 & 0 & 0 & 0 & 0 & 0 & 0 \\ -1 & 0 & 0 & 1 & 0 & 1 & 0 & -1 \\ 0 & 0 & 0 & -1 & -1 & 0 & 1 & 1 \\ -1 & 0 & 1 & 2 & 0 & 0 & -1 & -1 \\ 0 & 0 & 0 & 0 & 1 & 0 & 0 & 0 \\ 0 & 1 & 0 & -1 & -1 & 0 & 0 & 1 \\ -1 & 0 & 1 & 1 & 0 & 0 & 0 & -1 \\ 0 & 0 & -1 & -1 & -1 & 0 & 1 & 2 \end{pmatrix},$$

$$M_{1b} = \begin{pmatrix} 0 & 0 & 1 & -1 & 0 & -1 & 0 & 1 \\ 1 & 0 & 0 & 0 & 0 & -1 & 0 & 0 \\ 0 & 0 & 0 & 0 & 0 & 1 & 0 & 0 \\ 0 & 0 & 0 & 0 & 0 & -1 & 0 & 1 \\ 0 & -1 & 0 & 1 & 0 & 0 & 1 & -1 \\ 0 & -1 & 0 & 0 & 1 & 0 & 0 & 0 \\ 0 & 1 & 0 & 0 & 0 & 0 & 0 & 0 \\ 0 & -1 & 0 & 1 & 0 & 0 & 0 & 0 \end{pmatrix}, M_{2b} = \begin{pmatrix} 0 & 0 & 1 & 0 & 0 & -1 & 0 & 0 \\ 0 & -1 & 0 & 1 & 1 & 0 & 0 & -1 \\ 0 & 0 & 0 & 0 & 0 & 1 & 0 & 0 \\ 0 & -1 & 0 & 1 & 0 & 0 & 0 & 0 \\ 0 & -1 & 0 & 0 & 0 & 0 & 1 & 0 \\ 1 & 0 & 0 & -1 & 0 & -1 & 0 & 1 \\ 0 & 1 & 0 & 0 & 0 & 0 & 0 & 0 \\ 0 & 0 & 0 & 0 & 0 & -1 & 0 & 1 \end{pmatrix},$$

$$M_{1c} = \begin{pmatrix} 0 & 0 & -1 & 1 & 0 & 1 & 0 & -1 \\ 0 & 0 & 0 & 0 & 0 & 0 & 1 & 0 \\ 1 & 0 & 0 & 0 & 0 & 0 & -1 & 0 \\ 0 & 0 & -1 & 1 & 0 & 0 & 0 & 0 \\ 0 & 1 & 0 & -1 & 0 & 0 & -1 & 1 \\ 0 & 0 & 1 & 0 & 0 & 0 & 0 & 0 \\ 0 & 0 & -1 & 0 & 1 & 0 & 0 & 0 \\ 0 & 0 & 0 & 0 & 0 & 0 & -1 & 1 \end{pmatrix}, M_{2c} = \begin{pmatrix} 0 & 1 & 0 & 0 & 0 & 0 & -1 & 0 \\ 0 & 0 & 0 & 0 & 0 & 0 & -1 & 0 \\ 1 & 0 & -1 & -1 & 0 & 0 & 0 & 1 \\ 0 & 0 & -1 & 0 & 0 & 0 & 0 & 1 \\ 0 & 0 & -1 & 0 & 0 & 1 & 0 & 0 \\ 0 & 0 & 1 & 0 & 0 & 0 & 0 & 0 \\ 0 & 0 & 0 & 1 & 1 & 0 & -1 & -1 \\ 0 & 0 & 0 & 1 & 0 & 0 & -1 & 0 \end{pmatrix}.$$

It can be interesting to consider their inverses because fewer of their coefficients

are negative.

$$M_{1a}^{-1} = \begin{pmatrix} 1 & 0 & 0 & 0 & 0 & 0 & 0 & 0 \\ 1 & 1 & 0 & 0 & 0 & 0 & 0 & 0 \\ 1 & 0 & 1 & 0 & 0 & 0 & 0 & 0 \\ 1 & 0 & 0 & 1 & 0 & 0 & 0 & 0 \\ 0 & 0 & 0 & 0 & 1 & 0 & 0 & 0 \\ 0 & 0 & 0 & 0 & 1 & 1 & 0 & 0 \\ 0 & 0 & 0 & 0 & 1 & 0 & 1 & 0 \\ 0 & 0 & 0 & 0 & 1 & 0 & 0 & 1 \end{pmatrix}, M_{2a}^{-1} = \begin{pmatrix} 1 & 0 & 0 & 0 & 0 & 0 & 0 & 0 \\ 1 & 0 & -2 & -1 & 0 & 1 & 2 & 1 \\ 0 & 0 & 2 & 1 & 1 & 0 & -1 & -1 \\ 1 & 0 & -1 & 0 & 0 & 0 & 1 & 1 \\ 0 & 0 & 0 & 0 & 1 & 0 & 0 & 0 \\ 0 & 1 & 2 & 1 & 1 & 0 & -2 & -1 \\ 1 & 0 & -1 & -1 & 0 & 0 & 2 & 1 \\ 0 & 0 & 1 & 1 & 1 & 0 & -1 & 0 \end{pmatrix},$$

$$M_{1b}^{-1} = \begin{pmatrix} 0 & 0 & 1 & 1 & 0 & 0 & 0 & 0 \\ 0 & 0 & 0 & 0 & 0 & 0 & 1 & 0 \\ 1 & 0 & 0 & -1 & 0 & 0 & 1 & 1 \\ 0 & 0 & 0 & 0 & 0 & 0 & 1 & 1 \\ 0 & 0 & 0 & 0 & 0 & 1 & 1 & 0 \\ 0 & 1 & 0 & 0 & 0 & 0 & 0 & 0 \\ 0 & 0 & 1 & 1 & 1 & 0 & 0 & -1 \\ 0 & 0 & 1 & 1 & 0 & 0 & 0 & 0 \end{pmatrix}, M_{2b}^{-1} = \begin{pmatrix} 0 & 0 & 0 & 1 & 0 & 1 & 1 & -1 \\ 0 & 0 & 0 & 0 & 0 & 0 & 1 & 0 \\ 1 & 0 & 1 & 0 & 0 & 0 & 0 & 0 \\ 0 & 0 & 0 & 1 & 0 & 0 & 1 & 0 \\ 0 & 1 & 1 & -1 & 0 & 0 & 0 & 1 \\ 1 & 0 & 1 & 0 & 0 & 0 & 0 & 0 \\ 0 & 0 & 0 & 0 & 1 & 0 & 1 & 0 \\ 0 & 0 & 1 & 0 & 0 & 0 & 0 & 1 \end{pmatrix}$$

$$M_{1c}^{-1} = \begin{pmatrix} 0 & 0 & 1 & 1 & 0 & 0 & 0 & 0 \\ 0 & 0 & 0 & 1 & 1 & 1 & 0 & -1 \\ 0 & 0 & 0 & 0 & 0 & 1 & 0 & 0 \\ 0 & 0 & 0 & 1 & 0 & 1 & 1 & 0 \\ 0 & 0 & 0 & 0 & 0 & 1 & 1 & 0 \\ 1 & 1 & 0 & -1 & 0 & 0 & 0 & 1 \\ 0 & 1 & 0 & 0 & 0 & 0 & 0 & 0 \\ 0 & 1 & 0 & 0 & 0 & 0 & 0 & 1 \end{pmatrix}, M_{2c}^{-1} = \begin{pmatrix} 0 & 1 & 1 & -1 & 0 & 0 & 0 & 1 \\ 1 & 1 & 0 & 0 & 0 & 0 & 0 & 0 \\ 0 & 0 & 0 & 0 & 0 & 1 & 0 & 0 \\ 0 & 1 & 0 & 0 & 0 & 0 & 0 & 1 \\ 0 & 0 & 0 & 1 & 0 & 1 & 1 & -1 \\ 0 & 0 & 0 & 0 & 1 & 1 & 0 & 0 \\ 0 & 1 & 0 & 0 & 0 & 0 & 0 & 0 \\ 0 & 0 & 0 & 1 & 0 & 1 & 0 & 0 \end{pmatrix}.$$

Note that when the lengths are in the subspace S_1 (resp. S_2), the expressions can be simplified, see Table 4.5. We keep the same bases

$$\mathcal{B}_1 = \mathcal{B}_2 = (a_1, b_1, c_1, \tau_1, a_2, b_2, c_2, \tau_2)$$

to express the matrices.

4.3.3.c. An invariant hyperplane and equivariant spaces

All the propositions of this section are based on the following basic fact:

Lemma 4.9. *Let T an IETF with combinatorial type p_1 or p_2, satisfying conditions $(C0)$, $(C1)$, and $(C2)$. Let $x \in \{1a, 1b, 1c, 2a, 2b, 2c\}$ be the step of induction $\mathcal{R}$*

	induction on $p_1(A)$ or $p_2(A)$	the corresponding matrix
loser a	$\begin{aligned} a'_i &= a_i \\ b'_i &= b_i - a_{i+1} \\ c'_i &= c_i - a_{i+1} \\ \tau'_i &= \tau_i - a_i \end{aligned}$	$M_a^{(S)} = \begin{pmatrix} 1 & 0 & 0 & 0 & 0 & 0 & 0 & 0 \\ 0 & 1 & 0 & 0 & -1 & 0 & 0 & 0 \\ 0 & 0 & 1 & 0 & -1 & 0 & 0 & 0 \\ -1 & 0 & 0 & 1 & 0 & 0 & 0 & 0 \\ 0 & 0 & 0 & 0 & 1 & 0 & 0 & 0 \\ -1 & 0 & 0 & 0 & 0 & 1 & 0 & 0 \\ -1 & 0 & 0 & 0 & 0 & 0 & 1 & 0 \\ 0 & 0 & 0 & 0 & -1 & 0 & 0 & 1 \end{pmatrix}$
loser b	$\begin{aligned} a'_i &= c_i - b_{i+1} \\ b'_i &= a_i - b_{i+1} \\ c'_i &= b_{i+1} \\ \tau'_i &= \tau_{i+1} - b_{i+1} \end{aligned}$	$M_b^{(S)} = \begin{pmatrix} 0 & 0 & 1 & 0 & 0 & -1 & 0 & 0 \\ 1 & 0 & 0 & 0 & 0 & -1 & 0 & 0 \\ 0 & 0 & 0 & 0 & 0 & 1 & 0 & 0 \\ 0 & 0 & 0 & 0 & 0 & -1 & 0 & 1 \\ 0 & -1 & 0 & 0 & 0 & 0 & 1 & 0 \\ 0 & -1 & 0 & 0 & 1 & 0 & 0 & 0 \\ 0 & 1 & 0 & 0 & 0 & 0 & 0 & 0 \\ 0 & -1 & 0 & 1 & 0 & 0 & 0 & 0 \end{pmatrix}$
loser c	$\begin{aligned} a'_i &= b_i - c_{i+1} \\ b'_i &= c_{i+1} \\ c'_i &= a_i - c_{i+1} \\ \tau'_i &= \tau_{i+1} - c_i \end{aligned}$	$M_c^{(S)} = \begin{pmatrix} 0 & 1 & 0 & 0 & 0 & 0 & -1 & 0 \\ 0 & 0 & 0 & 0 & 0 & 0 & 1 & 0 \\ 1 & 0 & 0 & 0 & 0 & 0 & -1 & 0 \\ 0 & 0 & -1 & 0 & 0 & 0 & 0 & 1 \\ 0 & 0 & -1 & 0 & 0 & 1 & 0 & 0 \\ 0 & 0 & 1 & 0 & 0 & 0 & 0 & 0 \\ 0 & 0 & -1 & 0 & 1 & 0 & 0 & 0 \\ 0 & 0 & 0 & 1 & 0 & 0 & 1 & 0 \end{pmatrix}$

Table 4.5. – New lengths after induction with relabeling

that apply to T. Let M_x be the associated matrix. Let $u, u' \in \mathbb{R}^8$ be two vectors such that $u'M_x = u$. If $\lambda \in H = u^\perp$, then λ', the vector of lengths of $\mathcal{R}(T)$, is in $u'^\perp$.

Proof. — If $\lambda \in H = u^\perp$, then

$$u'.\lambda' = u'M_x.\lambda = u.\lambda = 0,$$

that is $\lambda' \perp u'$. ■

Proposition 4.10. *The hyperplane*

$$H_{\frac{1}{2}} = \left\{ (a_1, b_1, c_1, \tau_1, a_2, b_2, c_2, \tau_2) \in \mathbb{R}^8 \middle| \, \tau_1 + \tau_2 = \frac{1}{2}(a_1 + b_1 + c_1 + a_2 + b_2 + c_2) \right\}$$

is invariant under the induction.

Proof. — Let $u_{\frac{1}{2}} = \begin{pmatrix} 1 & 1 & 1 & -2 & 1 & 1 & 1 & -2 \end{pmatrix}$ be a vector normal to $H_{\frac{1}{2}}$. One can check that $u_{\frac{1}{2}}$ is a left-eigenvector of M_a, M_b and M_c (associated to eigenvalue 1). We conclude that if λ is in $H_{\frac{1}{2}}$, then so is λ'. ■

Proposition 4.11. *The hyperplane H_a associated to the combinatorial data p_1 and the hyperplane*

$$H_{b+c} = \left\{ (a_1, b_1, c_1, \tau_1, a_2, b_2, c_2, \tau_2) \in \mathbb{R}^8 \middle| \, b_1 + c_1 = b_2 + c_2) \right\}$$

associated to the combinatorial data p_2 are mapped to each other by the induction.

Proof. — As for the previous proposition, we define $u_a = \begin{pmatrix} 1 & 0 & 0 & 0 & -1 & 0 & 0 & 0 \end{pmatrix}$ (resp. $u_{b+c} = \begin{pmatrix} 0 & 1 & 1 & 0 & 0 & -1 & -1 & 0 \end{pmatrix}$) a vector normal to H_a (resp. H_{b+c}). Since we have $u_a M_{1a} = u_a$, $u_{b+c} M_{1b} = u_a$ and $u_{b+c} M_{1c} = u_a$ (resp. $u_{b+c} M_{2a} = -u_{b+c}$, $u_a M_{2b} = u_{b+c}$ and $u_a M_{2c} = u_{b+c}$), if λ is in H_a (resp. H_{b+c}), then λ' is either in H_{b+c} and $\mathcal{R}(T)$ has combinatorial type p_2 or in H_a and $\mathcal{R}(T)$ has combinatorial type p_1. ■

Proposition 4.12. *The space $H_l \cap H_a$ associated to the combinatorial data p_1 and the space*

$$K_{l'} = \left\{ (a_1, b_1, c_1, \tau_1, a_2, b_2, c_2, \tau_2) \in \mathbb{R}^8 \middle| \, a_1 + b_1 - c_1 - 2\tau_1 = a_2 + b_2 - c_2 - 2\tau_2 \right\} \cap H_{b+c}$$

associated to the combinatorial data p_2 are mapped to each other by the induction.

Proof. — Define $u_l = \begin{pmatrix} 1 & 1 & 1 & 0 & -1 & -1 & -1 & 0 \end{pmatrix}$, $u_a = \begin{pmatrix} 1 & 0 & 0 & 0 & -1 & 0 & 0 & 0 \end{pmatrix}$, $u_{b+c} = \begin{pmatrix} 0 & 1 & 1 & 0 & 0 & -1 & -1 & 0 \end{pmatrix}$ and $v = \begin{pmatrix} 1 & 1 & -1 & -2 & -1 & -1 & 1 & 2 \end{pmatrix}$ vectors that are respectively normal to each of the hyperplanes H_a, H_l, H_{b+c}, and $\{ (a_1, b_1, c_1, \tau_1, a_2, b_2, c_2, \tau_2) \in \mathbb{R}^8 | \, a_1 + b_1 - c_1 - 2\tau_1 = a_2 + b_2 - c_2 - 2\tau_2 \}$. Let λ be the vector of lengths of T an IETF of combinatorial type p_1 (resp. p_2). Note that

- $u_l M_{1a} = u_l - 2u_a$ (and $u_a M_{1a} = u_a$) so $H_a \cap H_l$ is sent to itself after a step $1a$ of the induction,
- $v M_{1b} = u_l$ (and $u_{b+c} M_{1b} = u_a$) so $H_a \cap H_l$ is sent to $K_{l'}$ after a step $1b$ of the induction,
- $v M_{1c} = -u_l$ (and $u_{b+c} M_{1c} = u_a$) so $H_a \cap H_l$ is sent to $K_{l'}$ after a step $1c$ of the induction,
- $v M_{2a} = v - 2u_{b+c}$ (and $u_{b+c} M_{2a} = -u_{b+c}$) so $K_{l'}$ is sent to itself after a step $2a$ of the induction,
- $u_l M_{2b} = -v$ (and $u_a M_{2b} = u_{b+c}$) so $K_{l'}$ is sent to $H_a \cap H_l$ after a step $2b$ of the induction,
- $u_l M_{2c} = v$ (and $u_{b+c} M_{2c} = u_a$) so $K_{l'}$ is sent to $H_a \cap H_l$ after a step $2c$ of the induction.

We conclude that if λ is in $H_a \cap H_l$ (resp. $K_{l'}$), then λ' is either in $K_{l'}$ and $\mathcal{R}(T)$ has combinatorial type p_2 or in $H_a \cap H_l$ and $\mathcal{R}(T)$ has combinatorial type p_1. ■

Proposition 4.13. *The space $H_\tau \cap H_a$ associated to the combinatorial data p_1 and the space*

$$K_{\tau'} = \left\{ (a_1, b_1, c_1, \tau_1, a_2, b_2, c_2, \tau_2) \in \mathbb{R}^8 \middle| \, c_1 + \tau_1 = c_2 + \tau_2 \right\} \cap H_{b+c}$$

associated to the combinatorial data p_2 are mapped to each other by the induction.

Proof. — Define $u_\tau = \begin{pmatrix} 0 & 0 & 0 & 1 & 0 & 0 & 0 & -1 \end{pmatrix}$, $u_a = \begin{pmatrix} 1 & 0 & 0 & 0 & -1 & 0 & 0 & 0 \end{pmatrix}$, $u_{b+c} = \begin{pmatrix} 0 & 1 & 1 & 0 & 0 & -1 & -1 & 0 \end{pmatrix}$ and $u_{\tau+c} = \begin{pmatrix} 0 & 0 & 1 & 1 & 0 & 0 & -1 & -1 \end{pmatrix}$ vectors that are respectively normal to each of the hyperplanes H_a, H_l, H_{b+c}, and $\{ (a_1, b_1, c_1, \tau_1, a_2, b_2, c_2, \tau_2) \in \mathbb{R}^8 | \, c_1 + \tau_1 = c_2 + \tau_2 \}$. Let λ be the vector of lengths of T an IETF of combinatorial type p_1 (resp. p_2). Note that

- $u_\tau M_{1a} = u_\tau - u_a$ (and $u_a M_{1a} = u_a$) so $H_a \cap H_\tau$ is sent to itself after a step $1a$ of the induction,
- $u_{\tau+c} M_{1b} = -u_\tau$ (and $u_{b+c} M_{1b} = u_a$) so $H_a \cap H_\tau$ is sent to $K_{\tau'}$ after a step $1b$ of the induction,
- $u_{\tau+c} M_{1c} = u_a + u_\tau$ (and $u_{b+c} M_{1c} = u_a$) so $H_a \cap H_\tau$ is sent to $K_{\tau'}$ after a step $1c$ of the induction,
- $u_{\tau+c} M_{2a} = u_{\tau+c}$ (and $u_{b+c} M_{2a} = -u_{b+c}$) so $K_{\tau'}$ is sent to itself after a step $2a$ of the induction,
- $u_\tau M_{2b} = u_{\tau+c} - u_{b+c}$ (and $u_a M_{2b} = u_{b+c}$) so $K_{\tau'}$ is sent to $H_a \cap H_\tau$ after a step $2b$ of the induction,
- $u_\tau M_{2c} = -u_{\tau+c}$ (and $u_{b+c} M_{2c} = u_a$) so $K_{\tau'}$ is sent to $H_a \cap H_\tau$ after a step $2c$ of the induction.

We conclude that if λ is in $H_a \cap H_\tau$ (resp. $K_{\tau'}$), then λ' is either in $K_{\tau'}$ and $\mathcal{R}(T)$ has combinatorial type p_2 or in $H_a \cap H_\tau$ and $\mathcal{R}(T)$ has combinatorial type p_1. ■

Proposition 4.14. *The space S_1 associated to the combinatorial data p_1 and the space S_2 associated to the combinatorial data p_2 are mapped to each other by the induction.*

Proof. — This follows directly from Propositions 4.12 and 4.13, because $S_1 = H_a \cap H_l \cap H_\tau$ and $S_2 = K'_l \cap K_{\tau'}$. ■

4.3.3.d. A new basis

The previous Propositions allow us to consider new matrices $N_{1a} = N_{2a}$, N_{1b}, N_{1c}, N_{2b} and N_{2c}, each in $\mathcal{M}_5(\mathbb{Z})$, that code the changes of lengths when the vector of lengths are in S_1 if the combinatorial type is p_1 and S_2 if the combinatorial type

is p_2. Indeed, we are in a subspace of dimension 5 only since we have 8 parameters together with 3 linear relations between them: $a_1 = a_2$, $b_1 + c_1 = b_2 + c_2$ and $\tau_1 = \tau_2$ if the combinatorial data is p_1, or $\tau_1 + c_1 = \tau_2 + c_2$ if the combinatorial data is p_2. We consider the basis $\mathcal{B} = (a_1 + a_2, b_1 + b_2, c_1 + c_2, \tau_1 + \tau_2, b_1 - b_2)$ of S_1 and S_2. We express the matrices N_x in this basis.

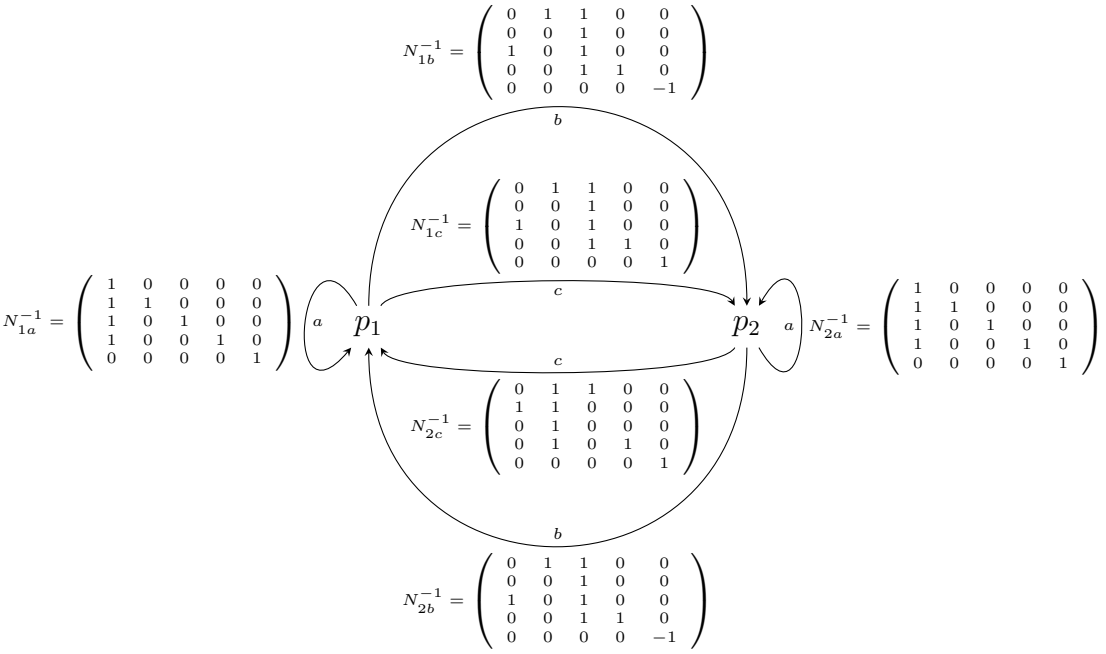

Figure 4.15. – The matrices of the the induction in the new basis
Each edge is labeled with the loser union of intervals and the matrix corresponding to the step of induction.

4.3.3.e. On the infinite paths

Lemma 4.15. *Let T be an IETF with combinatorial data p_1 or p_2. Assume that T and $\mathcal{R}(T)$ satisfy $(C0)$, $(C1)$ and $(C2)$. Assume that the labels of loser union of intervals are not the same for T and $\mathcal{R}(T)$ (without relabeling). Then the length $s(\mathbf{X})$ of the loser union of intervals for T is such that $s(\mathbf{X}) > \frac{l}{6}$, where $l = a_1 + b_1 + c_1 + a_2 + b_2 + c_2$.*

Proof. — Denote by X (resp. Y) the label of the loser union of intervals for T (resp. $\mathcal{R}(T)$), without relabeling. Denote by x (resp. y) the total length of the intervals X (resp. Y) for T and x' (resp. y') for $\mathcal{R}(T)$. Our computations on the induction give: $x' = x$ and $y' = y - x$. By definition of loser union of intervals, we have: $x < y$ and $y' < x'$. Note also that $y + x > \frac{l}{2}$ otherwise the third pair of intervals (for T) would be greater than the half of the total length and T would not satisfy $(C1)$ (see Remark 4.3). We conclude that $3x > y + x > \frac{l}{2}$. ■

Lemma 4.16. *Let T be an IETF with combinatorial data p_1 or p_2. If for every $k \in \mathbb{N}$, the induced map $\mathcal{R}^k(T)$ satisfies $(C0)$, $(C1)$, and $(C2)$, then $\tau_1 + \tau_2 = \frac{1}{2}(a_1 + b_1 + c_1 + a_2 + b_2 + c_2)$.*

Proof. — Let $\tau^{(k)} = \tau_1^{(k)} + \tau_2^{(k)}$ be the sum of parameters of shift of $\mathcal{R}^{(k)}(T)$, and $l^{(k)} = a_1^{(k)} + b_1^{(k)} + c_1^{(k)} + a_2^{(k)} + b_2^{(k)} + c_2^{(k)}$ be the total length of the domain of $\mathcal{R}^{(k)}(T)$. Let $x^{(k)} \in \{a, b, c\}$ be the length of the loser union of intervals of $\mathcal{R}^{(k)}(T)$. Set $\theta^{(k)} = \frac{\tau^{(k)}}{l^{(k)}}$ and $\xi^{(k)} = \frac{x^{(k)}}{l^{(k)}}$. Then

$$\theta^{(k+1)} = \theta^{(k)} + \frac{2\xi^{(k)}}{1 - 2\xi^{(k)}} \left(\theta^{(k)} - \frac{1}{2}\right).$$

We conclude that $\theta^{(k+1)} = \theta^{(k)}$ if and only if $\theta^{(k)} = \frac{1}{2}$. Moreover if we had $\theta > \frac{1}{2}$ (resp. $\theta < \frac{1}{2}$), then $(\theta^{(k)})_{k\in\mathbb{N}}$ would be increasing (resp. decreasing) and would eventually reach $\frac{2}{3}$ (resp. $\frac{1}{3}$). Indeed, no union of intervals can lose forever that infinitely often $\xi^{(k)} > \frac{1}{6}$, so that $\theta^{(k)} + \frac{2\xi^{(k)}}{1-2\xi^{(k)}} > \frac{1}{2}$ infinitely often as well. Then, for k large enough $\theta^{(k)} > \frac{2}{3}$ (resp. $\theta^{(k)} < \frac{1}{3}$), which means that $(C1)$ is not satisfied anymore (by Lemma 4.4). This contradicts the assumption. We conclude that if all the iterates $\mathcal{R}^{(k)}$ are defined, then $\theta^{(0)} = \frac{1}{2}$.

Proof (of Theorem D). — The inverses of matrices $N_{1a} = N_{2a}$, N_{1b}, N_{1c}, N_{2b} and N_{2c} can be decomposed as $N_x^{-1} = \left(\begin{array}{cc|c} \multicolumn{2}{c|}{\multirow{2}{*}{R_x}} & \\ & & \\ \hline 0 & & \pm 1 \end{array}\right)$, where $R_x \in \mathcal{M}_4(\mathbb{N})$ is a matrix with non-negative coefficients only.

Let $(x_i)_{i\in\mathbb{N}}$ be the infinite sequence of steps of induction followed by T. After n steps, the vector of lengths of $\mathcal{R}^n(T)$ is $\lambda^{(n)} = N_{x_n} \dots N_{x_2} N_{x_1} \lambda$, which means that λ is in the image of $N_{x_1}^{-1} N_{x_2}^{-1} \dots N_{x_n}^{-1}$. For any path $(x_i)_{i\in\mathbb{N}}$, the vector of lengths $\lambda^{(n)} = (a_1^{(n)} + a_2^{(n)}, b_1^{(n)} + b_2^{(n)}, c_1^{(n)} + c_2^{(n)}, b_1^{(n)} - b_2^{(n)}, \tau_1^{(n)} - \tau_2^{(n)})$ of the n-th induced map $\mathcal{R}(T)$ is such that

$$|b_1^{(n)} - b_2^{(n)}| = |b_1^{(0)} - b_2^{(0)}|.$$

Hence, if $|b_1^{(0)} - b_2^{(0)}| \neq 0$, then

$$\frac{|b_1^{(n)} - b_2^{(n)}|}{l^{(n)}} = \frac{|b_1^{(0)} - b_2^{(0)}|}{l^{(n)}} \underset{n\to\infty}{\longrightarrow} \infty,$$

which is impossible because $|b_1^{(n)} - b_2^{(n)}| < l^{(n)}$. We conclude that $b_1 = b_2$. Since $\lambda^{(0)} \in S_1$, we get $c_1 = c_2$. From Lemma 4.16, we know that $\tau_1 + \tau_2 = \frac{1}{2}(a_1 + b_1 + c_1 + a_2 + b_2 + c_2)$. Since $\lambda^{(0)} \in S_1$, we get $\tau_1 = \tau_2 = \frac{1}{2}(a_1 + b_1 + c_1) = \frac{1}{2}(a_2 + b_2 + c_2)$. This shows that T is a skew-product.

From results on IETFs on one circle (see Proposition 15 in [HP22] and [AR91]), we know that T is minimal and the tuple (a_1, b_1, c_1) is in the Rauzy gasket. ■

4.3.4. When a condition fails

The following cases are studied under the assumption that the lengths are in the subspace S_1 if the combinatorial data is p_1 or respectively S_2 if the combinatorial data is p_2.

4.3.4.a. When $(C0)$ is not satisfied, but $(C1)$ and $(C2)$ are

When the condition $(C0)$ is not fulfilled, but $(C1)$ and $(C2)$ are, we can choose to induce on the complementary of $\mathbf{M} \cup T^{-1}(\mathbf{M})$ in $\mathcal{C}_1 \cup \mathcal{C}_2$, for any $\mathbf{M}$ such that $s(\mathbf{M}) = \min s$ and $T(\mathbf{M}) \cap T^{-1}(\mathbf{M}) = \emptyset$ (i.e. that satisfies $(C2)$).

The induced IET is given by the same computations as before, but some intervals of continuity disappear (they have lengths 0). This lead to a few new combinatorial data with less intervals. There are a finite number of cases to consider.

4.3.4.b. When $(C1)$ is not satisfied

Since $(C1)$ is a conjunction of properties, there are several ways for $(C1)$ not to be true. In this section, we prove that when some interval $\mathbf{X}$ is such that $T(\mathbf{X}) \cap \mathbf{X} \neq \emptyset$, then T admits two cylinders of periodic points.

If $(C0)$, $(C2)$ hold and

$$\begin{array}{rl} \forall \{X, Y, Z\} = \{A, B, C\}, & T(\mathbf{X}) \subset \mathbf{Y} \cup \mathbf{Z} \\ \exists X \neq Y, & T(\mathbf{X}) \cap \mathbf{Y} = \emptyset \end{array} \tag{4.7}$$

then the configuration is "degenerated". The results can be adapted:

- Lemmas 4.2 and 4.4 hold up to replacing the signs $<$ and $>$ respectively by the signs $\leqslant$ and $\geqslant$.
- Lemma 4.5, Corollary 4.6, Lemmas 4.7 and 4.8, Theorem D and every expression given in Section 4.3.3 hold.

The case when the equations of (4.7) hold but $(C0)$ or $(C2)$ does not hold remains to be handled.

Lemma 4.17. *Let T be an IETF with combinatorial data p_1 (resp. p_2), with lengths in the subspace S_1 (resp. S_2). If T admits a union of intervals of continuity $\mathbf{X} = \mathbf{X}_1 \cup \mathbf{X}_2$ such that $T(\mathbf{X}) \cap \mathbf{X} \neq 0$, then T admits two cylinders of periodic points.*

Proof. — We give a proof by cases. We assume without loss of generality that the inequalities given by Lemma 4.2 are not satisfied for τ_1. Figure 4.16 shows periodic orbits of T, of period either 2 or 4, when T has combinatorial type p_1. The periodic cylinders are depicted with dotted lines. The case p_2 is analogous. ■

4.3.4.c. When $(C0)$, $(C1)$ are satisfied, but not $(C2)$

The cases of combinatorial data p_1 and p_2 are here distinct. In the first case, if $(C2)$ is not satisfied (but $(C0)$ and $(C1)$ are), then the IETF is not minimal: it admits two cylinders of periodic points, see Lemma 4.19. But in the second case, as Figure 4.17 illustrates it, the induced IETF can have a new combinatorial type:

$$p_3(A) = \left\{ \left(\begin{matrix} \overline{A_1} & \overline{B_1} & \overline{C_1} & \overline{D_1} \\ \overline{A_1} & \overline{B_2} \end{matrix} \right), \left(\begin{matrix} \overline{A_2} & \overline{B_2} & & \\ \overline{A_2} & \overline{B_1} & \overline{C_1} & \overline{D_1} \end{matrix} \right) \right\}.$$

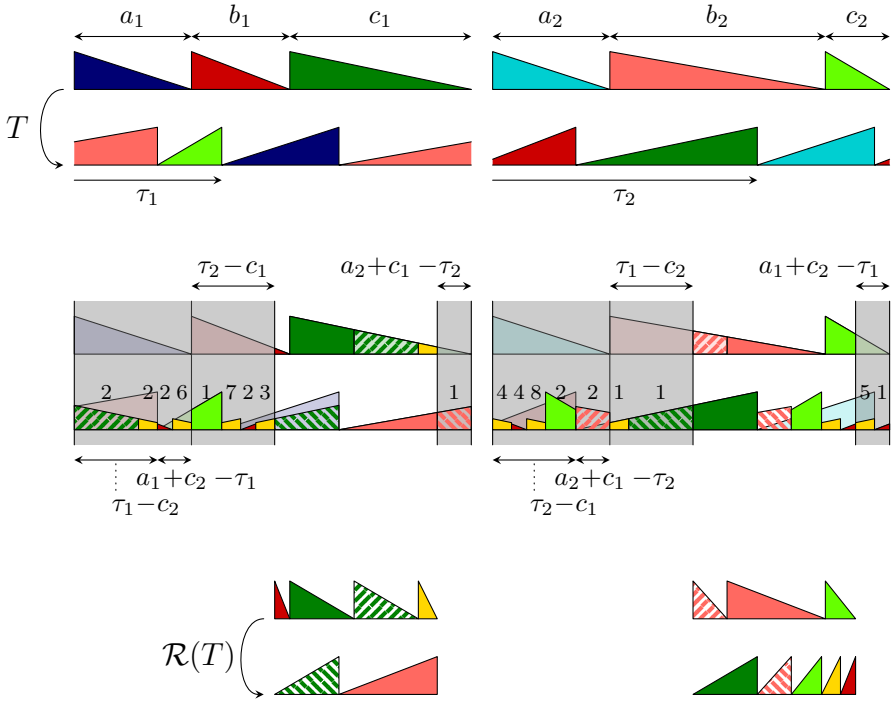

Figure 4.17. – An induced IETF with a new combinatorial data

However, I conjecture the following statement.

Conjecture 4.18. *Let T be an IETF with combinatorial data p_2, with lengths in the subspace S_2 and rationally independent. If T satisfies $(C0)$, $(C1)$, but not $(C2)$, then T has combinatorial type p_3.*

Lemma 4.19. *Let T be an IETF with combinatorial data p_1, with lengths in the subspace S_1. If T satisfies $(C0)$, $(C1)$, but not $(C2)$, then T admits a periodic orbit.*

Proof. — Recall that the condition $(C2)$ is given in terms of lengths in Table 4.1. For simplicity, we write τ instead of τ_1 or τ_2 and a instead of a_1 or a_2, since they are equal.

If s attains its minimum in B, then we can assume without loss of generality that the inequality not satisfied in $(C2)$ is $b_2 < a, c_1$. But if $b_2 > c_1$, then $b_1 = b_2 + c_2 - c_1 > c_2$, which contradicts that s attains its minimum in B. Hence we have

$$\begin{array}{c} c_1 \geqslant b_2 \geqslant a \geqslant b_1 \\ b_2 > b_1 \end{array} \tag{4.8}$$

The second line comes from the fact that $b_1 + b_2 = s(\mathbf{B}) < s(\mathbf{A}) = a_1 + a_2$. Since $(C1)$ is satisfied, $0 < \tau - c_1 < a$. The interval $J_1 = (0, \tau - c_1) \subset \mathbf{A}_1$ is such that:

- $T(J_1) = (a + c_1, \tau + a) \in \mathcal{C}_2$ is a subset of $\mathbf{C}_2$ because $c_1 \geqslant b_2$ by (4.8) and $\tau \leqslant b_2 + c_2$ by $(C1)$,
- $T^2(J_1) = (b_2, \tau + b_2 - c_1) \in \mathcal{C}_2$ is a subset of $\mathbf{B}_2$ because $b_2 \geqslant a$ by (4.8) and $\tau - c_1 \leqslant a$ by $(C1)$,
- $T^3(J_1) = (a + c_1 - c_2 - b_2, \tau + a - c_2 - b_2) = (a - b_1, \tau + a - b_1 - c_1) \in \mathcal{C}_2$ is a subset of $\mathbf{A}_2$ because $a - b_1 \geqslant 0$ by (4.8) and $\tau - b_1 - c_1 \leqslant a$ by $(C1)$,
- $T^4(J_1) = (b_1 + c_1, \tau + b_1) \in \mathcal{C}_1$ is a subset of $\mathbf{C}_1$ because $c_1 \geqslant a$ by (4.8) and $\tau \leqslant a + b_1$ by $(C1)$,
- $T^5(J_1) = (a, \tau + a - c_1) \in \mathcal{C}_1$ is a subset of $\mathbf{B}_1$ because $\tau - c_1 \leqslant b_1$ by $(C1)$,
- and $T^6(J_1) = J_1$, namely every points in J_1 is 6-periodic (the equality is pointwise since T^6 is an orientation preserving piecewise isometry and is continuous on the interval J_1).

There is another interval of 6-periodic points: $J_2 = (\tau - b_1, a) \in \mathcal{C}_2$, which is a subinterval of $\mathbf{A}_2$ because $\tau - b_1 \geqslant 0$ by $(C1)$. We have:

- $T(J_2) = (\tau, a + b_1) \subset \mathbf{B}_1$,
- $T^2(J_2) = (\tau + a, 2a + b_1) \subset \mathbf{C}_1$,
- $T^3(J_2) = (\tau - a, b_1) \subset \mathbf{A}_1$,
- $T^4(J_2) = (\tau + a - b_1, 2a) \subset \mathbf{B}_2$,
- $T^5(J_2) = (\tau + b_2, a + b_1 + b_2) \subset \mathbf{C}_2$,
- and $T^6(J_2) = J_2$.

If s attains its minimum in C, we can assume without loss of generality that the inequality not satisfied in $(C2)$ is $c_2 < a, b_1$. But if $c_2 > b_1$, then $c_1 = b_2 + c_2 - b_1 > b_2$, which contradicts that s attains its minimum in C. Hence we have

$$\begin{array}{c} b_1 \geqslant c_2 \geqslant a \geqslant c_1 \\ c_2 > c_1 \end{array} . \tag{4.9}$$

We have again two intervals of 6-periodic points. The interval $J_1 = (\tau - c_1, a) \subset \mathbf{A}_1$ is such that:

- $T(J_1) = (\tau, a + c_1) \subset \mathbf{B}_2$,

- $T^2(J_1) = (\tau + a + b_2 - c_1, 2a + b_2) \subset \mathbf{C}_2$,
- $T^3(J_1) = (\tau - a, c_1) \subset \mathbf{A}_2$,
- $T^4(J_1) = (\tau + a - c_1, 2a) \subset \mathbf{B}_1$,
- $T^5(J_1) = (\tau + b_1, a + b_1 + c_1) \subset \mathbf{C}_1$,
- and $T^6(J_1) = J_1$.

The interval $J_2 = (0, \tau - b_1) \subset \mathbf{A}_2$ is such that:

- $T(J_2) = (a + b_1, \tau + a) \subset \mathbf{C}_1$,
- $T^2(J_2) = (b_1, \tau) \subset \mathbf{B}_1$,
- $T^3(J_2) = (a - c_1, \tau + a - b_1 - c_1) \subset \mathbf{A}_1$,
- $T^4(J_2) = (b_1 + c_1, \tau + c_1) \subset \mathbf{C}_2$,
- $T^5(J_2) = (a + b_1 - c_2, \tau + a - c_2) \subset \mathbf{B}_2$,
- and $T^6(J_2) = J_2$.

If s attains its minimum in A, we can assume without loss of generality that $b_1 \geqslant b_2$ (hence $c_1 \leqslant c_2$). Then the fact that $(C2)$ is not satisfied implies either $a > b_2$ or $a > c_1$. If $b_2 \geqslant a > c_1$, then $b_1, b_2, c_2 \geqslant a > c_1$ and we can check that $J_1 = (\tau - c_1, a) \subset \mathbf{A}_1$ and $J_2 = (0, \tau - b_1) \subset \mathbf{A}_2$ are such that $T^6(J_1) = J_1$ and $T^6(J_2) = J_2$, as in the previous case. If $c_1 \geqslant a > b_2$, , then $b_1, b_1, c_2 \geqslant a > b_2$. With computations as in the first case (when s attains its minimum in B), we can check that $J_1 = (\tau - b_2, a) \subset \mathbf{A}_1$ and $J_2 = (0, \tau - c_2) \subset \mathbf{A}_2$ are such that $T^6(J_1) = J_1$ and $T^6(J_2) = J_2$.

If $a > c_1, b_2$, we assume without loss of generality that $b_2 \leqslant c_1$. Then the intervals $J_1 = (\tau - c_1, a) \subset \mathbf{A}_1$ and $J_2 = (0, \tau - b_1) \subset \mathbf{A}_2$ are such that $T^6(J_1) = J_1$ and $T^6(J_2) = J_2$. ■

4.3.4.d. When $(C1)$ is satisfied, but neither $(C2)$ nor $(C0)$

This is a degenerate case of the previous subsection, as subsection 4.3.4.a was a degenerate case of the case where the three conditions hold. This lead to the disappearance of one (or more) interval(s) of continuity.

4.4. Perspectives

4.4.1. Complete description of bi-triangle tiling billiards

To finish the study of bi-triangle tiling billiards, we must find a good induction on p_3. We cannot apply the definition that we give in Section 4.3 because the combinatorial data $p_3 = \left(\left(\sigma_0^{(1)}, \sigma_1^{(1)}\right), \left(\sigma_0^{(2)}, \sigma_1^{(2)}\right)\right)$ is not "symmetric", in the sense that $\sigma^{(1)} = \left(\sigma_0^{(1)}, \sigma_1^{(1)}\right)$ is not equivalent to $\sigma^{(2)} = \left(\sigma_0^{(2)}, \sigma_1^{(2)}\right)$ This would give answers to the questions on IETFs. We have then to translate these answers into

answers to the questions on tiling billiards. On the contrary to mono-triangle and cyclic quadrilateral tiling billiards, there could be some bi-triangle tiling billiards' trajectories that do not stay at bounded distance from a line, *even though* the associated IETF is not minimal. We explain this in the following paragraph.

Let $\mathcal{T}$ be a bi-triangle tiling. Let $\mathcal{D}$ be the associated Dynnikov's helicoid to the tiling billiard in $\mathcal{T}$ and let Λ be the lattice such that $\mathcal{D}$ is Λ-periodic. Set $\mathcal{S} = \mathcal{D}/\Lambda$. Roughly speaking, we can see a trajectory as wrapping around the quotient surface $\mathcal{S}$. We can show that if it wraps in a subsurface of genus at most 2, then the trajectory (in the tiling billiard) is either periodic or has an asymptotic direction. If there exists a cylinder of periodic trajectories, then these trajectories fill a cylinder of $\mathcal{S}$. It means that the other trajectories can wrap around a subsurface of genus at most 2, hence must be either periodic or with an asymptotic direction. This is why, in the case of mono-triangle and cyclic quadrilateral tiling billiards, only minimal IETFs can be associated to tiling billiards admitting trajectories without asymptotic direction. But in the case of bi-triangle tiling billiards, the surface $\mathcal{S}$ has genus 5, which leaves "enough place" to have both periodic cylinder *and* trajectories wrapping around a subsurface of genus 3, i.e. possibly without asymptotic direction.

4.4.2. Admissible tilings

Definition 4.20. *We call* admissible tiling *of the plane a tiling:*

(1) that is periodic,

(2) whose tiles are all cyclic polygons,

(3) and the circumcircles of tiles have all the same radius.

If $\mathcal{T}$ is an admissible tiling, with d tiles in a fundamental domain, there exists a 1-parameter family $(\Phi_\tau)_{\tau\in[0,\pi)}$ of IETFs on the union of d circles (corresponding to the d circumcircles of the d tiles) that describes the dynamics of the $\mathcal{T}$-tiling billiard. Each trajectory with parameter τ of the $\mathcal{T}$-tiling billiard corresponds to an orbit $(\Phi_\tau^k(x_0))_{k\in\mathbb{N}}$ of Φ_τ. The orbit is finite if and only if the trajectory is periodic or drift-periodic. The combinatorial data of the IETF is given by the dual graph of the tiling.

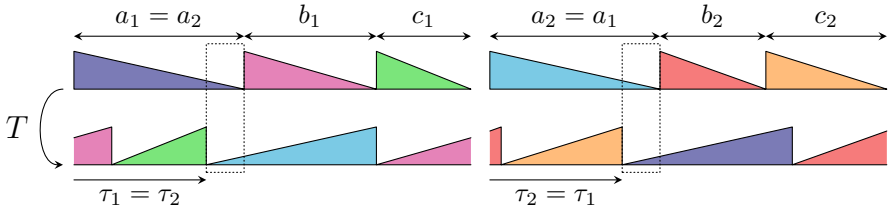

(a) If $\tau_1 < a_1$, then T admits a 4-periodic cylinder of width $a_1 - \tau_1 = a_2 - \tau_2$

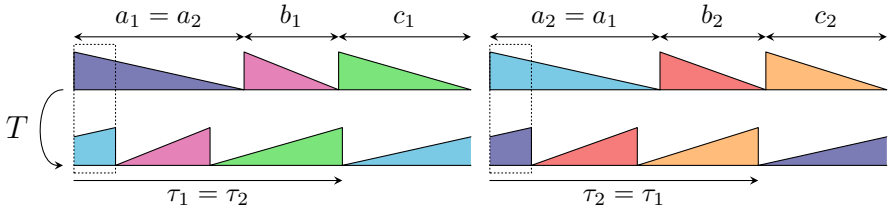

(b) If $b_1 + c_1 < \tau_1$, then T admits a 4-periodic cylinder of width $\tau_1 - b_1 - c_1 = \tau_2 - b_2 - c_2$

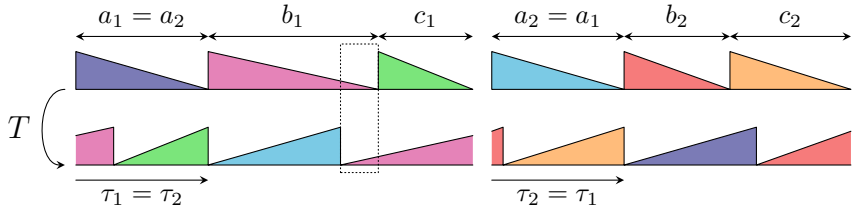

(c) If $\tau_1 < b_1$, then T admits a 2-periodic cylinder of width $b_1 - \tau_1$

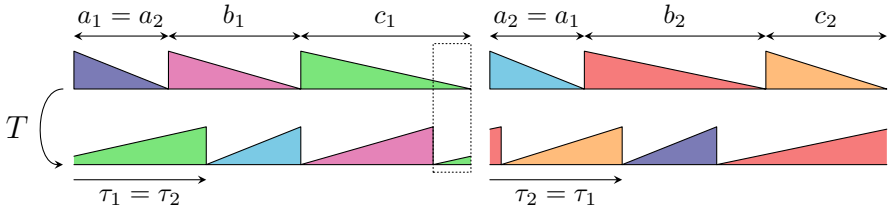

(d) If $\tau_1 < c_1$, then T admits a 2-periodic cylinder of width $c_1 - \tau_1$

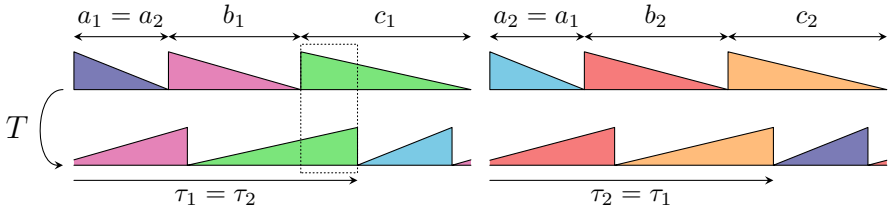

(e) If $a_1 + b_1 < \tau_1$, then T admits a 2-periodic cylinder of width $\tau_1 - a_1 - b_1$

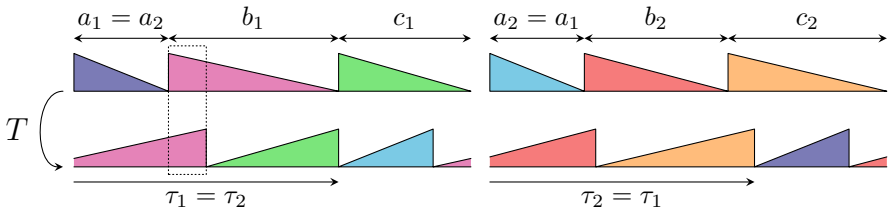

(f) If $a_1 + c_1 < \tau_1$, then T admits a 2-periodic cylinder of width $\tau_1 - c_1 - a_1$

Figure 4.16. – When $(C1)$ is not satisfied, T admits periodic points

5. The tiling billiard in the wind-tree model

5.1. Introduction

5.1.1. Setting

Let $\Lambda \subset \mathbb{R}^2$ be a lattice, let $a, b > 0$, and let $\theta \in [0, \pi)$. We consider an array of rectangles of size $a \times b$ placed on points of the lattice Λ, and making an angle θ with the horizontal. We will restrict to tuples (Λ, a, b, θ) where the rectangles are pairwise disjoint in the plane, and say these tuples are *admissible*. We consider the tiling billiard trajectories with initial *vertical* direction, from any point of the plane outside the rectangles. If a trajectory reaches a corner, it stops. We call this system *the wind-tree tiling billiard*, that we denote by $W(\Lambda, a, b, \theta)$. We prove the following Theorem, illustrated by Figure 5.1.

Theorem E. *For almost every admissible tuple (Λ, a, b, θ), there exist constants $C = C(\Lambda, a, b, \theta) > 0$ and $\Theta = \Theta(\Lambda, a, b, \theta) \in [0, \pi)$, such that every vertical trajectory in $W(\Lambda, a, b, \theta)$ is trapped in an infinite band of width $C > 0$ in direction Θ.*

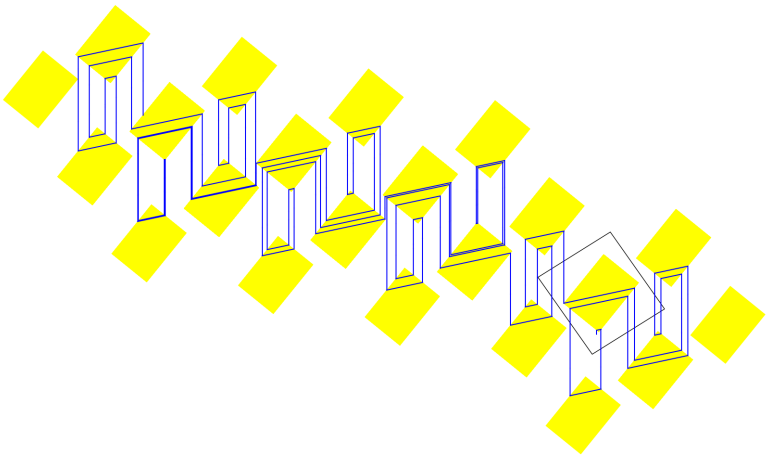

Figure 5.1. – Example of a trajectory

5.1.2. Strategy

To establish Theorem E, we transform our broken-line trajectory in the plane into a geodesic in some half-translation surface $X_{(\Lambda,a,b,\theta)}$ that corresponds to the system $W(\Lambda, a, b, \theta)$. This idea was already used by Frączek and Schmoll to study light rays in an Eaton lenses array [FS14]. One of the main points of this chapter is to build the surface $X_{(\Lambda,a,b,\theta)}$ corresponding to our case. This surface has four singularities, two of conical angle π and two of conical angle 3π. In other words $X_{(\Lambda,a,b,\theta)}$ lies in the stratum $\mathcal{Q}(1,1,-1,-1)$, that we denote by $\mathcal{Q}(1^2,-1^2)$ in the following. We prove the following Theorem, where γ_T is a cycle corresponding to the trajectory, defined in Section 5.3.

Theorem F. *Let $X \in \mathcal{Q}(1^2,-1^2)$ be a generic surface. There exist a cycle $w \in H_1(X,\mathbb{R})$ and a constant $C>0$ such that for every $p \in X$, and every $T>0$, the (algebraic) number of intersections between w and γ_T is bounded by C:*

$$|\iota(w,\gamma_T)| < C.$$

Here we use the term generic to say Birkhoff, Masur and Oseledets generic, all of which will be defined in Section 5.2.4. To get the bound, we decompose the cycle γ_T, as Forni did in [For02] and after him Delecroix, Hubert and Lelièvre in [DHL14]. We prove that Theorem F implies Theorem E with Lemma 5.15 in Section 5.3.1.

5.2. The corresponding surface

To each wind-tree with parameters (Λ, a, b, θ), we associate an infinite half-translation surface, which is the plane $\mathbb{R}^2$ with infinitely many singular points, of conical angle π or 3π. In this section, we explain how we build this surface and how it is related to our problem.

5.2.1. From foliations to an appropriate slit surface

There are two ways for a trajectory to pass through a rectangular obstacle: either it goes from a side to the opposite side, or it goes from a side to an adjacent side (and in this case, its direction is reversed), see Figue 5.2.

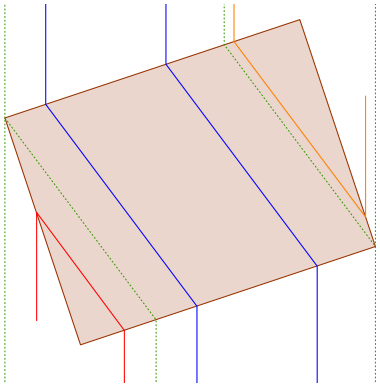

Figure 5.2. – The different ways to go through the obstacle

Two "crossing" trajectories in blue, and two "reversed" trajectories in red and orange. The singular leaves are drawn in dotted green.

This observation shows that one can replace the obstacle by a slit with identifications, as drawn in Figure 5.3. In this new setting, the trajectories of our problem become geodesics in an infinite half-translation surface. The surface in question is defined by Definition 5.1 and Lemma 5.4 states that the geodesics in the new surface are *equivalent* (see Definition 5.3) to the trajectories of the system $W(\Lambda, a, b, \theta)$.

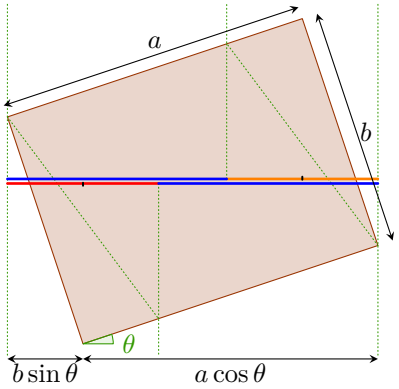

Figure 5.3. – From a rectangular obstacle to a slit with identifications

Definition 5.1. *Let (Λ, a, b, θ) be an admissible tuple. If the horizontal segments of length $a\cos\theta + b\sin\theta$ centered at each point of Λ are pairwise disjoint, we say that (Λ, a, b, θ) is a strongly admissible tuple. In this case, we denote by $S_{(\Lambda,a,b,\theta)}$ the plane $\mathbb{R}^2$ with an horizontal slit of length $a\cos\theta + b\sin\theta$ at each point of the lattice Λ, with the identifications as in Figure 5.4.*

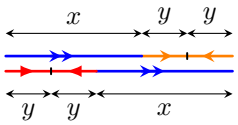

(a) If $a\cos\theta > b\sin\theta$ then $\begin{array}{l} x = b\sin\theta - a\cos\theta \\ y = a\cos\theta \end{array}$.

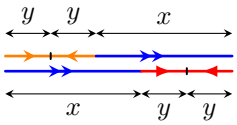

(b) If $a\cos\theta < b\sin\theta$ then $\begin{array}{l} x = a\cos\theta - b\sin\theta \\ y = b\sin\theta \end{array}$.

Figure 5.4. – Identifications of the slit

There is a geometric way to distinguish case (a) from case (b): if the singular leaves go through the interior of a side of length a (resp. b), then case (a) (resp. (b)) holds. Moreover, when case (a) (resp. (b)) holds, every trajectory entering in the obstacle by a side of length b (resp. a) goes out from an adjacent side.

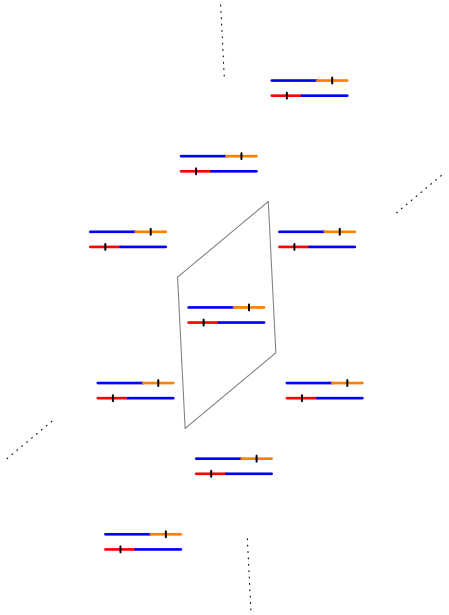

Figure 5.5. – The surface $S_{(\Lambda,a,b,\theta)}$
A fundamental domain of Λ is drawn in gray.

The assumption on the tuple is not always satisfied (see Figure 5.6) but almost always, as states Lemma 5.2. However, we can still associate a surface to the system, by taking the slit in slightly different direction. Indeed, the slit has to be transverse to vertical direction, but could be not horizontal. Nevertheless we continue with horizontal slit for simplicity.

Lemma 5.2. *Almost every admissible tuple* (Λ, a, b, θ) *is also strongly admissible.*

Proof. — The intervals are not pairwise disjoint if and only if there exists some horizontal vector $(x, 0)$ is in the lattice Λ, with $x < a\cos\theta + b\sin\theta$, which is, for almost every Λ, not the case. ■

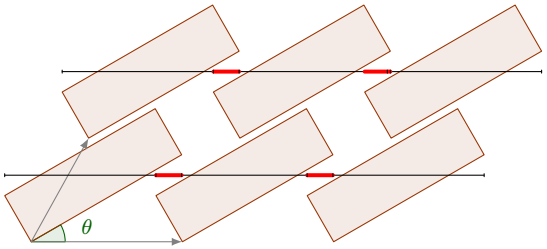

Figure 5.6. – An example where (Λ, a, b, θ) is admissible but not strongly admissible

The slit are simply drawn in black and the parts on which they overlap are drawn in bold red. The two grey vectors form a basis of the lattice Λ.

5.2.2. Equivalent trajectories

We denote by $\mathcal{I} \subset \mathbb{R}^2$ the set of horizontal segments of length $a\cos\theta + b\sin\theta$, centered at each point of Λ.

Note that the projection $\pi_S : \mathbb{R}^2 \setminus \mathcal{I} \longrightarrow S_{(\Lambda,a,b,\theta)}$ is well-defined.

Definition 5.3. *Let $\tilde{\gamma} \subset \mathbb{R}^2$ and $\gamma \subset S_{(\Lambda,a,b,\theta)}$ be two curves. Say that $\tilde{\gamma}$ and γ are equivalent if there exist two sets $\tilde{F} \subset \mathbb{R}^2$ and $F \subset S_{(\Lambda,a,b,\theta)}$ such that the images of the curves outside $\tilde{F}$ and F respectively are the same:*

$$\pi_S\left(Im(\tilde{\gamma}) \cap \left(\mathbb{R}^2 \setminus \tilde{F}\right)\right) = Im(\gamma) \cap \left(S_{(\Lambda,a,b,\theta)} \setminus F\right).$$

We have defined $S_{(\Lambda,a,b,\theta)}$ so that each vertical trajectory in the wind-tree model is equivalent to a vertical trajectory in $S_{(\Lambda,a,b,\theta)}$. This is what establishes the following lemma.

Lemma 5.4. *There exist a proper closed set $\tilde{F} \subset \mathbb{R}^2$ such that for any $p \in \mathbb{R}^2 \setminus \tilde{F}$, the vertical trajectory $\tilde{\gamma}$ starting at point $\tilde{p}$ in the wind-tree model of parameters (Λ, a, b, θ) is equivalent to the vertical trajectory starting at point p in $S_{(\Lambda,a,b,\theta)}$.*

Proof. — Denote by (A, B, C, D) the rectangular obstacle and (x_A, y_A) the coordinates of the point A (analogously for B, C and D). Let p and p' be the two intersection points between (A, B, C, D) and the segment $[q, q']$, where $q = \left(x_B, \frac{y_B+y_D}{2}\right)$ and $q' = \left(x_B, \frac{y_B+y_D}{2}\right)$. Let $\tilde{F}$ be the polygon $(p, q, A, B, q', p', C, D)$ if $y_B < y_D$, and $(p, q, D, A, p', q', B, C)$ if $y_B \geqslant y_D$. See Figure 5.7 below. The lengths of the slit are such that the trajectories coincide outside the region $\tilde{F}$ (see also Figure 5.3).

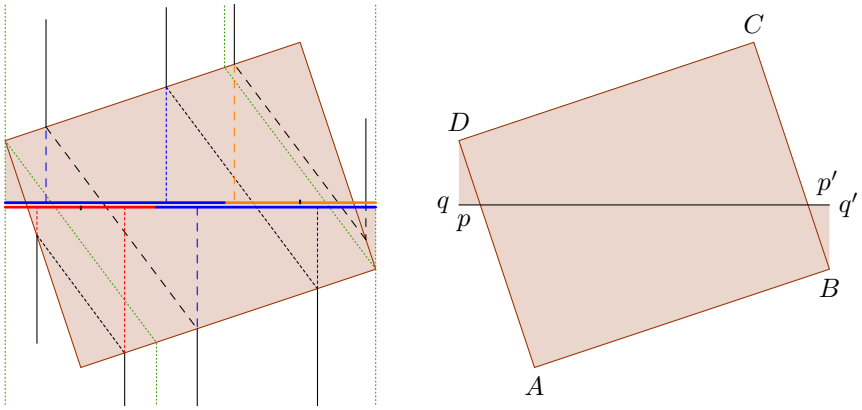

(a) Case $y_B < y_D$

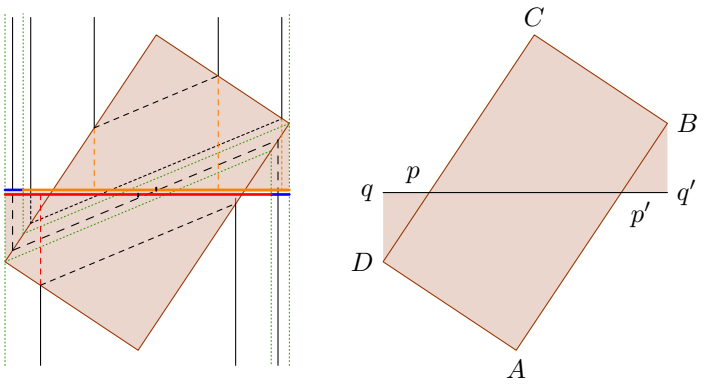

(b) Case $y_B < y_D$

Figure 5.7. – Definition of the set $\tilde{F}$

The trajectories in $\mathbb{R}^2$ (i.e. the trajectories of $W(\Lambda, a, b, \theta)$) are drawn in black, while the trajectories in $\pi(\tilde{F}) \subset S_{(\Lambda,a,b,\theta)}$ are drawn with dashed colored lines, according to the part of the slit they hit. The parts of the trajectories inside $\tilde{F}$ are drawn with dashed black lines. The trajectories in $\mathbb{R}^2 \setminus \tilde{F}$ and the ones in $S_{(\Lambda,a,b,\theta)} \setminus \pi(\tilde{F})$ coincide, they are drawn in black. ■

Remark 5.5. *We highlight that the parametrizations of the curves γ and $\tilde{\gamma}$ do not coincide. In fact, the difference in their parametrization may change at each crossing of an obstacle: sometimes γ has less distance to cover, sometimes more, see Figure 5.8a and 5.8b below.*

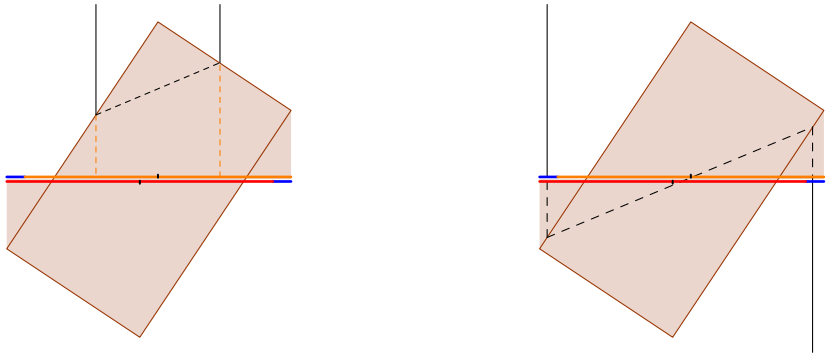

(a) γ may be longer than $\tilde{\gamma}$ (b) γ may be shorter than $\tilde{\gamma}$

Figure 5.8. – Changing the surface from $\mathbb{R}^2$ to $S_{(\Lambda,a,b,\theta)}$ changes the parametrization of γ

5.2.3. The finite half-translation surface we will work with

Since $S_{(\Lambda,a,b,\theta)}$ is a periodic surface, we can study a quotient of it instead of itself. This is more convenient because we will get a finite half-translation surface.

Lemma 5.6. *The quotient surface* $X_{(\Lambda,a,b,\theta)} = {}^{S_{(\Lambda,a,b,\theta)}}/_{\Lambda}$ *is in the stratum* $\mathcal{Q}(1^2,-1^2)$.

We call $X_{(\Lambda,a,b,\theta)}$ the *surface associated* to the tuple (Λ,a,b,θ). When the context is clear, we will simply write X instead of $X_{(\Lambda,a,b,\theta)}$, and call it the associated surface.

Proof. — All the singularities of X come from the identifications in the slit.



(a) If $a\cos\theta > b\sin\theta$ (b) If $a\cos\theta < b\sin\theta$

Figure 5.9. – Singularities on the slit

One can check on the picture above that X has four singularities. The middle of the red (resp. orange) segment (of length $2y$) has conical angle π, whereas the two endpoints of the blue segment (of length x) have conical angle 3π. ■

Remark 5.7. *We could have considered first the quotient of the plane with obstacles by the lattice and then have replaced the obstacle by a slit, we would have got the same surface* $X_{\Lambda,a,b,\theta}$. *The Figure below illustrates the equivalence of trajectories between the torus with an obstacle and the slit torus.*

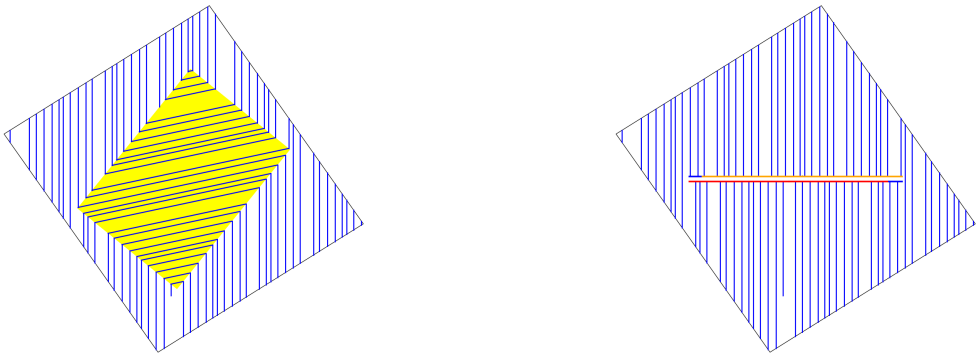

(a) On a torus with an obstacle (b) On a torus with a slit

Figure 5.10. – Two equivalent trajectories

Remark 5.8. *In our context, the natural way to picture X is as a slit torus, like in Figure 5.10b. However, as a half-translation surface, it can be represented as a polygon with parallel sides identified, like in Figure 5.12. Depending on what we do, it could be useful to think of X as in Figure 5.10b or as in Figure 5.12.*

We denote the canonical projections by $\pi : S_{(\Lambda,a,b,\theta)} \longrightarrow X_{(\Lambda,a,b,\theta)}$ and

$$\pi_X = \pi \circ \pi_S : \mathbb{R}^2 \setminus \mathcal{I} \longrightarrow X_{(\Lambda,a,b,\theta)}.$$

5.2.4. How generic is the surface?

Recall that the stratum $\mathcal{Q}(1^2, -1^2)$ is equipped with a finite measure μ, called the Masur-Veech measure. Denote by

$$\mathcal{X} = \left\{ X_{(\Lambda,a,b,\theta)} \middle| \, (\Lambda, a, b, \theta) \text{ is strongly admissible} \right\} \subset \mathcal{Q}(1^2, -1^2)$$

the set of surfaces corresponding to a system $W(\Lambda, a, b, \theta)$. These surfaces are specific. Indeed the set $\mathcal{X}$ has real dimension 6, whereas the stratum $\mathcal{Q}(1^2, -1^2)$ has real dimension 8. However, we show in this section that almost every $X \in \mathcal{X}$ is generic, meaning that:

(1) the surface satisfies Theorem 5.9 (i.e. is *Birkhoff genric*),

(2) the vertical flow on the surface is uniquely ergodic (i.e. the surface is *Masur generic*),

(3) the surface admits an Oseledets flag for the Kontsevich–Zorich cocycle (i.e. the surface is *Oseledets generic*).

Theorem 5.9. *For almost every $X \in \mathcal{Q}(1^2, -1^2)$, we have*

$$\forall \phi \in \mathcal{C}_c(\mathcal{Q}(1^2, -1^2)), \lim_{T\to\infty} \frac{1}{T} \int_0^T \phi(g_t X) dt = \int_{\mathcal{Q}(1^2,-1^2)} \phi d\mu.$$

This theorem is a consequence of Birkhoff ergodic theorem and the Masur–Veech theorem stating the ergodicity of the geodesic flow g_T on each stratum of the moduli space. We define the Kontsevich–Zorich cocycle in Sections 2.1.6 and 2.2.4 and Oseledets flag in Section 2.3.

Let $\mathcal{U}$ be a neighborhood of X such that all surface in $\mathcal{U}$ admit a presentation as a polygon with the same combinatorial data. Since $\mathcal{Q}(1^2,-1^2)$ has real dimension 8, we know that these polygons have 4 (linearly independent) pairs of parallel side. We consider them as vectors in $\mathbb{R}^2$ and denote them by $u_1(Y), u_2(Y), u_3(Y)$, and $u_4(Y)$. Denote by $h(u)$ the horizontal component of u and $v(u)$ the vertical component of u. We call

$$E^s(X) = \{Y \in \mathcal{U} | \forall i,\ h(u_i(Y)) = h(u_i(X))\}$$

the (local) *stable manifold* of X and

$$E^u(X) = \{Y \in \mathcal{U} | \forall i,\ v(u_i(Y)) = v(u_i(X))\}$$

the (local) *unstable manifold* of X. It follows directly from the expression of the Teichmüller flow g_t, that for every $Y \in E^s(X)$ the distance $\mathrm{d}(g_t(X), g_t(Y))$ tends exponentially fast to 0 when t goes to infinity, which explains the term *stable*. On the opposite, the orbit of every $Y \in E^u(X)$ goes away from the orbit of X. More precisely, the distance $\mathrm{d}(g_t(X), g_t(Y))$ tends exponentially fast to 0 when t goes to minus infinity.

Lemma 5.10. *Let $X \in \mathcal{Q}(1^2,-1^2)$. If X is Birkhoff, Masur and Oseledets generic, then any surface Y in the stable manifold $E^s(X)$ of X is Birkhoff, Masur and Oseledets generic.*

Proof. — Birkhoff, Masur and Oseledets genericity are properties that depend only on the future of X under the Teichmüller flow g_t, and not on its past. Since all surfaces in $E^s(X)$ have the same future, they are either all generic or all not generic. ■

Lemma 5.11. *Let (Λ, a, b, θ) be a strongly admissible tuple. For any surface Y in the unstable manifold of $X_{(\Lambda,a,b,\theta)}$, there exists a tuple $(\Lambda', a', b', \theta')$ such that $Y = X_{(\Lambda',a',b',\theta')}$.*

Note that this is a local property, as it works only for surfaces in $E^u(X) \subset \mathcal{U}$.

Proof. — The stable and unstable manifolds of a surface X in $\mathcal{Q}(1^2,-1^2)$ both have dimension 4. The tuple (Λ, a, b, θ) has 6 independent parameters, among which 4 make the surface vary in its unstable manifold:

- the two horizontal coordinates of a basis of Λ,
- the two lengths ($a\cos\theta$ and $b\sin\theta$) that defines the slit,

and 2 make the surface vary in its stable manifold:

- the two vertical coordinates of a basis of Λ.

We conclude that we can get every surface in the unstable manifold of $X_{(\Lambda,a,b,\theta)}$ by changing the tuple (Λ, a, b, θ). ■

Lemma 5.12. *For almost every strongly admissible tuple (Λ, a, b, θ), the associated half-translation surface X is Birkhoff, Masur and Oseledets generic.*

Proof. — Assume by contradiction that there is an open set $\Omega \subset \mathcal{X}$ containing X such that every surface $Y \in \Omega$ is not generic. The set $\mathcal{O} = \Omega \cap E^u(X)$ is an open set of $E^u(X)$ by Lemma 5.11 and $\mathcal{O}$ contains no generic element. But then the set

$$\mathcal{U} = \bigcup_{Y \in \mathcal{O}} E^u(Y)$$

is an open set in $\mathcal{Q}(1^2, -1^2)$ whose elements are all not generic by Lemma 5.10. This is impossible because almost every surface in $\mathcal{Q}(1^2, -1^2)$ (and more generally, in every stratum) is generic. ■

5.2.5. The new question

When we quotient the surface $S_{(\Lambda,a,b,\theta)}$ by the lattice Λ, we forget the position of the trajectory in the plane. But we can recover this information. Let (e_1, e_2) be a basis of Λ. The vectors e_1 and e_2 induce two curves respectively ζ_1 and ζ_2 such that (ζ_1, ζ_2) generates the fundamental group $\pi_1(X)$ of X. Their homology classes $([\zeta_1, \zeta_2])$ form a basis of $H_1(X, \mathbb{R})$. Then the (algebraic) number of intersections between the class $[\zeta_1]$ (resp. $[\zeta_2]$) and the trajectory (that we can consider as a class of homology γ_T up to connecting the start and end points of the trajectory - without crossing the curves ζ_1 or ζ_2) gives the position in the plane of the trajectory, relatively to the initial point. In the following we write the homology class ζ_1 and ζ_1 for simplicity. See Figure 5.11a.

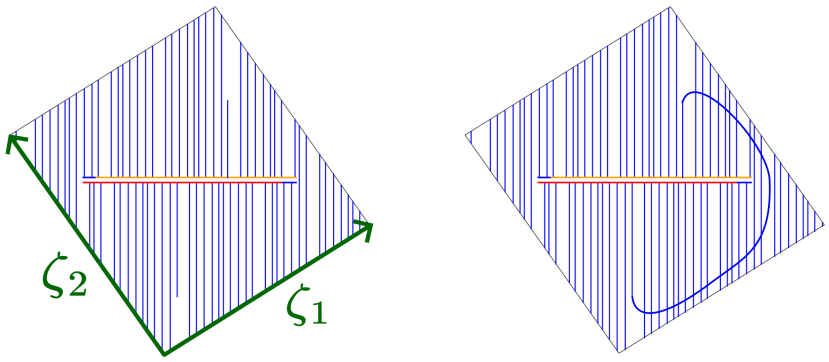

(a) Cycles ζ_1 and ζ_2 (b) Cycle γ_T

Figure 5.11. – The cycles which we consider

Hence our question is now: how many times does our curve γ_T (algebraically) intersect ζ_1 (resp. ζ_2)?

To answer this question, we first close the trajectory with a path that intersects neither ζ_1 nor ζ_2 (see Figure 5.11b), so that the trajectory can be seen as an element of the homology $H_1(X, \mathbb{R})$. Then we decompose the obtained closed curve γ into many closed curves $\gamma^{(k)}$. Finally we compute the algebraic intersection numbers between ζ_1 (resp. ζ_2) and each of the $\gamma^{(i)}$. To do this computation, we use the Teichmüller flow to "shorten" the curve $\gamma^{(k)}$ and the Kontsevich–Zorich cocycle to change from the basis (ζ_1, ζ_2) of $H_1(X, \mathbb{R})$ to a basis $(\zeta_1^{(k)}, \zeta_2^{(k)})$ such that $\gamma^{(k)}$ intersects many fewer times $(\zeta_1^{(k)}, \zeta_2^{(k)})$ than (ζ_1, ζ_2).

5.3. Decomposition of the trajectory

Let (Λ, a, b, θ) be a strongly admissible tuple, together with a basis (e_1, e_2). Let $X \in \mathcal{Q}(-1^2, 1^2) \subset \mathcal{M}$ be the half-translation surface associated to the tuple (Λ, a, b, θ). We assume that X is Birkhoff, Masur and Oseledets generic. Denote by (ζ_1, ζ_2) the two closed curves induced by (e_1, e_2) in the quotient. Fix s a singularity of X with no horizontal saddle connection. Choose a horizontal separatrix going out from s. Follow each vertical separatrix from s (there can be one or three of them depending on the conical angle of s), stop when it reaches the separatrix. If s has conical angle π, call this point x_0, if s has conical angle 3π call these points x_0, x_1, and x_2 (x_0 being the closest to s and x_2 the farthest). Let I be the horizontal segment starting at s and ending at x_0 (resp. x_2 if s has conical angle 3π).

Let $p \in X \setminus \pi(F)$. We assume that p is a regular point for the vertical flow in X, this is almost always the case. We consider the vertical trajectory in X starting at p. We will first explain in Subsection 5.3.1 that we can consider a cycle γ_T instead of a path. The goal of the current section is to decompose the cycle γ_T, this will be done in Subsection 5.3.3, using bounds established for surfaces in a neighborhood of X in Subsection 5.3.2.

Remark 5.13. *The same argument works for p not regular, it suffices to restrict ourselves to the times before the first time the vertical flow hits a singularity.*

5.3.1. From a path to a cycle

We want to close a path to get a closed curve. But we want to do it in a way that ensures that we can prove the result for trajectories in the plane by studying trajectories (seen as cycles) in the compact half-translation surface X. We will use the following

Lemma 5.14. *Given two points x and y in X, there exists a path δ such that:*

- *the path δ starts at x and ends at y,*

- *all but a finite number of points of δ are crossed either vertically or horizontally by δ,*
- *the path δ crosses neither the curve ζ_1 nor the curve ζ_2,*
- *the path δ is that of minimal length satisfying all the above properties.*

In the following, we denote by $\delta(x, y)$ any such path.

Proof. — We place ourselves in the cover S of X. Consider the fundamental domain $D = \{z_1 e_1 + z_2 e_2 \,|\, z_1, z_2 \in [0, 1]\}$ of Λ. Let $\tilde{x}$ and $\tilde{y}$ be the pre-images of x and y in D. Tile S with small squares (with horizontal and vertical sides). We can assume that both squares containing $\tilde{x}$ and $\tilde{y}$ are included in D (if needed, take smaller squares). Denote by l the segment between $\tilde{x}$ and $\tilde{y}$. Let b_x (resp. b_y) be the intersection point between l and the boundary of the square containing $\tilde{x}$ (resp. $\tilde{y}$). We build $\tilde{\delta}$ as the union of:

- a vertical and/or horizontal path that goes from $\tilde{x}$ to b_x,
- the path between b_x and b_y, following the boundaries of the squares,
- a vertical and/or horizontal path that goes from b_y to $\tilde{y}$.

The path $\delta = \pi(\tilde{\delta})$ satisfies the conclusion of the lemma. ■

We denote by

$$\Phi : \begin{array}{ccc} X \times \mathbb{R}_+ & \longrightarrow & X \\ (x, s) & \mapsto & \Phi_s(x) \end{array}$$

the vertical flow in X. In particular, for every x, $\Phi_0(x) = x$. For $s < t$, we denote by $\varphi_s^t(x)$ the part (of length $t - s$) of the vertical foliation of x which is between $\Phi_s(x)$ and $\Phi_t(x)$. Let $T_1, T_2 > 0$, and denote by $\gamma_{T_1,T_2}(p)$ the closed curve made of the union of $\varphi_{T_1}^{T_2}(p)$ and a path $\delta(\Phi_{T_2}(p), \Phi_{T_1}(p))$. For $T > 0$, we define

$$\gamma_T(p) = \gamma_{0,T}(p)$$

the cycle that starts at p, follows the vertical flow until time T and that comes back to p following a path $\delta(\Phi_T(p), p)$.

Finally, we denote by

$$\Psi : \begin{array}{ccc} \mathbb{R}^2 \times \mathbb{R}_+ & \longrightarrow & \mathbb{R}^2 \\ (x, s) & \mapsto & \Psi_s(x) \end{array}$$

the flow of the tiling billiard in the wind-tree model. Recall that we denote by ι the intersection form on $H_1(X, \mathbb{R}^2)$.

Lemma 5.15. *Let $w \in H_1(X, \mathbb{R})$. If*

$$\exists C > 0, \forall T > 0, \qquad |\iota(w, \gamma_T)| < C$$

then

$$\exists C' > 0,\ \exists z \in \mathbb{R}^2,\ \forall T > 0, \qquad | < z, \Psi_T(\tilde{p}) - \tilde{p} > | < C',$$

where $<,>$ *denotes the Euclidean scalar product and* $\tilde{p} \in \pi^{-1}(p)$.

The vector $\Psi_T(\tilde{p}) - \tilde{p}$ corresponds to the displacement of the tiling billiard trajectory in the plane, between times 0 and T. In other words, the trajectory of the tiling billiard in the wind-tree model is trapped in a strip of width $2C'$ and orthogonal to the vector z.

Proof. — We recall that the parametrization of Ψ_s does not necessarily coincide with the one of Φ_s, i.e. a priori $\pi_X(\Psi_s(\tilde{p})) \neq \Phi_s(p)$, for $\tilde{p} \in \mathbb{R}^2 \setminus \tilde{F}$ and $p = \pi_X(\tilde{p}) \in X$, where the set $\tilde{F}$ given by Lemma 5.4. Let $\mathcal{T}_r = \left\{ s \in \mathbb{R}_+ | \Psi_s(\tilde{p}) \notin \tilde{F} \right\}$ be the set of times when the tiling billiard trajectory in the plane lies outside $\tilde{F}$. Let $r : \mathbb{R}_+ \longrightarrow \mathbb{R}_+$ be a reparametrization function such that $\forall s \in \mathcal{T}_r$, $\pi_X(\Psi_s(\tilde{p})) = \Phi_{r(s)}(p)$. The values of r outside the set $\mathcal{T}_r$ do not matter.

Let $T \in r(\mathcal{T}_r)$, so that $\gamma_T(p) \notin F = \pi_X(\tilde{F})$, and let $s = r^{-1}(T)$. We have $\Psi_s(\tilde{p}) = \Phi_T(p)$.

Set $i_1 = \iota(\gamma_T, \zeta_1)$ and $i_2 = \iota(\gamma_T, \zeta_2)$ the algebraic intersection numbers of γ_T with the basis (ζ_1, ζ_2) of $H_1(X, \mathbb{R})$. Then the vector $\Psi_s(\tilde{p}) - \tilde{p}$ lies in

$$D_{i_1,i_2} := \{\, \beta_1 e_1 + \beta_2 e_2 \,|\, \lfloor \beta_1 \rfloor = i_1 \text{ and } \lfloor \beta_2 \rfloor = i_2 \} \subset \mathbb{R}^2$$

by the choice of the basis (e_1, e_2) of $\Lambda \subset \mathbb{R}^2$.

If $w = \alpha_1 \zeta_1 + \alpha_2 \zeta_2$, define $z = \alpha_1 e_1 + \alpha_2 e_2$. For the times $s \in \mathcal{T}_r$, we get $| < z, \Psi_T(\tilde{p}) - \tilde{p} > | < C$. For a time $T \notin \mathcal{T}_r$, we consider the closest time $s \in \mathcal{T}_r$ to T such that $T < s$. Then the difference vector $\epsilon = (\Psi_T(\tilde{p}) - \tilde{p}) - (\Psi_s(\tilde{p}) - \tilde{p})$ is such that its coefficients in the basis (e_1, e_2) are at most 1. Hence, up to take a bigger constant C', we have $| < z, \Psi_T(\tilde{p}) - \tilde{p} > | < C'$, which ends the proof. ■

Lemma 5.15 shows that Theorem F implies Theorem E.

5.3.2. Uniform bounds in a neighborhood of the surface X

Definition 5.16. *We call* vertical length *of a path* γ *its integral against the* 1*-form* dz*. We denote it by* l_v*:*

$$l_v(\gamma) = \int \gamma dz.$$

Lemma 5.17. *There exist a relatively compact neighborhood of* X *in* $\mathcal{Q}(1^2, -1^2)$ *and a constant* $K > 0$ *such that for every* $Y \in \overline{\mathcal{U}}$*, there exists a segment* $I(Y) \subset Y$ *such that, for* $i, j \in \{1, 2\}$*:*

- *every path* γ *on* Y *of* vertical length *at least* K *intersects at least once the segment* $I(Y)$*,*

- *every path γ on Y that intersects at least twice $I(Y)$ has* vertical length *at least K^{-1}.*

Moreover, for every $Y \in \overline{\mathcal{U}}$, the homology group $H_1(Y,\mathbb{R})$ can be identified to $H_1(X,\mathbb{R})$, and the basis $(\zeta_1(Y),\zeta_2(Y))$ of $H_1(Y,\mathbb{R})$ corresponding to the basis (ζ_1,ζ_2) of $H_1(X,\mathbb{R})$ is such that:

$$K^{-1} \leqslant l_v(\zeta_j(Y)) \leqslant K.$$

Proof. — Let $\mathcal{U}$ a relatively compact neighborhood of X in $\mathcal{Q}(1^2,-1^2)$, small enough so that every surface in $\mathcal{U}$, seen as a polygon with identified sides, has the combinatorial data as X (i.e. the sides are identified in the same order for every surface of $\mathcal{U}$). From this point of view, each singularity of a surface is a vertex of the polygon. Since all polygons have the same combinatorial type, there is a natural identification of the singularities of a surface of $\mathcal{U}$ to the singularities of any other surface in $\mathcal{U}$. For every $Y \in \mathcal{U}$, denote by $s(Y) \in Y$ the singularity corresponding to $s \in X$. Up to replacing $\mathcal{U}$ by a smaller neighborhood of X, we can assume that for every $Y \in \mathcal{U}$, the separatrix going out from $s(Y)$ is not a saddle connection. Then we can build a segment $I(Y) \subset Y$ in Y as we have built I in X. Consider the zippered rectangles presentation of Y. Up to considering a smaller neighborhood, we can assume that all the zippered rectangles in $\mathcal{U}$ have the same combinatorial data. For each surface, there is an upper and a lower bound for the height of the rectangles, say $K(Y)$ and $K(Y)^{-1}$. Since these bounds depend continuously on the surface Y, the constant $K = \max_{Y\in\overline{\mathcal{U}}} K(Y) \in (0,\infty)$ is well defined and satisfies the first two points of the lemma, together with $I(Y)$. Moreover, the curves (ζ_1,ζ_2) are not horizontal since s admits no horizontal saddle connection. Up to increasing K, we have also $K^{-1} < l_{\mathrm{v}}(\zeta_j(Y)) < K$ for every $Y \in \mathcal{U}$ and $j \in \{1,2\}$. ■

Denote by $(t_n)_{n\in\mathbb{N}}$ the sequence of return times of g_t in $\mathcal{U}$, with convention $t_0 = 0$.

Definition 5.18. *For $k \in \mathbb{N}$, we define*

$$\zeta_i^{(k)} = A^{KZ}(t_k, X).\zeta_i.$$

In particular $\left(\zeta_1^{(0)},\zeta_2^{(0)}\right) = (\zeta_1,\zeta_2)$.

Lemma 5.19. *For any $k \in \mathbb{N}$ and $j \in \{1,2\}$,*

$$K^{-1}e^{t_k} \leqslant l_v(\zeta_j^{(k)}) \leqslant Ke^{t_k}.$$

Proof. — This follows directly from the fact that $l_{\mathrm{v}}\left(\zeta_j^{(k)}\right) = e^{t_k} l_{\mathrm{v}}(\zeta_j)$. ■

5.3.3. Decomposition of the cycle

The following Lemma is an adaptation to the case of half-translation surfaces of Lemma 9.4 in [For02] for translation surfaces, rephrased in Lemma 9 of [DHL14].

Lemma 5.20. *There exists $T_0 = T_0(X)$ such that for every $T > T_0$, there exist an integer n, and a decomposition*

$$\forall p \in X, \gamma_T(p) = \sum_{k=0}^{n} \sum_{j=1}^{2} m_j^{(k)}(p) \zeta_j^{(k)} \qquad \text{in } H_1(X, \mathbb{R})$$

which satisfies:

- *for every $k \in \{0, \dots, n\}$, and $j \in \{1, 2\}$, the $m_j^{(k)}(p)$ are (possibly negative) integers,*
- *the sum $m_1^{(n)}(p) + m_2^{(n)}(p)$ is not zero,*
- *for every $k \in \{0, \dots, n\}$, $\sum_{j=1}^{2} |m_j^{(k)}(p)| \leqslant 2K^2 e^{t_{k+1} - t_k}$.*

Proof. — For each $k \in \mathbb{N}$, denote by $I^{(k)}$ the subinterval of I starting at s and of length $e^{-t_k} l(I)$.

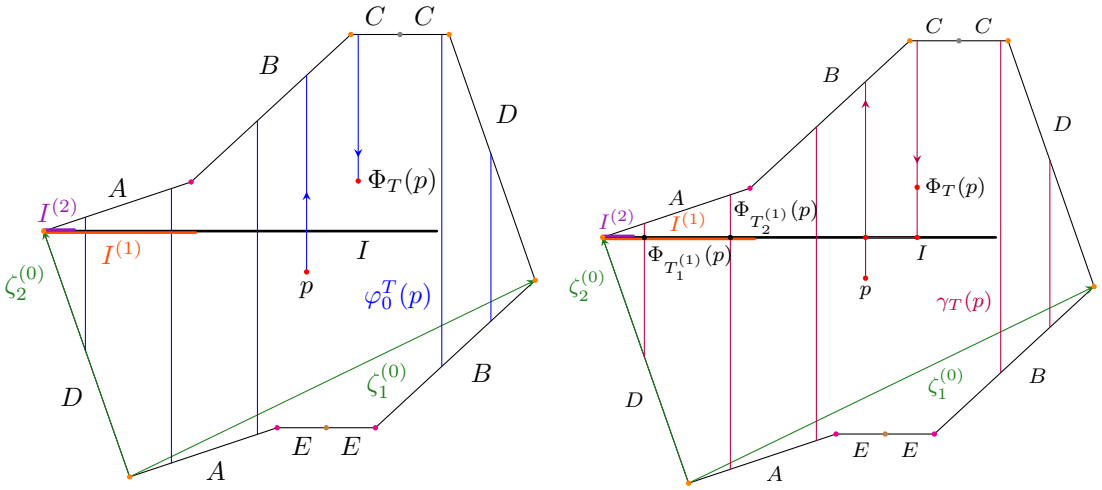

Figure 5.12. – Illustration of the different curves

If T is big enough, then the vertical path $\varphi_0^T(p)$ on X intersects the segment I several times by Lemma 5.17. It will also intersect several times the segments $I^{(k)}$ for the first integers k. Let n be the greatest integer such that γ intersects at least twice the segment $I^{(n)}$, and let $T_1^{(n)}$ (resp. $T_2^{(n)}$) be the first (resp. last) intersection time between $\varphi_0^T(p)$ and $I^{(n)}$.

Define

$$\gamma^{(n)} = \gamma_{T_1^{(n)}, T_2^{(n)}}(p)$$

the closed curve defined as the union of $\varphi_{T_1^{(n)}}^{T_2^{(n)}}(p)$ with a path $\delta(\Phi_{T_2^{(n)}}(p), \Phi_{T_1^{(n)}}(p))$. Define similarly

$$\begin{cases} \rho_1^{(n)} &= \gamma_{0,T_1^{(n)}}(p) \\ \rho_2^{(n)} &= \gamma_{T_2^{(n)},T}(p) \end{cases}.$$

Seen as elements of $H_1(X,\mathbb{R})$, γ, $\gamma^{(n)}$, $\rho_1^{(n)}$ and $\rho_2^{(n)}$ satify: $\gamma = \rho_1^{(n)} + \gamma^{(n)} + \rho_2^{(n)}$.

We now decompose $\rho_1^{(n)}$ and $\rho_2^{(n)}$ as we have decomposed γ. Let $T_1^{(n-1)}$ (resp. $T_2^{(n-1)}$) be the first (resp. last) intersection time between $\rho_1^{(n)}$ (resp. $\rho_2^{(n)}$) and $I^{(n-1)}$. Note that $\rho_1^{(n)}$ (resp. $\rho_2^{(n)}$) ends (resp. starts) in $I^{(n)} \subset I^{(n-1)}$ so $T_1^{(n-1)}$ (resp. $T_2^{(n-1)}$) is well-defined. Set

$$\begin{cases} \gamma_1^{(n-1)} &= \gamma_{T_1^{(n-1)},T_1^{(n)}}(p) \\ \gamma_2^{(n-1)} &= \gamma_{T_2^{(n)},T_2^{(n-1)}}(p) \end{cases}$$

and

$$\begin{cases} \rho_1^{(n-1)} &= \gamma_{0,T_1^{(n-1)}}(p) \\ \rho_2^{(n-1)} &= \gamma_{T_2^{(n-1)},T}(p) \end{cases}.$$

We may have $T_1^{(n-1)} = T_1^{(n)}$ (resp. $T_2^{(n-1)} = T_2^{(n)}$) and then $\gamma_1^{(n-1)}$ (resp. $\gamma_2^{(n-1)}$) is empty. By induction, we get an increasing sequence of times

$$0 \leqslant T_1^{(1)} \leqslant \cdots \leqslant T_1^{(n-1)} \leqslant T_1^{(n)} \leqslant T_2^{(n-1)} \cdots \leqslant T_2^{(1)} \leqslant T$$

such that

$$\gamma = \rho_1^{(0)} + \sum_{k=0}^{n-1} \gamma_1^{(k)}(p) + \gamma^{(n)} + \sum_{k=0}^{n-1} \gamma_2^{(k)} + \rho^{(0)},$$

where for any $k \in \{0,\dots,n-1\}$:

- $T_1^{(k)}$ (resp. $T_2^{(k)}$) is the first (resp. last) time in which $\varphi_0^T(p)$ intersects $I^{(k)}$,
- $\rho_1^{(0)} = \gamma_{0,T_1^{(0)}}(p)$ starts and ends at $\Phi_{T_1^{(0)}}(p) \in I^{(0)} = I$,
- $\gamma_1^{(k)} = \gamma_{T_1^{(k)},T_1^{(k+1)}}(p)$ starts in $I^{(k)}$ and ends in $I^{(k+1)}$,
- $\gamma^{(n)}$ starts in $I^{(n)}$, ends in $I^{(n)}$ and intersects at most once $I^{(n+1)}$,
- $\gamma_2^{(k)} = \gamma_{T_1^{(k+1)},T_1^{(k)}}(p)$ starts in $I^{(k+1)}$ and ends in $I^{(k)}$,
- $\rho_2^{(0)} = \gamma_{T_2^{(0)},T}(p)$ starts and ends at $\Phi_{T_2^{(0)}}(p) \in I^{(0)} = I$.

For $j \in \{1,2\}$, we write $\gamma_j^{(k)}(p)$, seen as an element of $H_1(X,\mathbb{R})$, in the basis $\left(\zeta_1^{(k)}, \zeta_2^{(k)}\right)$ (see Definition 5.18):

$$\gamma_j^{(k)} = n_{j,1}^{(k)}\zeta_1^{(k)} + n_{j,2}^{(k)}\zeta_2^{(k)}$$

and

$$\gamma^{(n)} = m_1^{(n)}\zeta_1^{(n)} + m_2^{(n)}\zeta_2^{(n)}.$$

Of course, the curves depends on p, hence the coefficients $n_{j,i}^{(k)}$ and $m_j^{(k)}$ depend also on p. However, we will bound their length from above by a constant that does not depend on p. The curve $\gamma_i^{(k)}$ can not be too long because it intersects at most once the segment $I^{(k+1)}$, which is such that $g_{t_{k+1}}.I^{(k+1)} = I\left(g_{t_{k+1}}.X\right)$ (this is why we defined $I^{(k)}$ this way) and Lemma 5.17 applied to $g_{t_{k+1}}.\gamma_i^{(k)} \subset g_{t_{k+1}}(X)$ gives:

$$e^{-t_{k+1}} l_{\mathrm{v}}\left(\gamma_i^{(k)}\right) = l_{\mathrm{v}}\left(g_{t_{k+1}}.\gamma_i^{(k)}\right) \leqslant K.$$

Moreover, $l_{\mathrm{v}}\left(\gamma_i^{(k)}\right) = \sum_{j=1}^{2} \left|n_{i,j}^{(k)}\right| l_{\mathrm{v}}\left(\zeta_j^{(n)}\right)$ is bounded from below thanks to Lemma 5.19:

$$l_{\mathrm{v}}(\gamma_i^{(k)}) \geqslant \sum_{j=1}^{2} \left|n_{i,j}^{(k)}\right| K^{-1} e^{t_k}.$$

From these two bounds, we get, for $i = 1$ and $i = 2$:

$$\sum_{j=1}^{2} \left|n_{i,j}^{(k)}\right| \leqslant K^2 e^{t_{k+1}-t_k}.$$

We define $m_1^{(k)} = n_{1,1}^{(k)} + n_{2,1}^{(k)}$ and $m_2^{(k)} = n_{1,2}^{(k)} + n_{2,2}^{(k)}$ so that:

$$\gamma_1^{(k)} + \gamma_2^{(k)} = m_1^{(k)}\zeta_1^{(k)} + m_2^{(k)}\zeta_2^{(k)}.$$

Then we get the bound announced:

$$\sum_{j=1}^{2} \left|m_j^{(k)}\right| \leqslant \sum_{i,j=1}^{2} \left|n_{i,j}^{(k)}\right| \leqslant 2K^2 e^{t_{k+1}-t_k}.$$

■

5.4. Conclusion

5.4.1. Computation of the algebraic intersection number

Take $w \in H_1(X, \mathbb{R})$ and write $(w_1^{(k)}, w_2^{(k)})$ the coordinates of w in the basis $\left(\zeta_1^{(k)}, \zeta_2^{(k)}\right)$, then we have:

$$\begin{aligned}\iota(\gamma_{0,T}(p), w) &= \sum_{k=0}^{n-1} \iota\left(\gamma_1^{(k)} + \gamma_2^{(k)}, w\right) + \iota\left(\gamma^{(n)}, w\right) + \iota\left(\rho_1^{(0)} + \rho_2^{(0)}, w\right) \\ &= \sum_{k=0}^{n} \sum_{i,j=1}^{2} m_i^{(k)} w_j^{(k)} \iota\left(\zeta_i^{(k)}, \zeta_j^{(k)}\right) + \sum_{j=1}^{2} w_j^{(0)} \iota\left(\rho_1^{(0)} + \rho_2^{(0)}, \zeta_j^{(0)}\right) \\ &= \sum_{k=0}^{n} \left(m_1^{(k)} w_2^{(k)} + m_2^{(k)} w_1^{(k)}\right) + 0.\end{aligned}$$

We will control the m_j with Lemma 5.20 and the $w_j^{(k)}$ with the Oseledets theorem applied to the Kontsevich–Zorich cocycle.

5.4.2. Conclusion using the Oseledets theorem

We have everything to prove Theorem F.

Theorem F. *Let $X \in \mathcal{Q}(1^2, -1^2)$ be a generic surface. There exist a cycle $w \in H_1(X, \mathbb{R})$ and a constant $C > 0$ such that for every $p \in X$, and every $T > 0$, the (algebraic) number of intersections between w and γ_T is bounded by C:*

$$|\iota(w, \gamma_T)| < C.$$

Proof. — The surface X is Oseledets generic, so the Oseledets theorem applied to the Kontsevich–Zorich cocycle gives two Lyapunov exponents $\theta_1 \leqslant \theta_2$ and a flag decomposition $\{0\} = E_0 \subset E_1 \subset E_2 = H_1(X, \mathbb{R})$ such that

$$\forall v \in E_i \setminus E_{i-1}, \ \frac{\log \left|\left|A_{KZ}^{(n)} v\right|\right|}{n} \underset{n\to\infty}{\longrightarrow} \theta_i.$$

Moreover, Bell, Delecroix, Gadre, Gutierez-Romo and Schleimer [BDGGS21] showed that the plus and minus Lyapunov spectra of any component of any stratum of half-translation surfaces are simple, in particular here $\theta_1 < \theta_2$. Furthermore, the Kontsevich–Zorich cocycle is symplectic, which implies that $\theta_1 = -\theta_2$. We conclude that $\theta_1 < 0$, namely $\lambda := e^{\frac{\theta_1}{2}} < 1$.

Let $w \in H_1(X, \mathbb{R})$ be a vector in the contracted direction E_1, and let $\varepsilon \in (0, \frac{\theta_2}{2})$. Then there exists k_0 such that:

$$\forall k \geqslant k_0, \ \log \left|\left|w^{(k)}\right|\right| = \log \left|\left|A_{KZ}^{(k)} w\right|\right| \leqslant k(\theta_1 + \varepsilon) < k\frac{\theta_1}{2}.$$

Then $\left|\left|w_j^{(k)}\right|\right| \leqslant \lambda^k ||w||$ and

$$\begin{aligned}|\iota(\gamma_{0,T}(p), w)| &\leqslant \sum_{k=0}^{n} \left|\left|w^{(k)}\right|\right| \left(\left|m_1^{(k)}\right| + \left|m_2^{(k)}\right|\right) \\ &\leqslant \sum_{k=0}^{n} \lambda^k ||w|| \left(\left|m_1^{(k)}\right| + \left|m_2^{(k)}\right|\right) \\ &< ||w|| \sum_{k=0}^{n} \lambda^k K^2 e^{t_{k+1}-t_k}\end{aligned}$$

Write $M = \frac{1}{\mu(\mathcal{U})}$ the inverse of the measure of $\mathcal{U}$ in $\mathcal{Q}(1^2, -1^2)$. By Kac's lemma $\frac{t_k}{k} \underset{k\to\infty}{\longrightarrow} M$, so for any $\delta > 0$, there exists $k_0 \in \mathbb{N}$ such that

$$\forall k \geqslant k_0, \quad M - \delta(2k+1) \leqslant t_{k+1} - t_k \leqslant M + \delta(2k+1),$$

which leads to

$$|\iota(\gamma_{0,T}(p), w)| < ||w||_\infty \left(\sum_{k=0}^{k_0-1} \lambda^k K^2 e^{t_{k+1}-t_k} + e^{M+\delta} \sum_{k=k_0}^{n} \lambda^k e^{2k\delta} \right).$$

For δ small enough, this is a convergent geometric sum. This shows the lemma, for

$$C = ||w||_\infty \left(\frac{e^{M+\delta}}{1 - \lambda e^{2\delta}} + \sum_{k=0}^{k_0-1} \lambda^k K^2 e^{t_{k+1}-t_k} \right).$$

Note that this value depends on the surface X (because of the times t_k, for $k \in \{0, k_0 - 1\}$). ■

This proves by the same occasion Theorem E as a corollary, as stated by Lemma 5.15 .

Goujard [Gou15] gives the exact value of volumes of strata of small genus. Together with the formula of Eskin, Kontsevich and Zorich [EKZ11] on the sum of Lyapunov exponents, we get that the exact values of the Lyapunov exponents *for the Teichmüller flow* in the stratum $\mathcal{Q}(1^2, -1^2)$ are $\theta_1 = -\frac{2}{3}$ and $\theta_2 = \frac{2}{3}$.

5.5. Perspectives

We showed that the vertical trajories are trapped in a strip for *almost every* lattice Λ according to which we place the obstacles. This result reminds the result for Eaton lenses [FS14], which was generalized by Frączek , Shi, and Ulcigrai [FSU18]. They show that for *every* lattice Λ, the trajectories in *almost every* direction are trapped in a strip of the plane. In the future, we hope to prove the same result for tiling billiards in the wind-tree model with analogous methods.

Moreover, we have good reasons to believe in the following conjecture, where we denote by q_v the orthogonal projection onto the subspace $\mathrm{Vect}(v)$ spanned by v.

Conjecture 5.21. *For almost every admissible tuple (Λ, a, b, θ), for almost every initial point $\tilde{p}$:*

$$\begin{cases} \limsup_{n\to\infty} |q_v\left(\Psi_t(\tilde{p}) - \tilde{p}\right)| = \infty \\ q_v\left(\Psi_t(\tilde{p}) - \tilde{p}\right) \geqslant 0 \text{ infinitely often} \\ q_v\left(\Psi_t(\tilde{p}) - \tilde{p}\right) \leqslant 0 \text{ infinitely often} \end{cases},$$

where $v \in \mathbb{R}^2$ gives the direction of the strip in which the trajectory is trapped.

The first line comes from the fact that there is only one direction of $H_1(X, \mathbb{R})$ contracted by the Kontsevich–Zorich cocycle, so that a generic trajectory can not be bounded in every direction.

The second and third lines express the fact that the trajectory is conjectured to be recurrent, as in the classical wind-tree model.

Conclusion

Tiling billiards are a young subject, rich of exciting open questions. To conclude this PhD thesis, I briefly come back to the links between my work and the following question:

What can be said in general about tiling billiards in periodic polygonal tilings?

For periodic tilings composed by cyclic polygons whose circumcircles have all the same radius, namely admissible tilings defined in Section 4.4.2, this question can be reduced to a question on the family $\mathcal{F}$ of IETFs related to the tiling billiards. Every element of $\mathcal{F}$ is flipping all its intervals of continuity. It can be defined on one or more circles. In Chapter 4, we begin the study of bi-triangle tiling billiards. We defined an induction that allows to study a subfamily of $\mathcal{F}$. This is a first step to understand the entire family and thus to describe the trajectories in any periodic tiling billiard. In particular we are interested in the following

Question 5.1. *In which admissible tilings do there exist some trajectories that are not periodic nor linearly escaping?*

The family $\mathcal{G}$ of IETFs involved in the study of generalized tiling billiards, defined and explored in Chapter 3, is a generalization of the subfamilies $\mathcal{F}_3$ and $\mathcal{F}_4$ of $\mathcal{F}$, whose elements are the IETFs corresponding respectively to the triangle and cyclic quadrilateral tiling billiards. Chapter 3 handles the case of polygons inscribed in a half-circle.

Question 5.2. *What happens for generalized tiling billiards defined with cyclic polygons that are not inscribed in a half-circle?*

Even though generalized tilings are not periodic tilings (since they are not tilings), their study involves fully flipping IETFs, as the study of admissible tiling billiards does.

For locally foldable periodic tilings with a centrally symmetric fundamental domain, the Dynnikov helicoid is a strong connection between our question and the Novikov problem. In both of the so far known cases (triangle and cyclic quadrilateral tiling billiards), the Dynnikov helicoid has genus 3. In the case of bi-triangle tiling billiards studied in Chapter 4, the Dynnikov helicoid has genus 5.

Question 5.3. *Are there some new behaviors for tiling billiards whose Dynnikov helicoid has genus more than* 3*?*

The wind-tree model, that can be considered as a polygonal tiling with one infinite tile (corresponding to the plane but the union of rectangular obstacles), offers another nice setting to study tiling billiards. We proved in Chapter 5 that for almost every configuration of the wind-tree, every trajectory with vertical initial direction is trapped in a strip of bounded width.

Question 5.4. *How does a generic trajectory fill the strip in which it is trapped? In particular, does it go arbitrarily far away in both directions of the strip?*

In another direction, one can ask

Question 5.5. *What happens for the tiling billiard in the wind-tree model if we replace the rectangular obstacle by another right-angled polygon?*

The fact that the polygon is right-angled ensures that the trajectories will still have the same direction outside the obstacle. Thus, we can associated a new slit surface to this system. We have then to check that we can apply the argument of Chapter 5 in the stratum of this new surface. For the classical wind-tree model, this is done by Delecroix-Zorich [DZ20] for connected shape and then by Fougeron [Fou20] for non connected shape.

Bibliographie

[Ada04] Boris Adamczewski. Symbolic discrepancy and self-similar dynamics. *Annales de l'Institut Fourier*, 54(7) :2201-2234, 2004. doi : 10.5802/aif.2079. url : http://www.numdam.org/articles/10.5802/aif.2079/ (cf. page 51).

[AI01] Pierre Arnoux et Shunji Ito. Pisot substitutions and Rauzy fractals. In tome 8, numéro 2, pages 181-207. 2001. url : http://projecteuclid.org/euclid.bbms/1102714169. Journées Montoises d'Informatique Théorique (Marne-la-Vallée, 2000) (cf. page 40).

[AR91] Pierre Arnoux et Gérard Rauzy. Geometric representation of sequences of complexity $2n + 1$. *Bull. Soc. Math. Fr.*, 119(2) :199-215, 1991. issn : 0037-9484. doi : 10.24033/bsmf.2164 (cf. pages 31, 96).

[AS13] Pierre Arnoux et Štěpán Starosta. The Rauzy gasket. In *Further developments in fractals and related fields. Mathematical foundations and connections. Outgrowth of the 2nd international conference on fractals and related fields, Porquerolles Island, France, June 2011*, pages 1-23. New York, NY : Birkhäuser/Springer, 2013. isbn : 978-0-8176-8399-3 ; 978-0-8176-8400-6. doi : 10.1007/978-0-8176-8400-6_1 (cf. page 82).

[AH20] A. Avila et P. Hubert. Recurrence for the wind-tree model. *Ann. Inst. Henri Poincaré, Anal. Non Linéaire*, 37(1) :1-11, 2020. issn : 0294-1449. doi : 10.1016/j.anihpc.2017.11.006 (cf. page 24).

[Avi10] Artur Avila. Dynamics of renormalization operators. In *Proceedings of the International Congress of Mathematicians. Volume I*, pages 154-175. Hindustan Book Agency, New Delhi, 2010. isbn : 978-81-85931-08-3 ; 978-981-4324-31-1 ; 981-4324-31-0 (cf. page 29).

[BDFI24] Paul Baird-Smith, Diana Davis, Elijah Fromm et Sumun Iyer. Tiling Billards on Triangle Tilings, and Interval Exchange Transformations. *J. Lond. Math. Soc.*, 109(1) :e12854, 2024. doi : https://doi.org/10.1112/jlms.12854 (cf. pages 18, 20, 47, 49, 55, 74, 84).

[Bar23] Simon Barazer. Average diffusion rate of Ehrenfest Wind-tree billiards. preprint, 2023. arXiv : 2312.12126 [math.DS] (cf. page 24).

[BDGGS21] Mark Bell, Vincent Delecroix, Vaibhav Gadre, Rodolfo Gutiérrez-Romo et Saul Schleimer. The flow group of rooted abelian or quadratic differentials. 2021. arXiv : 2101.12197 [math.DS] (cf. page 120).

[Bir31] George D. Birkhoff. Proof of the ergodic theorem. *Proc. Natl. Acad. Sci. USA*, 17 :656-660, 1931. issn : 0027-8424. doi : 10.1073/pnas.17.12.656 (cf. page 30).

[Cof88] John Coffey. Some remarks concerning an example of a minimal, non-uniquely ergodic interval exchange transformation. *Math. Z.*, 199(4) :577-580, 1988. ISSN : 0025-5874. DOI : 10.1007/BF01161646 (cf. page 27).

[DN90] Claude Danthony et Arnaldo Nogueira. Measured foliations on nonorientable surfaces. *Annales scientifiques de l'École Normale Supérieure*, Ser. 4, 23(3) :469-494, 1990. DOI : 10.24033/asens.1608. URL : http://www.numdam.org/articles/10.24033/asens.1608/ (cf. page 28).

[DDRS18] Diana Davis, Kelsey DiPietro, Jenny Rustad et Alexander St Laurent. Negative refraction and tiling billiards. *Adv. Geom.*, 18(2) :133-159, 2018. ISSN : 1615-715X. DOI : 10.1515/advgeom-2017-0053 (cf. page 16).

[DH18] Diana Davis et W. Patrick Hooper. Periodicity and ergodicity in the trihexagonal tiling. *Comment. Math. Helv.*, 93(4) :661-707, 2018. ISSN : 0010-2571. DOI : 10.4171/CMH/447 (cf. page 21).

[Del16] Vincent Delecroix. Interval exchange transformations, 2016 (cf. page 40).

[DHL14] Vincent Delecroix, Pascal Hubert et Samuel Lelièvre. Diffusion for the periodic wind-tree model. *Ann. Sci. Éc. Norm. Supér. (4)*, 47(6) :1085-1110, 2014. ISSN : 0012-9593. DOI : 10.24033/asens.2234 (cf. pages 24, 31, 104, 117).

[DZ20] Vincent Delecroix et Anton Zorich. Cries and whispers in wind-tree forests. In *What's next ?—the mathematical legacy of William P. Thurston*. Tome 205, Ann. of Math. Stud. Pages 83-115. Princeton Univ. Press, Princeton, NJ, 2020. ISBN : 978-0-691-18589-7 ; 978-0-691-16776-3 ; 978-0-691-16777-0. DOI : 10.2307/j.ctvthhdvv.8 (cf. page 124).

[DD09] Roberto DeLeo et Ivan Dynnikov. Geometry of plane sections of the infinite regular skew polyhedron 4, 6 | 4. *Geometriae Dedicata*, 138 :51-67, 2009. DOI : 10.1007/s10711-008-9298-1 (cf. page 28).

[DHMPS] I. Dynnikov, P. Hubert, P. Mercat, O. Paris-Romaskevich et A. Skripchenko. The Lebesgue measure of Novikov's gasket is zero. En cours d'écriture (cf. pages 16, 18, 28, 47, 49, 73).

[Dyn92] I. A. Dynnikov. Proof of S. P. Novikov's conjecture for the case of small perturbations of rational magnetic fields. *Russ. Math. Surv.*, 47(3) :172-173, 1992. ISSN : 0036-0279. DOI : 10.1070/RM1992v047n03ABEH000901 (cf. page 28).

[Dyn97] I. A. Dynnikov. Semiclassical motion of the electron. A proof of the Novikov conjecture in general position and counterexamples. In *Solitons, geometry, and topology : on the crossroad*, pages 45-73. Providence, RI : American Mathematical Society, 1997. ISBN : 0-8218-0666-1 (cf. page 28).

[Dyn99] I. A. Dynnikov. Semiclassical electron motion and Novikov's conjecture. *J. Math. Sci., New York*, 94(4) :1, 1999. ISSN : 1072-3374. DOI : 10.1007/BF02365205 (cf. page 28).

[Eat52] J. E. Eaton. On spherically symmetric lenses. *Transactions of the IRE Professional Group on Antennas and Propagation* :66-71, 1952 (cf. page 25).

[EE12] Paul Ehrenfest et Tatiana Ehrenfest. Begriffliche Grundlagen der statistischen Auffassung in der Mechanik. *Encykl. d. math. Wissensch.*, IV 2 II, 1912 (cf. page 24).

[EKZ11] A. V. Eskin, Maxim Kontsevich et Anton Zorich. Sum of Lyapunov exponents of the Hodge bundle with respect to the Teichmüller geodesic flow. *Publications mathématiques de l'IHÉS*, 120 :207-333, 2011. URL : https://api.semanticscholar.org/CorpusID:119307741 (cf. pages 50, 121).

[For02] Giovanni Forni. Deviation of Ergodic Averages for Area-Preserving Flows on Surfaces of Higher Genus. *Annals of Mathematics*, 155(1) :1-103, 2002. ISSN : 0003486X. URL : http://www.jstor.org/stable/3062150 (visité le 05/02/2024) (cf. pages 31, 50, 104, 117).

[Fou20] Charles Fougeron. Diffusion rate of windtree models and Lyapunov exponents. *Bull. Soc. Math. France*, 148(1) :25-49, 2020. ISSN : 0037-9484,2102-622X. DOI : 10.24033/bsmf.2798 (cf. page 124).

[FS14] Krzysztof Frączek et Martin Schmoll. Directional localization of light rays in a periodic array of retro-reflector lenses. *Nonlinearity*, 27(7) :1689-1707, 2014. ISSN : 0951-7715. DOI : 10.1088/0951-7715/27/7/1689 (cf. pages 24-26, 31, 104, 121).

[FSU18] Krzysztof Frączek, Ronggang Shi et Corinna Ulcigrai. Genericity on curves and applications : pseudo-integrable billiards, Eaton lenses and gap distributions. *J. Mod. Dyn.*, 12 :55-122, 2018. ISSN : 1930-5311. DOI : 10.3934/jmd.2018004 (cf. pages 26, 31, 45, 121).

[Gou15] Elise Goujard. Siegel-Veech constants for strata of moduli spaces of quadratic differentials. *Geom. Funct. Anal.*, 25(5) :1440-1492, 2015. ISSN : 1016-443X,1420-8970. DOI : 10.1007/s00039-015-0345-4 (cf. page 121).

[Ham23] Ursula Hamenstädt. Typical properties of periodic Teichmüller geodesics : Lyapunov exponents. *Ergodic Theory Dynam. Systems*, 43(2) :556-584, 2023. ISSN : 0143-3857,1469-4417. DOI : 10.1017/etds.2021.113 (cf. page 66).

[HP22] Pascal Hubert et Olga Paris-Romaskevich. Triangle tiling billiards and the exceptional family of their escaping trajectories : circumcenters and Rauzy gasket. *Exp. Math.*, 31(1) :58-87, 2022. ISSN : 1058-6458. DOI : 10.1080/10586458.2019.1583615 (cf. pages 18, 47, 49, 96).

[Jay] Magali Jay. Deviations for generalized tiling billiards in cyclic polygons. Preprint (cf. page 5).

[KS67] A. B. Katok et A. M. Stepin. Approximations in ergodic theory. *Usp. Mat. Nauk*, 22(5(137)) :81-106, 1967. ISSN : 0042-1316 (cf. page 27).

[Kea75] Michael Keane. Interval exchange transformations. *Math. Z.*, 141 :25-31, 1975. ISSN : 0025-5874. DOI : 10.1007/BF01236981 (cf. page 30).

[Kea77] Michael KEANE. Non-ergodic interval exchange transformations. *Isr. J. Math.*, 26 :188-196, 1977. ISSN : 0021-2172. DOI : 10.1007/BF03007668 (cf. page 27).

[KN76] Harvey B. KEYNES et Dan NEWTON. A 'minimal', non-uniquely ergodic interval exchange transformation. *Math. Z.*, 148 :101-105, 1976. ISSN : 0025-5874. DOI : 10.1007/BF01214699 (cf. page 27).

[Leo03] Roberto De LEO. Characterization of the set of "ergodic directions" in Novikov's problem of quasi-electron orbits in normal metals. *Russian Mathematical Surveys*, 58(5) :1042, 2003. DOI : 10.1070/RM2003v058n05ABEH000669 (cf. page 28).

[Leo05] Roberto De LEO. A proof of Dynnikov's conjecture on the location of stability zones in the Novikov problem on plane sections of periodic surfaces. *Russian Mathematical Surveys*, 60(3) :566-567, 2005. DOI : https://doi.org/10.1070/RM2005v060n03ABEH000850 (cf. page 28).

[Leo06] Roberto De LEO. Topology of Plane Sections of Periodic Polyhedra with an Application to the Truncated Octahedron. *Experimental Mathematics*, 15(1) :109-124, 2006. DOI : 10.1080/10586458.2006.10128949 (cf. page 28).

[LH64] Rudolf Karl LUNEBERG et Max HERZBERGER. *Mathematical Theory of Optics*. University of California Press, 1re édition, 1964. ISBN : 9780520368507. URL : http://www.jstor.org/stable/jj.8501483 (cf. page 25).

[MMY05] S. MARMI, P. MOUSSA et J.-C. YOCCOZ. The cohomological equation for Roth-type interval exchange maps. *J. AMER. MATH. SOC*, 18(4) :823-872, 2005 (cf. pages 34, 43, 51).

[Mas82] Howard MASUR. Interval Exchange Transformations and Measured Foliations. *Ann. of Math. (2)*, 115(1) :169-200, 1982. ISSN : 0003486X. URL : http://www.jstor.org/stable/1971341 (visité le 12/02/2024) (cf. pages 30, 52, 58).

[Nog89] Arnaldo NOGUEIRA. Almost all interval exchange transformations with flips are nonergodic. *Ergodic Theory Dyn. Syst.*, 9(3) :515-525, 1989. ISSN : 0143-3857. DOI : 10.1017/S0143385700005150 (cf. pages 16, 28, 30).

[Nov82] S. P. NOVIKOV. The Hamiltonian formalism and a many-valued analogue of Morse theory. *Russ. Math. Surv.*, 37(5) :1-56, 1982. ISSN : 0036-0279. DOI : 10.1070/RM1982v037n05ABEH004020 (cf. pages 28, 73).

[Ose68] Valeriy I. OSELEDETS. A multiplicative ergodic theorem. Characteristic Ljapunov, exponents of dynamical systems. *Trudy Moskov. Mat. Obšč.*, 19 :179-210, 1968. ISSN : 0134-8663 (cf. page 30).

[Par19] Olga PARIS-ROMASKEVICH. Trees and flowers on a billiard table. preprint, 2019. URL : https://hal.science/hal-02169195 (cf. pages 18, 20, 31, 47, 49).

[Par21] Olga PARIS-ROMASKEVICH. Tiling billiards and Dynnikov's helicoid. *Trans. Mosc. Math. Soc.*, 2021 :133-147, 2021. ISSN : 0077-1554. DOI : 10.1090/mosc/317 (cf. pages 16, 28, 47, 49, 73).

[Poi90] Henri POINCARÉ. On the three-body problem and the equations of dynamics. *Acta Math.*, 13 :1-270, 1890. ISSN : 0001-5962 (cf. page 27).

[Que10a] Martine QUEFFÉLEC. *Dynamical Systems Arising from Substitutions*. In *Substitution Dynamical Systems - Spectral Analysis*. 2e édition. Springer Berlin Heidelberg, Berlin, Heidelberg, 2e édition, 2010, pages 125-160. ISBN : 978-3-642-11212-6. DOI : 10.1007/978-3-642-11212-6_5 (cf. pages 40-42).

[Que10b] Martine QUEFFÉLEC. *Substitution Dynamical Systems-Spectral Analysis*, tome 1294 de *Lecture Notes in Mathematics*. Springer-Verlag, Berlin, 2e édition, 2010, pages xv, 351. ISBN : 978-3-642-11211-9. DOI : 10.1007/978-3-642-11212-6 (cf. page 39).

[Sat76] Evgeni Anatolevich SATAEV. On the number of invariant measures for flows on orientable surfaces. *Math. USSR, Izv.*, 9 :813-830, 1976. ISSN : 0025-5726. DOI : 10.1070/IM1975v009n04ABEH001499 (cf. page 27).

[SSS01] R. A. SHELBY, D. R. SMITH et S. SCHULTZ. Experimental Verification of a Negative Index of Refraction. *Science*, 2001 (cf. page 16).

[SPW04] D. R. SMITH, J. B. PENDRY et M. WILTSHIRE. Metamaterials and negative refractive index. *Science*, 2004 (cf. page 16).

[Vee82] William A. VEECH. Gauss Measures for Transformations on the Space of Interval Exchange Maps. *Annals of Mathematics*, 115(2) :201-242, 1982. ISSN : 0003486X. URL : http://www.jstor.org/stable/1971391 (visité le 12/02/2024) (cf. pages 27, 30, 43, 52, 58).

[Via06] M. VIANA. Ergodic theory of interval exchange maps. *Revista Matemática de la Universidad Complutense de Madrid*, 19 :7-100, 2006. URL : http://dml.mathdoc.fr/item/urn:eudml:doc:40876 (cf. pages 43, 51).

[Yoc10] Jean-Christophe YOCCOZ. Interval exchange maps and translation surfaces. *Clay Math. Proc.*, 10, 2010 (cf. page 51).

[Zor84] Anton ZORICH. A problem of Novikov on the semiclassical motion of an electron in a uniform almost rational magnetic field. *Russian Mathematical Surveys*, 39(5) :287, 1984. DOI : 10.1070/RM1984v039n05ABEH004091 (cf. page 28).

[Zor96] Anton ZORICH. Finite Gauss measure on the space of interval exchange transformations. Lyapunov exponents. *Annales de l'Institut Fourier*, 46(2) :325-370, 1996. DOI : 10.5802/aif.1517. URL : http://www.numdam.org/articles/10.5802/aif.1517/ (cf. pages 36, 46).

[Zor97] Anton ZORICH. Deviation for interval exchange transformations. *Ergodic Theory and Dynamical Systems - ERGOD THEOR DYN SYST*, 17 :1477-1499, 1997. DOI : 10.1017/S0143385797086215 (cf. page 30).

[Zor99] Anton Zorich. How do the leaves of a closed 1-form wind around a surface ? *Pseudoperiodic Topology, Translations of the AMS*, 197 :135-178, 1999. doi : 10.1090/trans2/197/05 (cf. pages 30, 37, 46, 52, 60).

[Zor06] Anton Zorich. Flat surfaces. In *Frontiers in number theory, physics, and geometry. I*, pages 437-583. Springer, Berlin, 2006. isbn : 978-3-540-23189-9 ; 3-540-23189-7 (cf. page 28).